NO_x Control Options and Integration for US Coal Fired Boilers

Quarterly Progress Report

Reporting Period Start Date April 1, 2003
Reporting Period End Date: June 30, 2003

Mike Bockelie, REI
Kevin Davis, REI
Temi Linjewile, REI
Connie Senior, REI
Eric Eddings, University of Utah
Kevin Whitty, University of Utah
Larry Baxter, Brigham Young University
Calvin Bartholomew, Brigham Young University
William Hecker, Brigham Young University
Stan Harding, N.S. Harding & Associates

July 31, 2003

DOE Cooperative Agreement No: DE-FC26-00NT40753

Reaction Engineering International
77 West 200 South, Suite 210
Salt Lake City, UT 84101

Disclaimer

Abstract

This is the twelfth Quarterly Technical Report for DOE Cooperative Agreement No: DE-FC26-00NT40753. The goal of the project is to develop cost effective analysis tools and techniques for demonstrating and evaluating low NO_x control strategies and their possible impact on boiler performance for boilers firing US coals. The Electric Power Research Institute (EPRI) is providing co-funding for this program. This program contains multiple tasks and good progress is being made on all fronts.

During this quarter, a new effort was begun on the development of a corrosion management system for minimizing the impacts of low NO_x combustion systems on waterwalls; a kickoff meeting was held at the host site, AEP's Gavin Plant, and work commenced on fabrication of the probes. FTIR experiments for SCR catalyst sulfation were finished at BYU and indicated no vanadium/vanadyl sulfate formation at reactor conditions. Improvements on the mass-spectrometer system at BYU have been made and work on the steady state reactor system shakedown neared completion. The slipstream reactor continued to operate at AEP's Rockport plant; at the end of the quarter, the catalysts had been exposed to flue gas for about 1000 hours. Some operational problems were addressed that enable the reactor to run without excessive downtime by the end of the quarter.

Table of Contents

1

Executive Summary

The work to be conducted in this project received funding from the Department of Energy under Cooperative Agreement No: DE-FC26-00NT40753. This project has a period of performance that started February 14, 2000 and continues through December 30, 2004.

Our program contains five major technical tasks:

- evaluation of Rich Reagent Injection (RRI) for in-furnace NO_x control
- demonstration of RRI technologies in full-scale field tests at utility boiler
- impacts of combustion modifications (including corrosion and soot)
- ammonia adsorption / removal from fly ash
- SCR catalyst testing

To date good progress is being made on the overall program. We have seen considerable interest from industry in the program due to our successful initial field tests of the RRI technology and the corrosion monitor.

During the last three months, our accomplishments include the following:

- A new effort was begun on the development of a corrosion management system for minimizing the impacts of low NO_x combustion systems on waterwalls; a kickoff meeting was held at the host site, AEP's Gavin Plant.
- At BYU, new 5 wt% V_2O_5/TiO_2 catalyst samples were prepared for further sulfation treatments. There was evidence of increased surface acidity on the sulfate formed under wet conditions.
- Adsorption tests indicated that ammonia appeared to adsorb on Brønsted acid sites present on the sulfated surface, suggesting sulfating the catalyst produced Brønsted acid sites. NO did not appear to adsorb on the sulfated catalyst surface, with or without pre-adsorption of ammonia.
- Improvements on the mass-spectrometer system at BYU have been made and work on the steady state reactor system shakedown neared completion.
- Physical dimensions of monolith and plate catalysts have been measured and methods for laboratory testing of monoliths and plates have been considered.
- During this quarter, the slipstream reactor was operated at AEP's Rockport plant and a significant amount of hours on flue gas were accumulated. At the end of the performance period, the catalysts had been exposed to flue gas for about 1000 hours.
- This quarter saw a number of operational and equipment problems with the slipstream reaction. Chief among these were sample line plugging, catalyst plugging, heater malfunction and ammonia tank pressure build-up and venting. Minor modifications were made to the reactor to address some of the operational problems; in addition, operating procedures were changed to prevent plugging. As a result of these changes, the reactor ran well for the latter part of the quarter.

2

Experimental Methods

Within this section we present in order, brief discussions on the different tasks that are contained within this program. For simplicity, the discussion items are presented in the order of the Tasks as outlined in our original proposal.

Task 1 - Program Management

During the last performance period, a new effort to develop methods to manage waterwall corrosion in coal-fired utility boilers was initiated. Funding for the effort is being provided through a joint program that involves the Ohio Coal Development Office (OCDO) and the DOE. Project team members include REI, American Electric Power (AEP), EPRI, Corrosion Management, Ltd, the University of Utah and NS Harding and Associates. All project team members are contributing cost share for the project. To facilitate the DOE portion of the funding, and to provide the time required to perform the work effort and field tests, the cooperative agreement between REI and DOE has been modified; the project end date is now December 30, 2004. The funds from OCDO are being provided to REI through a sub-contract from AEP. All required agreements for the project were completed. On Thursday June 12, 2003 a project kick-off meeting was held at the Gavin AEP Plant, in Chesire, Ohio. Present at the meeting were JJ Letcavits – Program Manager (AEP – Columbus), Randy Sheidler – Senior Coordinator (AEP Gavin), Fred Wheeler – Regional Engineer (AEP Gavin), Howard Johnson – Program Manager (OCDO), Bruce Lani – Program Manager (DOE/NETL), Wate Bakker (EPRI), Brad Adams (REI), Kevin Davis (REI), Stan Harding (NS Harding & Associates) and Temi M. Linjewile (REI). The Powerpoint presentations made at the kick-off meeting are provided in the Appendix to this report.

Industry Involvement

Results from portions of this research program have been reported to industry through technical presentations at recent conferences:

- A poster presentation entitled "Improved Rich Reagent Injection (RRI) Performance for NO_x Control in Coal Fired Utility Boilers," was presented at the 2003 DOE-EPRI-EPA-AWMA Combined Power Plant Air Pollution Control Mega Symposium, May 19-22, 2003 in Washington, DC [Cremer et al, 2003]. The poster highlighted the use of RRI for reducing NO_x emissions for coal-fired, electric utility cyclone barrel fired furnaces. Previous demonstrations of RRI have shown 30% NO_x reduction. Recent modeling studies for two furnaces predict 55-60% NO_x reductions are achievable.
- Two papers and a poster were accepted for presentation at the DOE NETL Conference on SCR and SNCR for Control of NO_x to be held October 29-30, 2003 in Pittsburgh, PA:
    - Marc Cremer, David Wang, E. Schindler, "Improved Rich Reagent Injection (RRI) Performance For NO_x Control In Two Coal Fired Utility Boilers."
    - Constance Senior, Temi Linjewile, Michael Bockelie, Eric Eddings, Kevin Whitty, Larry Baxter, "SCR Deactivation Mechanisms Related to Alkali and Alkaline Earth Elements."

- Dave Swensen and Darren Shino, “Control Systems for Long-Term Field-Testing Applications.” (poster)

Task 3 - Minimization of Impacts

Task 3.1 Waterwall Wastage

Reaction Engineering International (REI) and its project partners (American Electric Power (AEP), Corrosion Management, N.S. Harding & Associates, the University of Utah, EPRI and the Ohio Coal Development Office (OCDO)) have teamed up with DOE to develop a multi-pronged process for managing waterwall corrosion in coal-fired utility boilers. The project is based upon a novel multi-sensor real-time corrosion monitoring system using an advanced electrochemical technology; feasibility of the sensor was demonstrated in the field previously on this program. In the new effort, the corrosion measurements will be coupled with REI's in-house CFD modeling tools and the recently developed EPRI-REI corrosion correlations for utility boilers for the identification of key corrosion locations and to provide up-front insight as to how corrosion patterns might change during variations in operating conditions and fuel selection. In addition, an advanced precision metrology technique and simple screw-in type coupons will be used to verify predicted and measured corrosion rates.

The objectives of this effort are as follows:

- Refinement and application of CFD tools as a guide for sensor placement and corrosion management
- Development, testing, and application of a multi-sensor system
- Development of a methodology for combining predictions and validated measurements (over a range of operating conditions) into corrosion management guidelines for a coal-fired boiler.

The schedule and milestones are summarized in Figure 1.

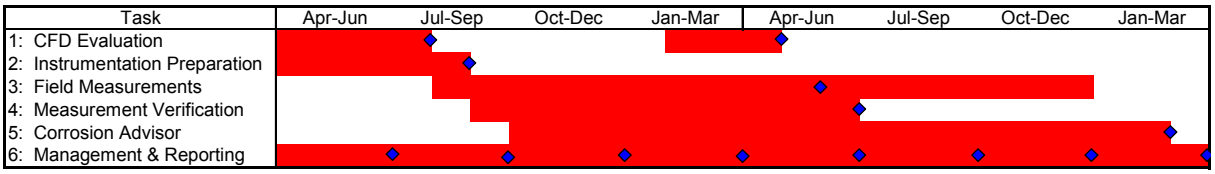

Table 1. Schedule and Milestones for Corrosion Management Effort.

Each of the diamonds represents a milestone. For Task 1 the first milestone includes the completion of the baseline simulation and the second milestone involves subsequent modeling to guide the field-testing involved in Task 3. The Task 2 milestone is the completion of shakedown testing of the instrumentation. The Task 3 milestone is the performance of the controlled field-testing and will be subject to unit demand. During Task 3 and shortly thereafter, regular checks on the sensor accuracy will be performed under Task 4. The Task 4 milestone is the completion of these evaluations. The development of the corrosion advisor is the basis for Task 5, which will end with a software deliverable that serves as the Task 5 milestone. Task 6 milestones include quarterly and final reports.

The program will be carried out at AEP's James Gavin Station on the banks of the Ohio River near Chesire, Ohio. This 2600 MW station is the largest coal-fired power plants in the state of Ohio and consumes 7 million tons of coal per year. REI will lead the CFD modeling. Corrosion Management and REI will lead the multi-sensor monitor development. AEP will lead the field tests at Gavin Station. N.S. Harding & Associates will lead the development of the Corrosion Advisor. REI and AEP will share management and reporting responsibilities.

On Thursday June 12, 2003 a project kick-off meeting was held at the Gavin AEP Plant, in Chesire OH. Present at the meeting were JJ Letcavits – Program Manager (AEP – Columbus), Randy Sheidler – Senior Coordinator (AEP Gavin), Fred Wheeler – Regional Engineer (AEP Gavin), Howard Johnson – Program Manager (OCDO), Bruce Lani – Program Manager (DOE/NETL), Wate Bakker (EPRI), Brad Adams (REI), Kevin Davis (REI), Stan Harding (NS Harding & Associates) and Temi M. Linjewile (REI). After self-introductions, the meeting started with presentations on the REI electrochemical noise (EN) probe and the KEMCOP passive corrosion probes (screw-in coupons), followed by a review of the project status, a roundtable discussion on reporting issues, plans and responsibilities. The Powerpoint presentations made at the kick-off meeting are provided in the Appendix to this report.

A plant site visit was conducted in the afternoon. The meeting attendees were able to inspect the locations where the REI EN probe and the EPRI passive probes (screw-in coupons) would be installed. There are five probe locations on the South wall and one probe location in the North wall. At each probe location there is a 3-inch port for the REI EN probe. In addition, at each probe location an array of small access ports have been provided for placing three T-11 KEMCOP screw-in coupons and one Inconel 625 probe. During the site visit, attendees also inspected the control room where the host PC would be located.

Work has begun on the fabrication of electrochemical noise probes and the KEMCOP screw-in coupons.

Task 4 - SCR Catalyst Testing

The purpose of this task is to perform a combination of basic and applied R&D, with heavy focus on laboratory and field tests, to develop a better understanding of the "real" costs associated with using selective catalytic reduction (SCR) for coal-fired boilers using US coals and a coal/biomass blend. Within this task there are four principal sub-tasks:

Task 4.1: Technology assessment on fundamental analysis of chemical poisoning of SCR catalysts by alkali and alkaline earth materials

Task 4.2: Evaluation of commercial catalysts in a continuous flow system that simulates commercial operation

Task 4.3: Evaluation of the effectiveness of catalyst regeneration

Task 4.4: Develop a model of deactivation of SCR catalysts suitable for use in a CFD code

Sub-tasks 1 and 3 are being principally performed at Brigham Young University under the direction of Professors Larry Baxter and Calvin Bartholomew. The work effort for sub-tasks 2 and 4 is being performed by REI, under the supervision of Dr. Constance Senior, with assistance from the University of Utah (Professor Eric Eddings and Dr. Kevin Whitty) on sub-task 2.

Task 4.1 Technology Assessment

The objectives of this subtask are (1) to supplement the largely complete SCR-catalyst-deactivation literature with results from new laboratory-scale, experimental investigations conducted under well-controlled and commercially relevant conditions, and (2) to provide a laboratory-based catalyst test reactor useful for characterization and analysis of SCR deactivation suitable for samples from commercial facilities, slipstream reactors, and laboratory experiments. Two catalyst flow reactors and several additional characterization systems provide the analytical tools required to achieve these objectives. The flow reactors include the *in situ* surface spectroscopy reactor (ISSR) and the catalyst characterization system (CCS), both of which were described in more detail in the Technical Quarterly Report for July through September 2002. The ancillary characterization systems include a temperature-programmable surface area and pore size distribution analyzer, scanning electron microscopes and microprobes, and catalyst preparation systems.

The sample test matrix includes two classes of catalysts: commercial, vendor-supplied SCR catalysts and BYU-manufactured, research catalysts. The commercial catalysts provide immediate relevance to practical application while the research catalyst provides less fettered ability to publish details of catalyst properties. The five commercial catalysts selected for use come from most commercially significant catalyst manufacturers and provide a wide range of catalyst designs and compositions. The in-house catalyst allows detailed analysis and publication of results that may be more difficult with the commercial systems. This catalyst suite provides a comprehensive test and analysis platform from which to determine rates and mechanisms of catalyst deactivation. The result of this task will be a mathematical model capable of describing rates and mechanisms of deactivation.

Within the last performance period, *in situ*, spectroscopic experiments partially reported last quarter were completed. The most significant finding of these investigations is a consistent indication that vanadium does not sulfate during SCR activity in the presence of gas-phase SO_2 while both the substrate (anatase) and modifiers (molybdenum) do. In addition, mass-spectroscopy-based analyses of product gases from this reactor system are being completed that will allow analysis of fundamental kinetics and deactivation mechanisms.

ISSR Overview

The purpose of the FTIR-ISSR is to provide definitive indication of surface-active species through *in situ* monitoring of infrared spectra from catalytic surfaces exposed to a variety of laboratory and field conditions. The ISSR provides in situ transmission FTIR spectrometer measurements of SO_2, NH_3, and NO_x, among other species. Absorption and desorption behaviors of these and other species are monitored. Quantitative indications of critical parameters, including Brønsted and Lewis acidities on fresh and exposed catalysts will be included. There are a number of important reasons for investigating the interaction of SO_2 with vanadia/titania SCR catalysts:

1. Given that several hundred ppm of SO_2 is typically present in the flue gas of a biomass-fired or coal-fired boiler and since it is known to adsorb on a number of metal oxides, it would be important to understand and model the effects of the adsorbed SO_2 on catalytic activity and stability.

2. While a few previous studies have addressed the effects of SO_2 on vandium SCR catalysts, the results of this work are contradictory. Some investigators report the SO_2 increases activity and resistance to deactivation of vanadium catalysts, while others report that SO_2 has no effect on activity. Mechanisms of SO_2 interaction with vanadia/titania catalysts have not been adequately addressed. For example, it is unclear if vandia or titania or both are sulfated by SO_2.

3. The role of SO_2 in deactivation of vanadium SCR catalysts is unclear. For example, while $CaSO_4$ deposits have been found to foul and mask the surfaces of vanadium catalysts, the mechanism of $CaSO_4$ formation is unclear, i.e., whether it involves formation in the gas phase or if SO_2 is oxidized on the catalyst surface to SO_3, which then interacts with CaO surface deposits.

The objectives of this study are to (1) understand at a fundamental level the interactions of SO_2 with vanadia/titania and how these interactions affect activity, selectivity, and deactivation of the catalyst and (2) determine the extent to which and rates at which vanadia and/or titania are sulfated under reaction conditions.

Furthermore, indications of coadsorption of NH_3 and NO_x will help elucidate mechanisms and rates of both reactions and deactivation.

FTIR transient test reactor

Repeat sulfation treatments of 5% V_2O_5/TiO_2 under both dry and wet conditions

Sulfation treatments of 5 wt% V_2O_5/TiO_2 were repeated under both dry and wet conditions (Table 1) as shown in Figure 2 (dry) and Figure 4 (wet) for a newly prepared 5 wt% V_2O_5/TiO_2; spectra obtained previously for a similar 5 wt% V_2O_5/TiO_2 catalyst are provided in Figure 3 (dry) and Figure 5 (wet) for purposes of comparison. While the new and old spectra are qualitatively similar, there are important quantitative differences. For example, more intense peaks were observed under both dry and wet sulfation conditions for the newly prepared 5% vanadia catalyst. The location of the sulfate peak for the new catalyst during dry sulfation is constant at about 1370 cm^{-1} from the beginning until the end of sulfation test; however, during the wet sulfation test, the corresponding sulfate peak shifts about 10 cm^{-1} lower in the first 10 hours, and changes to 1372 cm^{-1} by the end of sulfation. The shift in the sulfate peak from low wave number to high wave numbers suggests a strengthening of the acidity of the sulfate formed on the catalyst surface under wet sulfation.

Table 1. Conditions of sulfation experiments

Experiment description	Sample Details	Notes	Gas Stream Composition, %				Flow (sccm)	Temp (°C)	Window Type
			He	O_2	SO_2	H_2O			
Dry Sulfation	5% V_2O_5/TiO_2	Preoxidation	90	10		0	50	380	KCl+CaF_2
	24hrs	Sulfation	90	8	0.2	0	72	380	
Wet Sulfation	5% V_2O_5/TiO_2	Preoxidation	90	10		0	50	380	KCl+CaF_2
	24hrs	Sulfation	88	8	0.2	2	72.5	380	

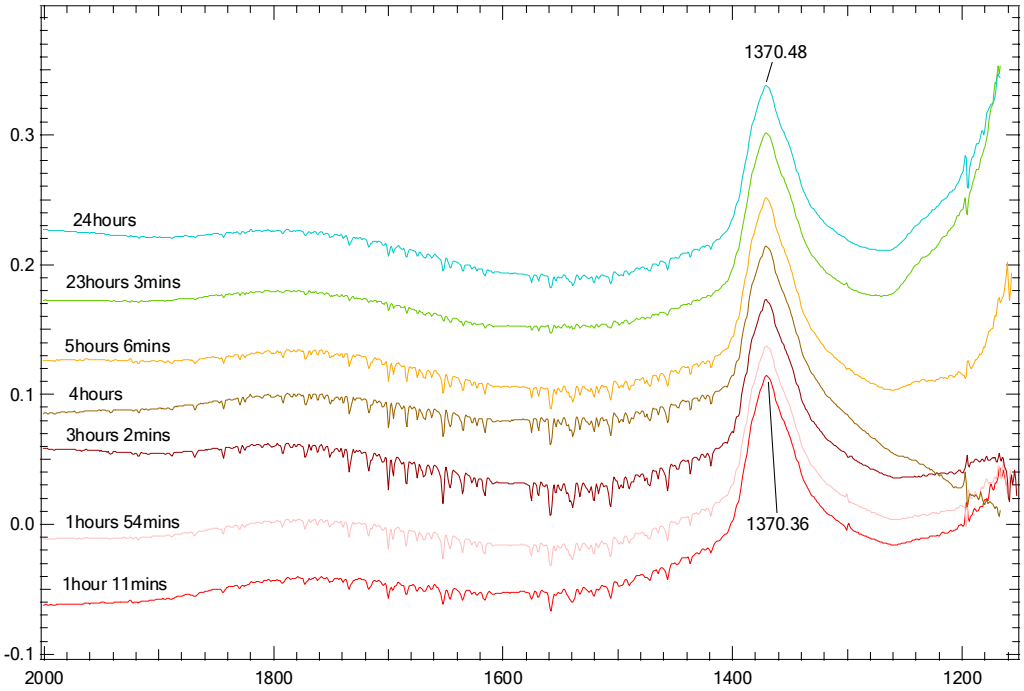

Figure 2. Dry sulfation of 5% V_2O_5/TiO_2---new catalyst sample.

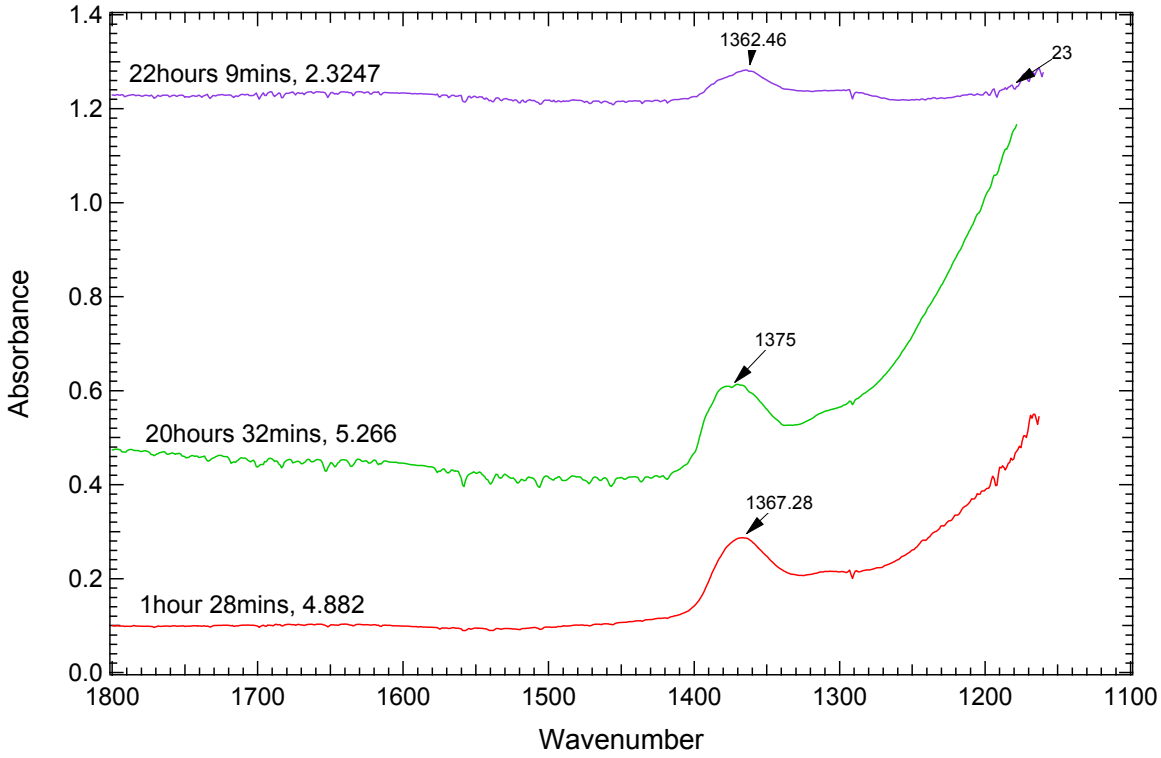

Figure 3. Dry sulfation of 5% V_2O_5/TiO_2---old catalyst sample.

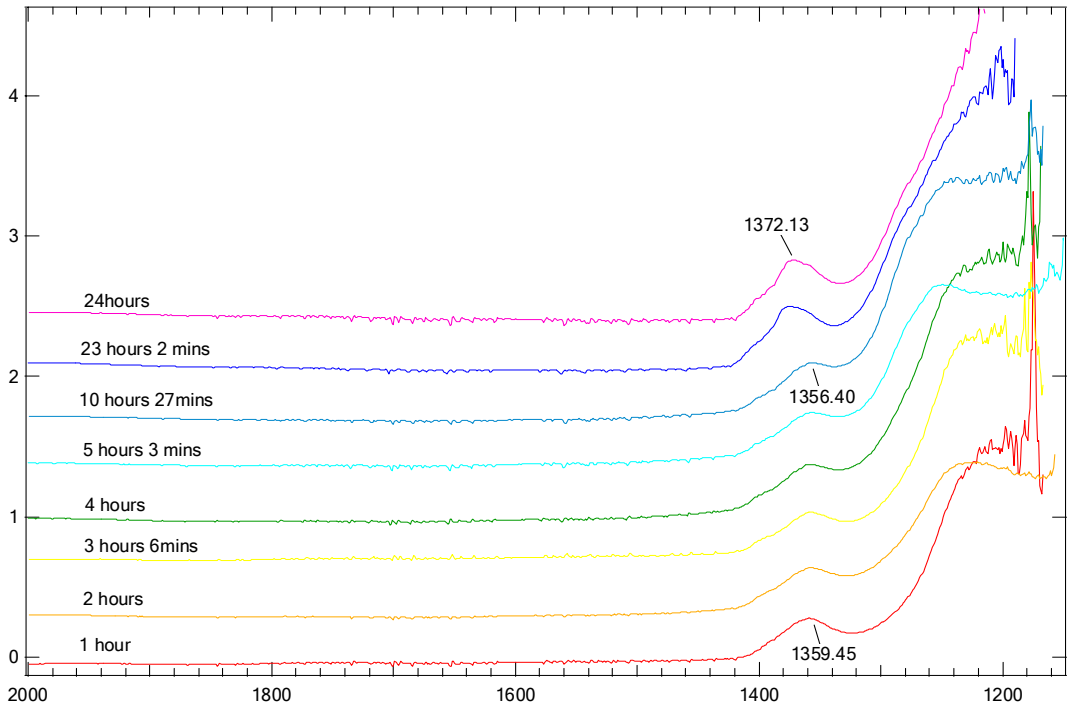

Figure 4. Wet sulfation of 5% V_2O_5/TiO_2---new catalyst sample.

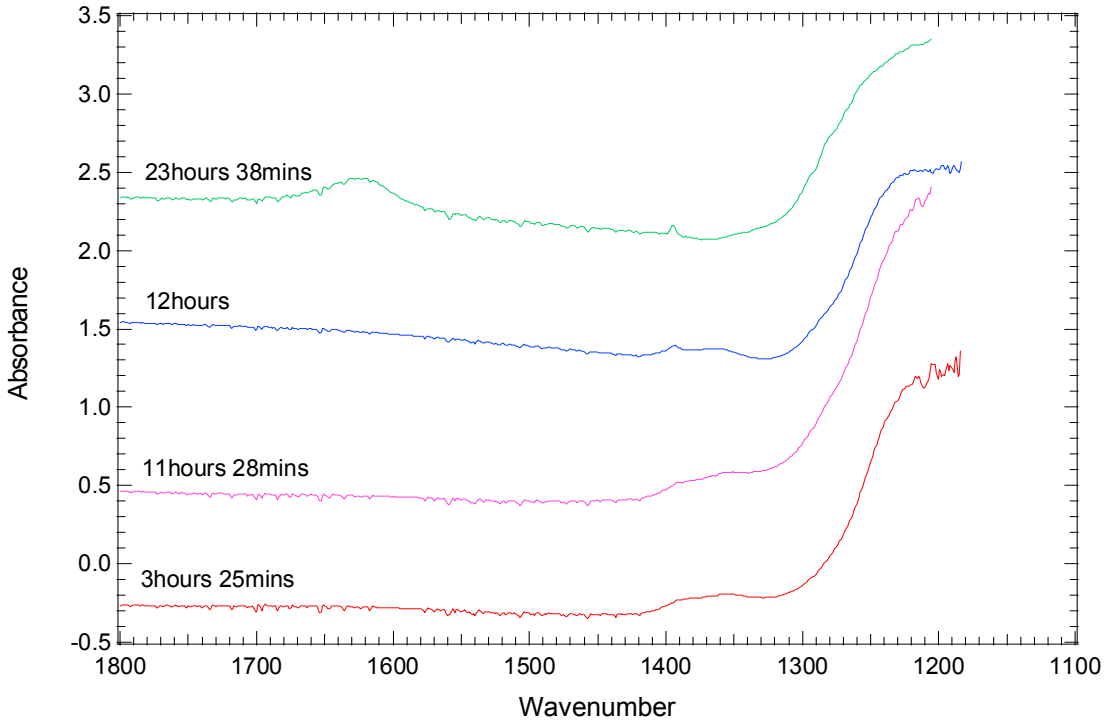

Figure 5. Wet sulfation of 5% V_2O_5/TiO_2---old catalyst sample.

NH_3 and NO adsorptions on dry sulfated 5 wt% vanadia

NH_3 and NO adsorption experiments were conducted on a 5 wt% vanadia catalyst that was previously sulfated under dry conditions.

NH_3 adsorption at room temperature

NH_3 was introduced to the sulfated catalyst at room temperature (RT) for about 25 minutes, following which the ammonia flow was stopped, helium was introduced, and the temperature was raised from 25 ˚C to 380 ˚C (see Figure 6).

Upon ammonia adsorption, new peaks show up at 1433 cm^{-1}, and two new overlapping peaks appear between 2900 to 3350 cm^{-1}. The IR absorption peak at 1433 cm^{-1} indicates a bending vibration of ammonia chemisorbed on Brønsted acid sites on the sulfated catalyst surface. No absorption was observed at 1640 cm^{-1}, a peak that reportedly corresponds to the vibration of ammonia chemisorbed on Lewis acid sites. The absorption peaks observed at 2900-3350 cm^{-1} can be assigned to the stretching vibration of ammonia adsorbed on both Brønsted (~ 3030 cm^{-1}) and Lewis acid (~3350 cm^{-1}) sites on the catalyst surface. The results show that ammonia is mainly adsorbed on Brønsted acid sites on the sulfated catalyst surface; this observation suggests that after sulfation the acid sites on the catalyst surface are principally of the Brønsted type.

Some NH_3 remains on the catalyst surface even after the temperature was increased to 200 ˚C; however, it is completely desorbed at 300 ˚C.

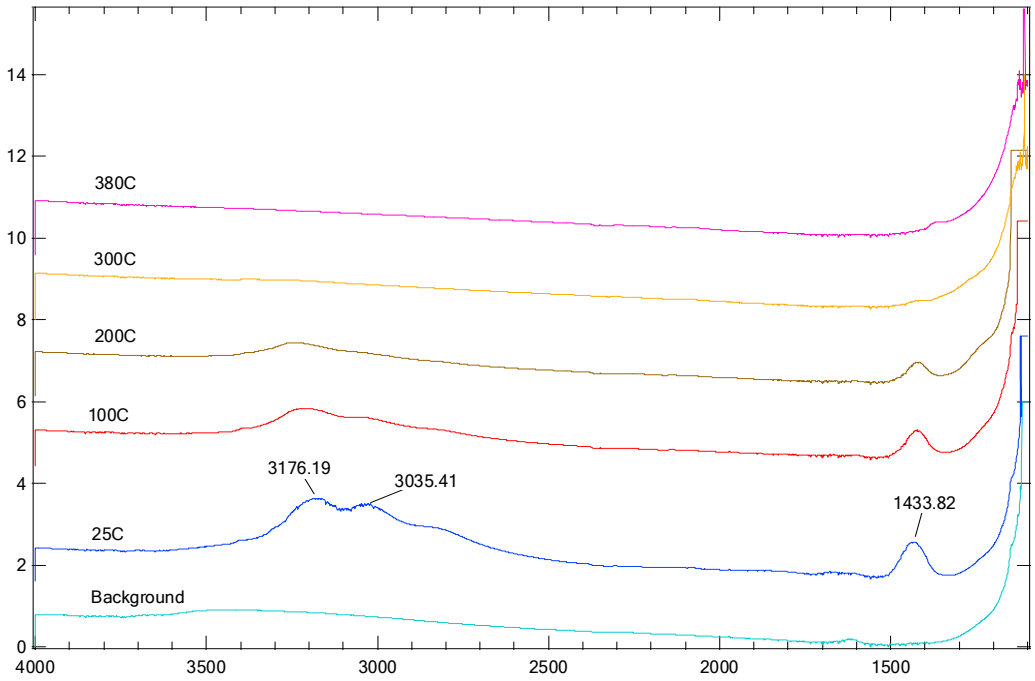

Figure 6. NH_3 adsorption at 25˚C (RT), desorption at raised temperatures.

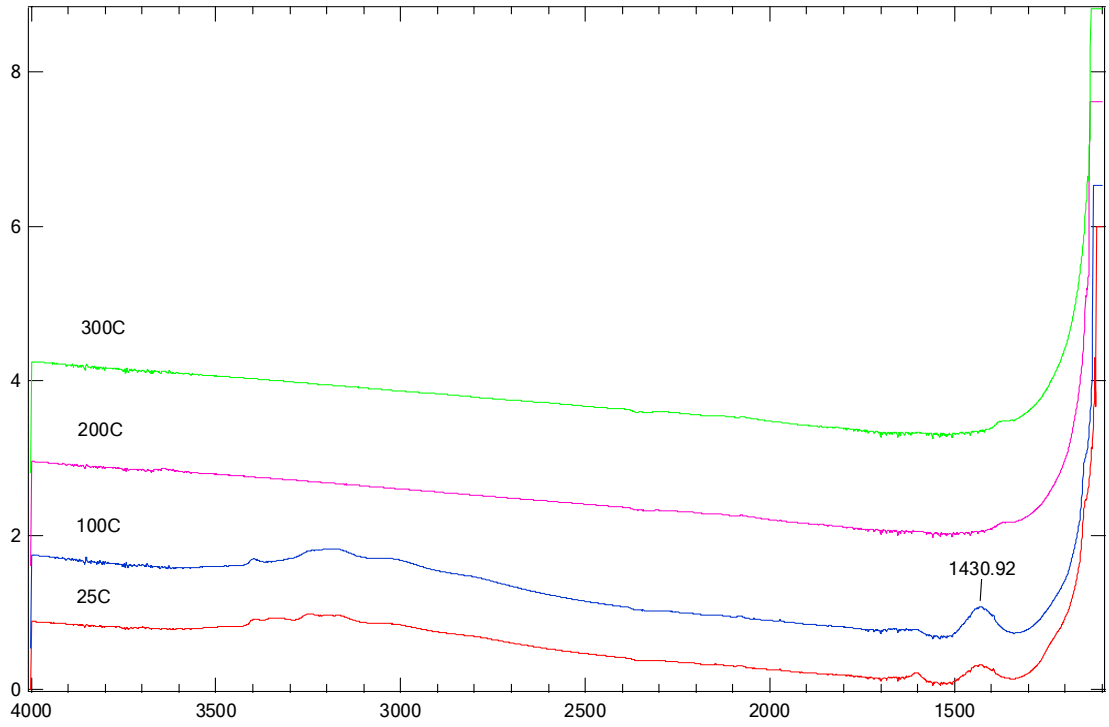

ere

Figure 8. NO adsorption at different temperatures.

Figure 7. NH_3 adsorption at different temperatures.

NO adsorption at different temperatures

NO adsorption experiments were conducted at 25°C with and without oxygen (about 5%) using a gas containing 100 ppm NO in N_2; additional experiments were conducted without oxygen (gas composition otherwise the same) at 100-380°C. A 5 wt% vanadia catalyst which had been sulfated for 24 hours under dry conditions was used in this experiments. Gas flow was 32 sccm; catalyst sample size was 0.1 g.

With or without oxygen present, no NO adsorption (1615 cm-1 in IR spectra) was observed at room temperature. Since there was no difference, only one spectrum is shown in Figure 8.

Based on our results, NO apparently adsorbs on reduced vanadia surfaces but does not adsorb on fully oxidized vanadia surfaces. It is reported that NO adsorption is usually negligible at reaction temperatures, particularly in the presence of NH_3.

NO does not adsorb on NH_3-preadsorbed surfaces--- probably because all the available VO_x sites have been occupied by NH_3. In our test, an ammonia adsorption peak is still apparently observed during NO adsorption at RT, which indicates that some ammonia remained on the catalyst surface, although surface vanadia species could have been reduced by ammonia [Busca et al., 1998]. The most believable mechanistic schemes involve gas phase NO reacting with adsorbed NH_3. Thus, NO adsorption would not be predicted on a catalyst pretreated with ammonia.

Mass Spectrometer Troubleshooting

Sample Flow Control

Samples are introduced to the mass spectrometer through a capillary tube. Previously, the total flow rate introduced to the MS was 50 sccm; however, recently this flow decreased, indicating that the flow to MS was hindered somehow. This problem was thought to be due to either a decrease in the capacity of the rotary pump or an increase in pressure drop caused by plugging of the capillary tube.

To address this problem, the rotary pump oil was changed and the capillary tube was cleaned with acetone and 3% HCl. Each of these measures increased the total flow rate into the MS and the current flow rate is sufficient.

Delay of MS response

A delay in the MS response was observed (see Figure 9) due to the installation of a 3-way valve at the inlet to the MS (flow configuration shown in Figure 10), which caused all of the flowing gas to enter the MS capillary and build up pressure. This problem was resolved by replacing the two 3-way valves shown immediately before and after the reactor in Figure 10 with tees, and installing a single 3-way valve at the MS inlet (see Figure 11). This scenario allows excess flow to proceed to the vent, while sampling a small portion of the inlet (or outlet) stream. The resulting improvement in response time can be seen in Figure 12.

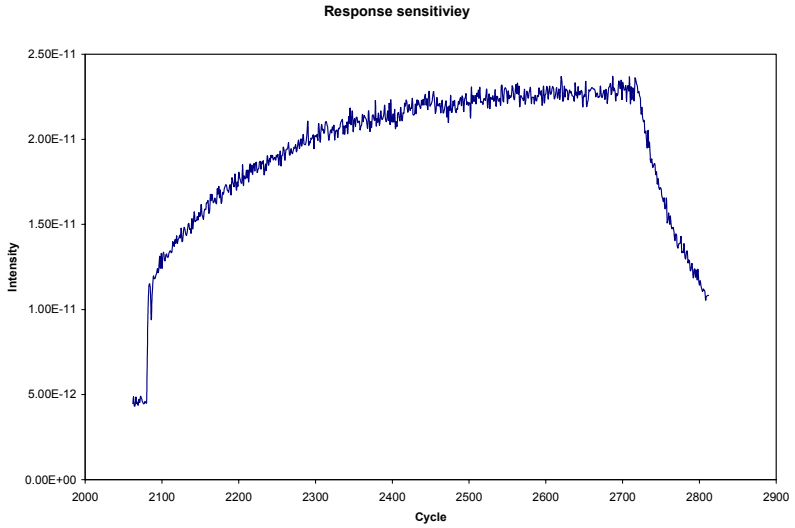

Figure 9. Response delay with valve set up.

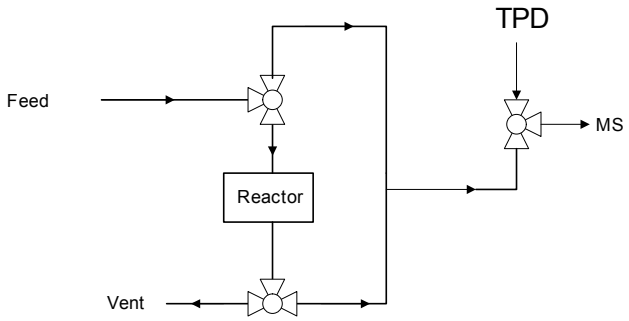

Figure 10. Old 3-way valve configuration.

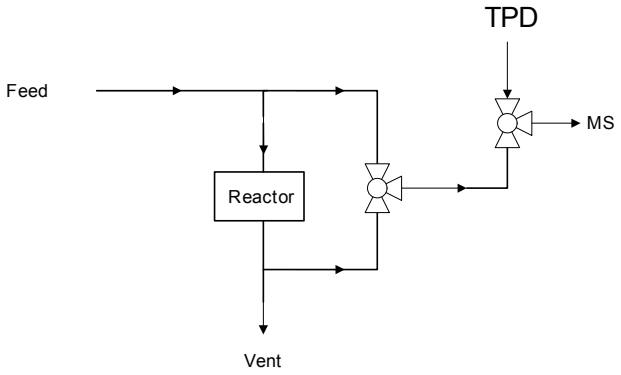

Figure 11. New 3-way valve configuration.

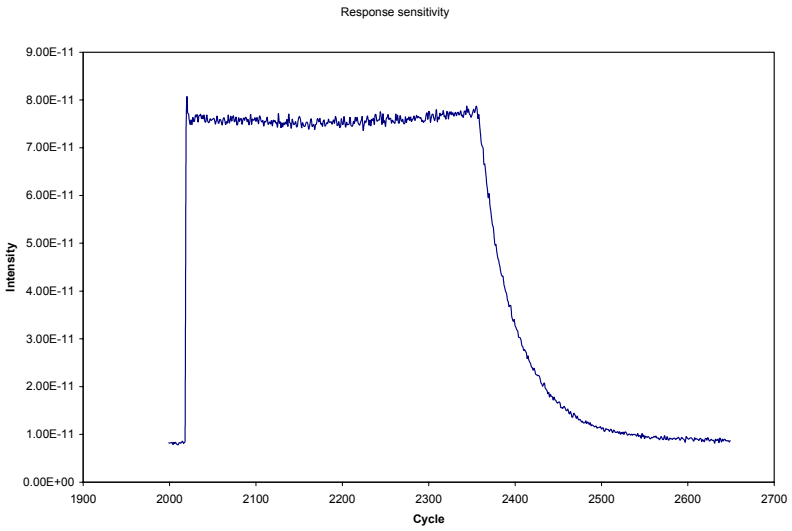

Figure 12. Instantaneous MS response with Tee set up.

Sequencer set up

A sequencer was configured for MS sampling, which allows a code written for the MF software to be used to automatically select either the FTIR inlet or outlet stream for analysis. Figure 13 shows the location of the FTIR cell (Reactor) and the solenoid valves that perform the sampling selection. This new flow system does not increase sample delay times as discussed above.

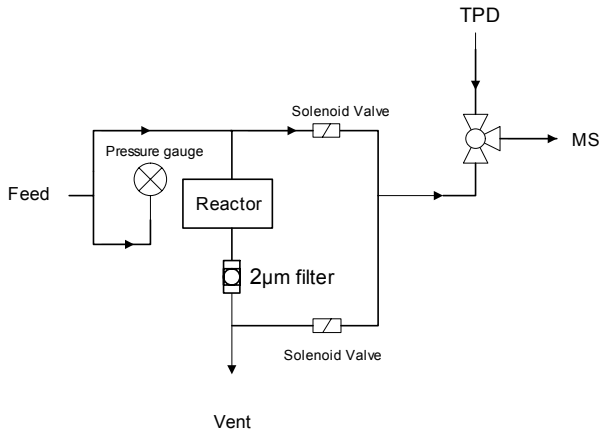

Figure 13. Sequencer set up

CCS Overview

The catalyst characterization system (CCS) provides capabilities for long-term catalyst exposure tests required for ascertaining deactivation rates and mechanisms and a characterization facility for samples from the slipstream reactor to determine changes in reactivity and responses to well-controlled environments. This system simulates industrial flows by providing a test gas with the following compositions: NO, 0.10%; NH_3, 0.1%; SO_2, 0.1%; O_2, 2%; H_2O, 10%; and He, 87.7%. Both custom and commercial catalysts are tested as fresh samples and after a variety of laboratory and field exposures under steady conditions.

The purpose of the CCS is to quantitatively determine deactivation mechanisms by measuring specific, intrinsic catalyst reactivity of custom (laboratory) and commercial catalysts under a variety of conditions. These catalysts will be impregnated with a variety of contaminants, including Ca, Na, and K. In addition, the CCS will characterize samples of catalyst from slipstream field tests to determine similar data and changes in characteristics with exposure. Advanced surface and composition analyses will be used to determine composition, pore size distribution, surface area, and surface properties (acidity, extent of sulfation, etc.).

Catalyst packing

The method of catalyst sample loading has been improved. The previous catalyst loading technique consisted of placing glass wool inside the 3/8” reactor tube; pouring a small amount (around 0.1 to 0.4 grams) of catalyst through the tube on top of the glass wool; placing additional glass wool on top of the catalyst; and finally inserting the thermocouple into the reactor. With such a small amount of catalyst, it was found that the powder did not lay flat on the glass wool, resulting in non-uniform flow across the catalyst bed. Furthermore, it was determined that the thermocouple was unlikely to reside inside the catalyst bed, but rather leaned against the side of the reactor tube, giving an inaccurate catalyst temperature reading.

An improved method for catalyst packing was devised to remedy these two concerns. A stainless steel frit was placed on top of a stainless steel split ring that was press-fit inside the reactor tube (Figure 14). This design allows powdered catalyst to lie flat (i.e. more uniform) on the split ring and frit, and further guarantees that the thermocouple will be in the correct vertical position, just touching the top of the catalyst. To prevent the thermocouple from touching the reactor wall, spacers that slide on the thermocouple tip (not shown in Figure 14) are used to direct the thermocouple tip toward the center of the reactor tube.

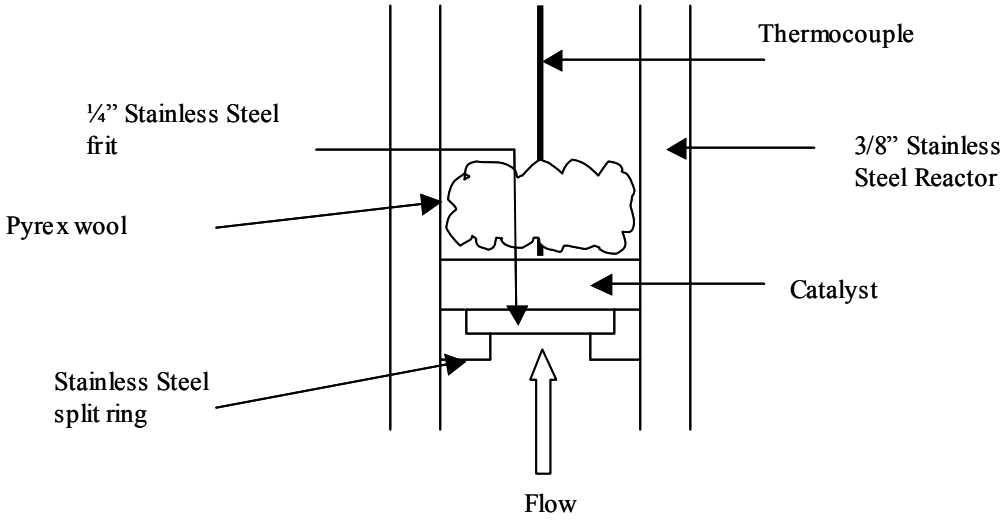

Figure 14. Improved catalyst packing method.

Water bubbler floats

The water levels inside each of the four bubblers is indicated by floats, which are attached to a small capillary tube that can be observed to rise and fall with the water level. It was discovered that the original floats, which consisted of polyethylene tubes sealed at the ends with epoxy, had lost their buoyancy. It turns out that the epoxy seals did not hold, but instead had leaked water inside the tubing. To solve this problem, new floats were constructed out of glass tubes, sealed by a glassblower on each end (Figure 15). These floats will not leak water, nor will they release any volatile plasticizers into the bubbler (which could ultimately poison the downstream catalyst).

Water condenser

The previous water condenser, consisting of a 250 cm^3 stainless steel vessel submerged in ice water, was found to be ineffective. To improve this design, one-meter of 1/8" OD stainless steel tubing was coiled 17 times and attached to the top of the container (see Figure 16).

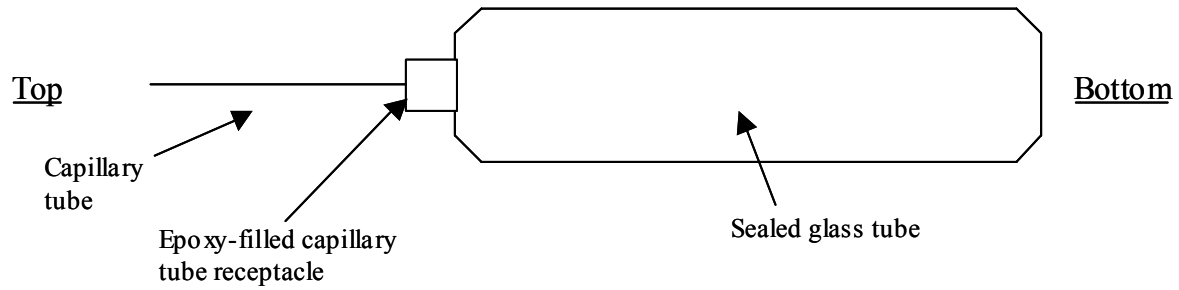

Figure 15. Glass Float for Bubbler.

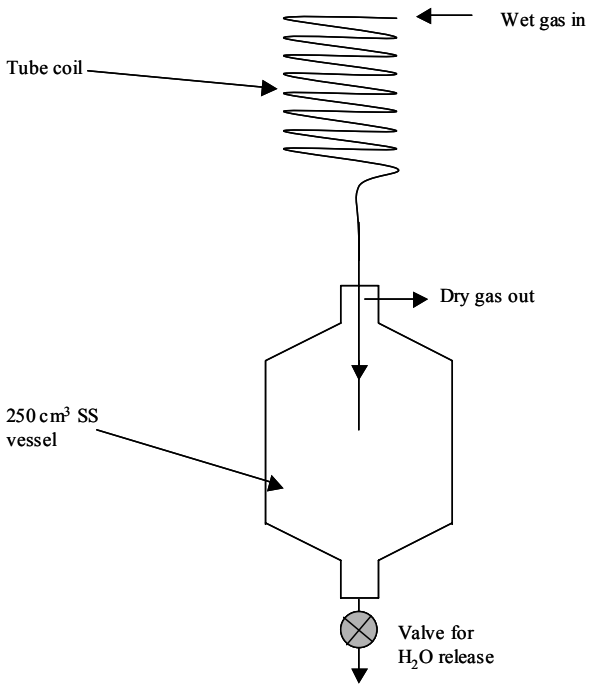

Figure 16. Condenser for water knockout.

Gas analyzers

NH_3/SO_2 Analyzer

Delay times

Several tests were performed in order to determine the effect of delay time that results from extended lengths of tubing and various dead volumes that exist in the reactor system. Figure 17 is a simplified version of the flow system that was used to perform these tests. Note the letters "*a"*, "*b"*, and "*c"* in boxes. Hereafter, "*a"* is referred to as "reactor bypass", "*b"* as "whole system", and"*c"* as "analyzer inlet tube."

Also note that there are three mass flow controllers (MFC's) shown in the figure; these were used to control the flow of the gases whose delay times are of interest. MFC 3 (calibrated for 0-300 sccm of 0.75% NO) was used for helium (purge) flow, MFC 4 (calibrated for 1% NH_3) was used with 914 ppm NH_3, and MFC 5 (calibrated for 3% SO_2) was used with 940 ppm SO_2. These tests were performed at nominal flows of 200 sccm, as this flow rate is around what is expected for powdered samples.

Table 2 displays a summary of the results obtained. Note that in all cases, ammonia delay times are significantly larger than SO_2 delay times, indicative of either NH_3 adsorption on the stainless steel tubing or possibly a greater lag in the analyzer ammonia channel response. Either way, the NH_3 delay times should be utilized in order to determine valve-switching and data-logging times.

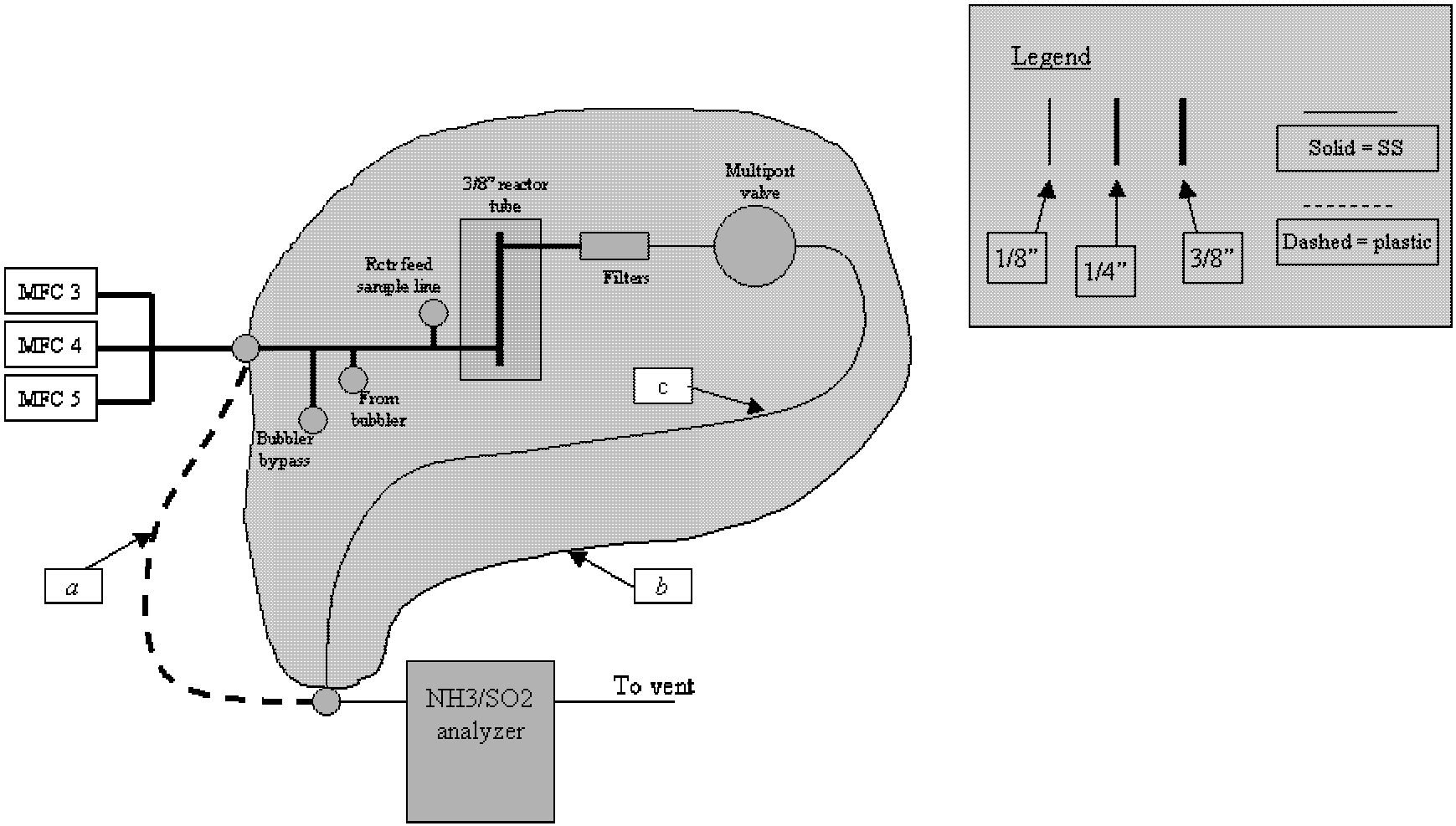

Figure 17. Schematic of flow paths for NH_3 and SO_2 delay times analyses. "*a*" = "reactor bypass", "*b*" (shaded area) = "whole system", and "*c*" = "analyzer inlet tube."

Table 2. Delay times (seconds) for analyzer to reach 90, 95, or 99 % of cylinder concentration at 200 sccm flow. Note that these gases are dry and that times are approximate.

	Reactor Bypass		Whole System		Analyzer Inlet Tube	
Gas	**Zero to Max**	**Max to Zero**	**Zero to Max**	**Max to Zero**	**Zero to Max**	**Max to Zero**
NH_3 (max = 914 ppm)	t_{90} = 17 t_{95} = 21 t_{99} = 70	t_{90} = 18 t_{95} = 26 t_{99} = 182	t_{90} = 40 t_{95} = 50 t_{99} = 100	t_{90} = 48 t_{95} = 81 t_{99} = 437	t_{90} = 11 t_{95} = 13 t_{99} = 18	t_{90} = 9 t_{95} = 12 t_{99} = 35
SO_2 (max = 940 ppm)	t_{90} = 12 t_{95} = 13 t_{99} = 26	t_{90} = 10 t_{95} = 12 t_{99} = 20	t_{90} = 28 t_{95} = 34 t_{99} = NA[1]	t_{90} = 29 t_{95} = 34 t_{99} = 54	t_{90} = N/A[2] t_{95} = N/A t_{99} = N/A	t_{90} = N/A t_{95} = N/A t_{99} = N/A

1. The value obtained, 350 seconds, is assumed to result from an unequilibrated upstream line and is not considered valid.
2. Analyzer inlet tube delay times for SO_2 were not determined since in all previous cases, SO_2 has a faster response time than NH_3, the limiting species.

Flow rate effects

It has been observed that the flow rate to the NH_3/SO_2 analyzer significantly affects the registered NH_3/SO_2 concentration. This is due to several factors. According to the manual, the analyzer's detectors (UV/VIS) are designed to be operated at flow rates between 0.2 – 1.5 L/min *at pressures less than 0.15 kPa (1.48 x 10^{-3} atm or 0.0218 psi).* This corresponds to a vacuum of about 25 in. Hg relative to ambient pressure. However, at present we are operating at near ambient pressure.

Thus, drifts in concentration and other quirks observed in the past can be attributed to analyzer pressure sensitivity (and a leaky valve that was removed), as we have been operating significantly outside of its specs. A vacuum pump downstream of the analyzer could be used to obtain the correct pressure inside the analyzer; however this measure would greatly complicate the flow system since water vapor is present in the line at high concentrations and the NO_x analyzer and gas chromatograph are downstream from the NH_3/SO_2 analyzer.

Fortunately, correlations relating flow to analyzer readout can be used to adjust for the pressure (i.e. flow rate) effects without using a vacuum pump, provided that the concentration/flow rate relationship behaves according to Figure 18. This figure illustrates four hypothetical gases that are 800, 900, 1000, or 1100 ppm in NH_3 (or SO_2). In order to utilize such correlations for analyzer readout, two important criteria must be met:

1. The relationship between concentration and flow rate is linear.

2. The lines are parallel.

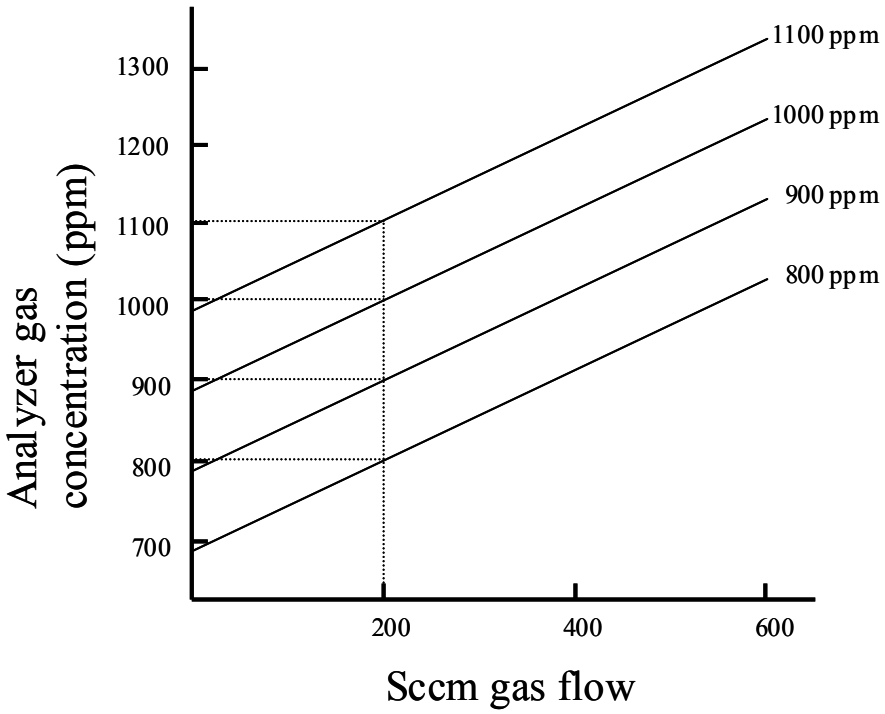

Figure 18. Illustration of flow rate/registered gas concentration relationship.

Tests were performed by varying calibration gas flow rates (914 ppm NH_3, 940 ppm SO_2) from 0-1200 sccm. The results indicate the flow rate-readout relationships can indeed be represented by a straight line with only minor deviations. Graphs of residuals versus fitted data show that a linear model gives NH_3 residuals ranging from ±6 ppm, while SO_2 residuals are within ±4—both less than 1% of 900 ppm, and about 1.5% of 400 ppm (slipstream conditions). Due to spread in data taken to formulate calibration curves, somewhat greater uncertainty in actual concentration is expected, probably not to exceed a few percent (i.e. 3-4%) of actual full-scale.

If the lines in Figure 18 are parallel, the concentration-flow relationship is concentration-independent; that is, the slope of the line is independent of the actual concentration of gas fed to the instrument. This assumption cannot be tested because there is only one certified cylinder for each calibration gas (SO_2 and NH_3) that falls within the analyzer's range, so it will be assumed that this criterion is met.

Thus, a linear function can be used to estimate the actual concentration in the following manner: Eq. (1) is the general linear equation relating observed analyzer ppm (ppm_{obs}) to the flow rate (*flow*), with *m* and *b* being, respectively, the slope and intercept. Eq. (2) is similar to Eq. (1), except that it identifies what the *actual* ppm (ppm_{act}) of the gas is since it is reported at the calibration flowrate value, $flow_{cal}$. Subtracting Eq. (1) from Eq. (2) and rearranging gives Eq. (3).

$$ppm_{obs} = m \cdot flow + b \qquad (1)$$

$$ppm_{act} = m \cdot flow_{cal} + b \quad (2)$$

$$ppm_{act} = ppm_{obs} + m \cdot (flow_{cal} - flow) \quad (3)$$

The slope of a flow rate-concentration calibration line (*m*), the calibration flow rate ($flow_{cal}$), and the process flow rate (*flow*) are three parameters needed in order to convert any observed NH_3/SO_2 analyzer readout to actual concentration. Values for *flow* and $flow_{cal}$ are easily computed from mass flow controller set points (and/or readouts). This may become tricky if water vapor is introduced.

NO_x Analyzer

There are two identical NO_x analyzers. One had been in the repair shop because it had a burned out converter heater. Recently, the heater in the other unit, installed in our reactor system burned out. Fortunately, the recently repaired unit has proved to be a satisfactory replacement, thus far.

Flow rate dependencies are not observed in the case of the NO_x analyzer since it draws in only 15-20 sccm of sample gas from a tee in the sample line, regardless of the inlet flow rate, while the rest of the gas flows to vent. In the near future, a portion of the flow to vent will be sent to a chromatograph for analysis of N_2. Since the NO_x analyzer also requires about 175 sccm of dry air from the room for the converter, air is dried by passing it through a canister containing Drierite. In order to measure total NO_x, NO_2 is converted to NO, the gas that the analyzer can detect, by heating the gas sample to around 625 °C. The transformation of NO_2 to NO takes place inside the converter in a stainless steel reactor tube heated to about 625 °C.

Tests exploring the delay times of gases introduced into the NO_x analyzer are currently being performed.

Mass flow controllers

MFC calibrations

One task in the reactor shakedown has been to check the mass flow controllers' performance to ensure that calibrations done at the factory were (still) valid and that the space velocities used to compute catalyst activity were correct. Several significant errors, which can explain quirks observed in the laboratory, were discovered. Mass flow controller flow rates were determined with a Gilian™ Gilibrator, which is a device that measures the time required for a bubble, driven upward by gas flow, to rise inside a glass column of known volume. Room temperature and ambient pressure were then used to convert the observed flow rate to standard conditions, and this value was compared against the predicted MFC flow rate under standard conditions.

Several mass flow controllers showed significant and consistent errors ranging anywhere from minus 8% to plus 40%! These errors explain observed discrepancies between gas concentration setpoint and actual value. For example, the analyzer NO concentration readout was significantly higher than it should have been—a result of the NO MFC's being off by 40%! Fortunately, large deviations like this can be fixed by adjusting the MFC control circuit according to the manufacturer's calibration procedure.

The calibration procedure entails connecting the Gilibrator to the outlet of the MFC and then adjusting the zero, span, and linearity potentiometers at various flow rates. Experience has shown that the mass flow controllers are accurate to within around ± 1-2% after calibration, which is close to the manufacturer's specification of ±1%. Deviations in flow rate may be exacerbated by plugging of mass flow controllers (see below).

MFC inconsistencies

Tests were performed in order to determine the differences in the flow rates of mass flow controllers 7-14, which are connected according to Figure 19. The purpose of the tests was to quantify the uncontrollable inconsistencies in MFC flow rates. Ideally, each group of four MFC's (7–10 and 11-14) would give *exactly* the same flow rates into each reactor, but in practice this is not so. Since two MFC's connected in parallel feed each reactor (Figure 19), it is important to observe the maximum deviations in MFC's performance and do several tests with catalysts to observe the effect that the deviations in flow rate have on the observed conversion/catalyst activity. This is important to do in order to compare activity of different catalysts placed in different reactors—it is imperative to substantiate that observed differences in activity are due to the catalyst, not the reactor.

Each MFC was run at 0, 20, 40, 60, 80, and 100% of max flow (MFC 7-10 max = 200 sccm; MFC 11-14 max 500 sccm). Five data points at each set point were taken each day, and the data were taken on two days to see how time might affect response (repeatability). Multiple data points allow for the use of statistical methods to compare means with appropriate confidence intervals.

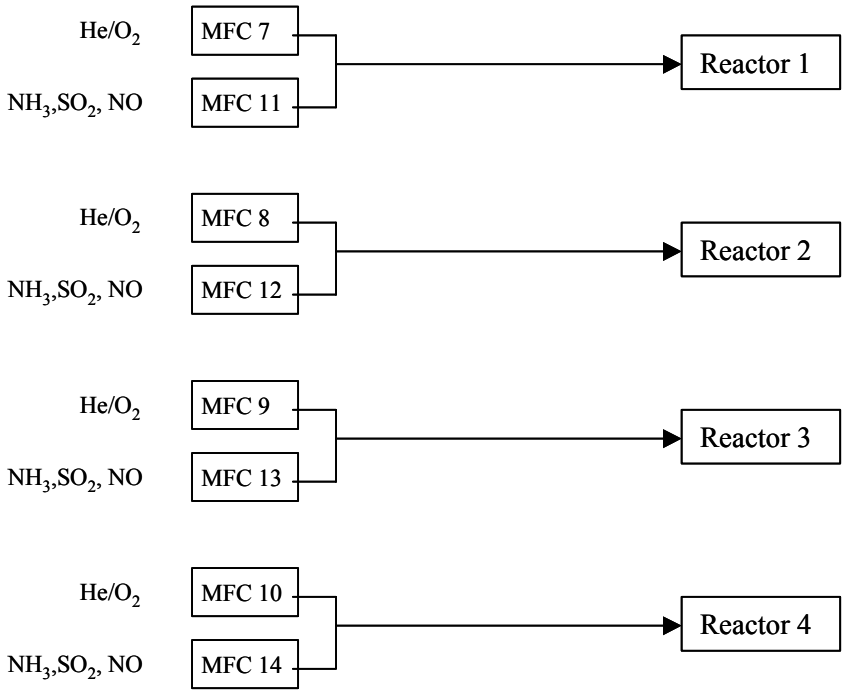

Figure 19. Simplified schematic of reactor feed mass flow controller layout.

The data were analyzed using Minitab, a statistical computer package. Analysis of variance (ANOVA) statistical tools were used to compare the observed averages and standard deviations

in order to determine if there is evidence of variation in flow rates between similar mass flow controllers. In all cases, the p-value for the ANOVA tests was <0.0005, indicating with considerable certainty that the flow rates do indeed differ.

This having been established, pair-wise comparisons were made for each percent set point on each date to quantify the difference in mass flow controller flow rates (for 4 MFC's there are a total of 6 pair-wise comparisons to be made). These comparisons were made based on the Tukey family-wise comparisons method. This procedure was performed with a family-wise confidence of 95%, meaning that the results report the true difference in means of *all* comparisons 95% of the time. This turns out to be a 98.9% confidence for each pair-wise comparison, indicating that given a single pair of means, 98.9% of the time, the true difference in their values lies within the selected confidence interval.

Because there were so many comparisons to be made and given the fact that the worst-case scenarios are of greatest interest, the maximum differences in mean flow rates (largest MFC flow rate – smallest MFC flow rate) at each percent set point were gathered. These results are reported in Table 3, Table 4, and Table 5. Table 3 shows the largest observed differences at each percent set point in sccm. Table 4 displays the sccm differences reported in Table 3 as percentages relative to the "Set point" column, while Table 5 shows the differences as percentages relative to full-scale.

Table 3. MFC comparison data: flowrates reported as standard cm^3/min.

Date	Comparison	% flow	Set point	Largest diff. in means	Low diff. @ 98.9% conf.	Hi diff. @ 98.9% conf.	Pair (larger flow listed first)
June 27, 2003	MFC 7-10	20%	100	0.84	0.50	1.19	(7 or 10) and 9
		40%	200	1.70	1.29	2.11	8 and 9
		60%	300	2.64	2.08	3.20	8 and 9
		80%	400	3.53	2.54	4.53	8 and 9
		100%	500	5.83	5.16	6.50	7 and 9
June 30, 2003	MFC 7-10	20%	100	0.84	0.69	0.99	10 and 9
		40%	200	1.00	0.53	1.47	8 and 9
		60%	300	1.53	0.92	2.14	8 and 9
		80%	400	3.11	1.71	4.51	8 and 9
		100%	500	4.74	3.80	5.67	8 and 9
June 27, 2003	MFC 11-14	20%	40	1.17	0.78	1.57	13 and 12
		40%	80	1.70	0.99	2.41	13 and 11
		60%	120	2.30	1.51	3.09	13 and 11
		80%	160	3.49	2.77	4.20	13 and 11
		100%	200	4.39	2.58	6.21	13 and 11
June 30, 2003	MFC 11-14	20%	40	1.16	0.62	1.71	13 and 12
		40%	80	1.45	0.65	2.26	13 and 14
		60%	120	2.31	1.06	3.57	13 and 11
		80%	160	4.19	2.85	5.53	13 and 11
		100%	200	5.58	3.47	7.69	13 and 11

Table 4. MFC comparison data: differences reported as percent of set point.

Date	Comparison	% flow	Set point	Largest diff. in means	Low diff. @ 98.9% conf.	Hi diff. @ 98.9% conf.	Pair (larger flow listed first)
June 27, 2003	MFC 7-10	20%	100	0.84%	0.50%	1.19%	(7 or 10) and 9
		40%	200	0.85%	0.65%	1.06%	8 and 9
		60%	300	0.88%	0.69%	1.07%	8 and 9
		80%	400	0.88%	0.63%	1.13%	8 and 9
		100%	500	1.17%	1.03%	1.30%	7 and 9
June 30, 2003	MFC 7-10	20%	100	0.84%	0.69%	0.99%	10 and 9
		40%	200	0.50%	0.27%	0.73%	8 and 9
		60%	300	0.51%	0.31%	0.71%	8 and 9
		80%	400	0.78%	0.43%	1.13%	8 and 9
		100%	500	0.95%	0.76%	1.13%	8 and 9
June 27, 2003	MFC 11-14	20%	40	2.93%	1.94%	3.93%	13 and 12
		40%	80	2.13%	1.24%	3.02%	13 and 11
		60%	120	1.91%	1.25%	2.57%	13 and 11
		80%	160	2.18%	1.73%	2.63%	13 and 11
		100%	200	2.20%	1.29%	3.10%	13 and 11
June 30, 2003	MFC 11-14	20%	40	2.91%	1.55%	4.27%	13 and 12
		40%	80	1.82%	0.81%	2.83%	13 and 14
		60%	120	1.93%	0.88%	2.98%	13 and 11
		80%	160	2.62%	1.78%	3.46%	13 and 11
		100%	200	2.79%	1.73%	3.85%	13 and 11

Table 5. MFC comparison data: differences reported as percent of full-scale.

Date	Comparison	% flow	Setpoint	Largest diff. in means	Low diff. @ 98.9% conf.	Hi diff. @ 98.9% conf.	Pair (larger flow listed first)
June 27, 2003	MFC 7-10	20%	100.00	0.17%	0.10%	0.24%	(7 or 10) and 9
		40%	200.00	0.34%	0.26%	0.42%	8 and 9
		60%	300.00	0.53%	0.42%	0.64%	8 and 9
		80%	400.00	0.71%	0.51%	0.91%	8 and 9
		100%	500.00	1.17%	1.03%	1.30%	7 and 9
June 30, 2003	MFC 7-10	20%	100.00	0.17%	0.14%	0.20%	10 and 9
		40%	200.00	0.20%	0.11%	0.29%	8 and 9
		60%	300.00	0.31%	0.18%	0.43%	8 and 9
		80%	400.00	0.62%	0.34%	0.90%	8 and 9
		100%	500.00	0.95%	0.76%	1.13%	8 and 9
June 27, 2003	MFC 11-14	20%	40.00	0.59%	0.39%	0.79%	13 and 12
		40%	80.00	0.85%	0.50%	1.21%	13 and 11
		60%	120.00	1.15%	0.75%	1.54%	13 and 11
		80%	160.00	1.74%	1.39%	2.10%	13 and 11
		100%	200.00	2.20%	1.29%	3.10%	13 and 11
June 30, 2003	MFC 11-14	20%	40.00	0.58%	0.31%	0.85%	13 and 12
		40%	80.00	0.73%	0.32%	1.13%	13 and 14
		60%	120.00	1.16%	0.53%	1.79%	13 and 11
		80%	160.00	2.09%	1.42%	2.77%	13 and 11
		100%	200.00	2.79%	1.73%	3.85%	13 and 11

Table 5 is most informative because it contains the values in terms of percent of full-scale flow—the same type of values that the manual mass flow control equipment uses. If it can be assumed that the differences in future MFC performance will be similar to the results given in Table 5, then an experiment can be designed that will quantify the differences in conversion that such MFC deviations would produce. Specifically, the following two questions are of interest: 1) What is the greatest possible discrepancy in MFC flow rates under typical operating conditions? 2) What effect does the discrepancy have on observed catalyst performance?

MFC plugging

We have a concern regarding MFC's 11-14. In the past when the reactor system has been run with process gases, it has been observed that some of these MFC's behave as if they are becoming plugged. Fortunately, after periods of non-use, the MFC's have performed satisfactorily. Perhaps whatever may be inhibiting their performance is volatile and disappears, or maybe another problem (such as inconsistent upstream pressure) may be responsible. Although the exact cause of this behavior has not been determined, it is thought likely to be due to reactions between the $NO/SO_2/NH_3$ mixture that may form ammonium nitrate and/or ammonium sulfate compounds. Dana Overacker (Department of Chemical Engineering, University of Utah) has mentioned that he has experienced such plugging issues.

If ammonium sulfate or ammonium nitrate is the culprit of MFC plugging, MFC's 11-14 may show deviations in flow performance that exceed those in this report. The MFC manufacturer has been contacted and has provided instructions for cleaning/maintenance to deal with this problem.

Operating procedures

A complete Safe Operating Procedure (SOP) had not been previously written for the laboratory equipment in use. Since the last QPR, progress on this document has been made. Procedures for changing gas cylinders with the laboratory's gas manifold system have been written. Calibration procedures for gas analyzers have also been produced. These documents mark the beginning of a SOP, which will be completed as time allows.

Monolith catalysts

Physical Dimensions

One of our objectives is to test monolith and plate catalysts obtained from vendors or prepared in our laboratory. Physical dimensions of the catalyst samples from vendors and BYU were measured as accurately as possible with calipers and a tape measure. A summary of this information is contained in Table 6. Table 7 presents other geometric properties of the catalyst, including area open to flow, total cross sectional areas, total geometric surface area available to reaction, and total volume available to gas flow. In the case of Monolith 3, the calculations reported are approximate because of the irregularity of the shape of its channels. Figures 20 through 32 show details of the catalysts.

Table 6. Physical dimensions of the six catalyst samples under investigation.

Catalyst	Length (in/cm)	Width 1 (in/cm)	Width 2 (in/cm)	Cell width (in/mm)[1]	Wall Thickness (in/mm)[1]	Pitch (in/mm)[1]
M1	19.75/50.17	2.09/5.32	2.063/5.24	0.24/6.2	0.047/1.2	0.29/7.4
M2	21.63/54.93 (BYU = 20.25/51.4)[2]	2.0/5.08	2.0/5.08	0.25/6.3	0.030/0.77	0.28/7.07
M3	19.31/49.054	2.13/5.40	2.13/5.40	NA	~1mm flat piece, ~0.9mm curved	NA
M3 stainless case	20.06/50.96	2.25/5.72	2.25/5.72	NA	~1mm thick	NA
M4 (BYU)	6.0/15.24 (x4 = 24.0/60.96)[3]	2.0/5.08 (1.82/4.62 for 7x7 cell cross-section)[4]	2.0/5.08 (1.82/4.62 for 7x7 cell cross-section)[4]	0.20/5.0	0.055/1.4	0.25/6.4
P1	21.5/54.615 (BYU = 19.75/50.2)[2]	3.875/9.84	NA	NA	0.039/01.0	0.2231/5.667
P2	19.75/50.17[5] (BYU = 18.75/47.6)[2]	4.375/11.11	NA	NA	0.035/0.90	0.2231/5.667

Table 7. Exterior surface area and open flow area information for catalysts in the slipstream reactor.

Catalyst	Total Cells	Single-cell Open Area (in^2/cm^2)	Total Open Area (in^2/cm^2)	Total Frontal Area (in^2/cm^2)	% Open Frontal Area	Total surface area for reaction[6] (in^2/cm^2)	Total open volume[6] (in^3/cm^3)
M1	49	0.0596/0.384	2.92/18.84	4.32/27.9	67.61	995/6096	57.7/945
M2	49	0.0615/0.397	3.01/19.45	4.0/25.8	75.36	1051/6782	65.2/1068
M3	~45	~0.070/~0.45	~3.1/~20	4.52/29.1	~70	~925/~5970	~61/~993
M4 (BYU)	49 or 64	0.0388/0.250	49: 1.90/12.25 64: 2.48/16.0	49: 3.31/21.3 64: 4.29/27.7	49: 57.4 64: 57.8	49: 231/1493-6" 926/5974-24" 64: 302/1951-6" 1209/7803-24"	49: 11.4/187-6" 45.6/747-24" 64: 14.9/244-6" 59.5/975-24"
P1	21[7]	NA	14.86/95.87	17.81/114.92	83.42	6450/41613	639/10470[8]
P2	21[7]	NA	17.18/110.81	20.19/130.24	85.08	6715/43323	678/11118[8]

1 Note: metric measurements are more accurate than inches on cell width, wall thickness, and pitch.
2 In order to test methods of cutting catalysts, these fresh catalyst samples were cut at BYU and the lengths reported next to this footnote subscript are the cut lengths.
3 Four 6-inch M4 catalysts are placed in series in the slipstream reactor, making 24" total length.
4 See Monolith 4 section below.
5 Because two plate sections are installed in series, twice the plate length (2*21.5" = 43.0" for P1 and 2*19.75" = 39.50" for P2) should be used in calculating space velocities.
6 Total surface areas and volumes for monolith catalysts are ¼ what they are for the entire catalyst in the reactor since there are four monolith pieces in the slipstream reactor (see Figure 33).
7 Nineteen cells of one equal size are between the plates and two of another equal size on either side of the end plates between the plates and the chamber wall.
8 Important note: the volumes reported for the plate catalysts include only the volume where there is catalyst material, not the dead volume between the top and bottom sections of catalyst.

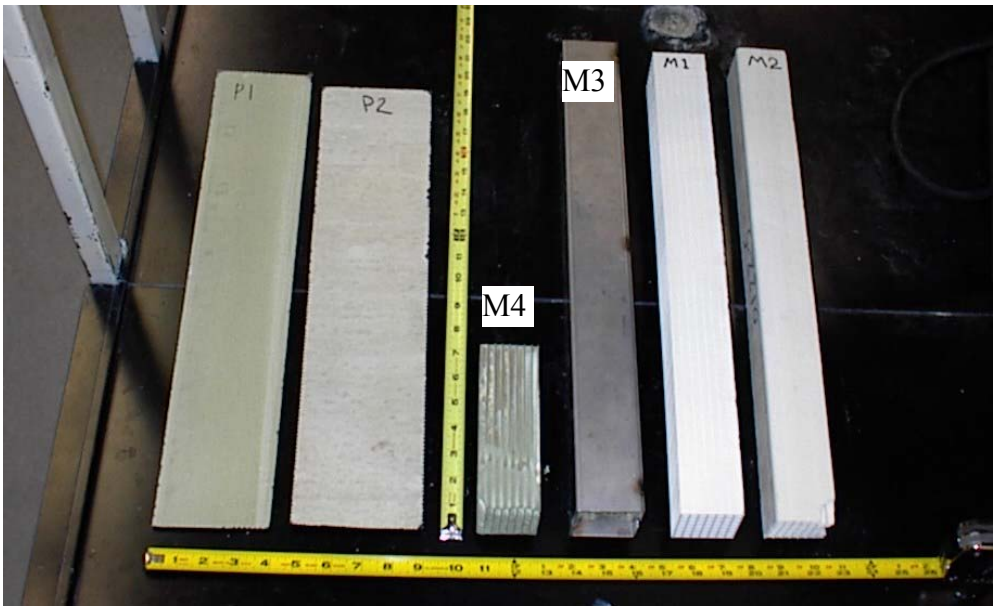

Figure 20. Photograph showing all six catalyst samples alongside one another [order from left to right = P1, P2, M4 (BYU), M3 (SS-encased), M1, M2].

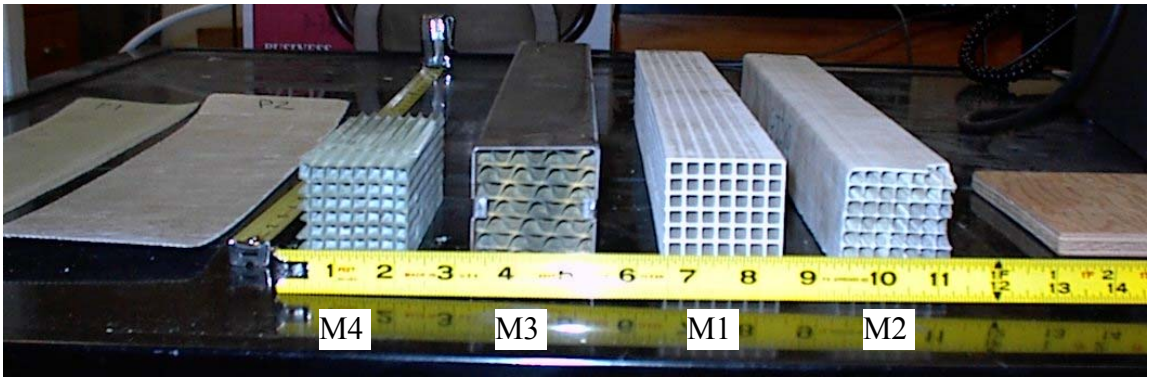

Figure 21. Photograph showing all six catalyst sample faces [order from left to right = P1, P2, M4 (BYU), M3 (SS-encased), M1, M2].

Monolith 1

Extruded monolith. The wall pitch is the thicker of the two square commercial monoliths, and is thus the more robust of the two commercial square-channel monoliths.

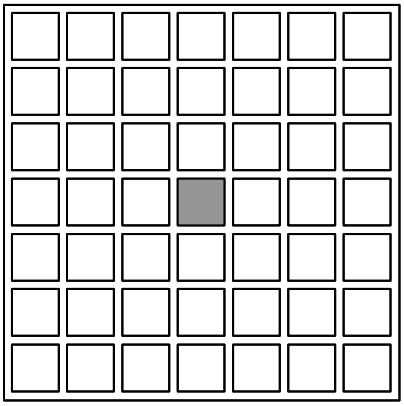

Figure 22. To-scale schematic of Monolith 1.

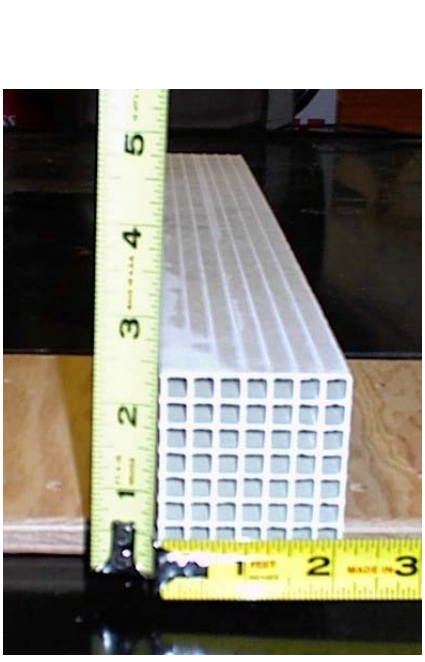
a.

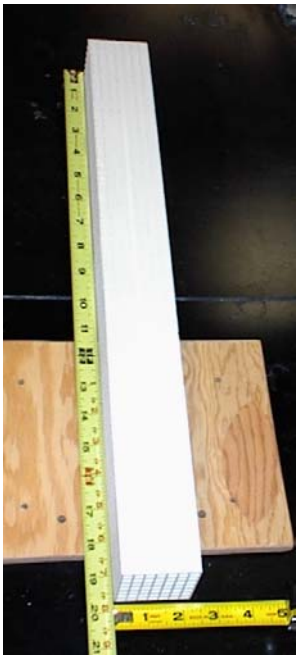
b.

Figure 23. Photos of (a) the face and (b) the length of Monolith 1.

Monolith 2

Extruded monolith. The wall pitch is thinner than Monolith 1, while the channel width is essentially the same.

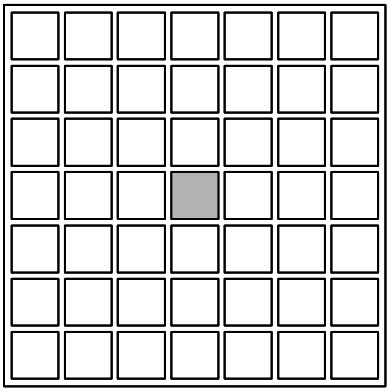

Figure 24. To-scale schematic of Monolith 2.

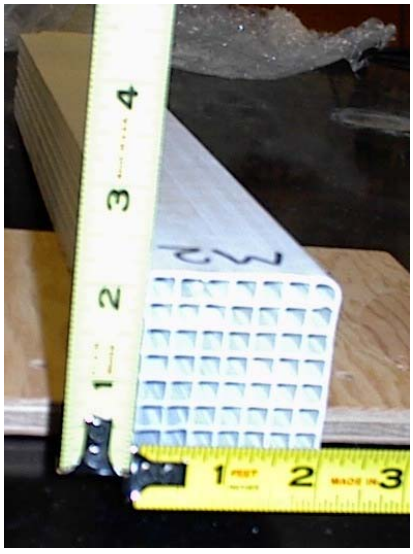
a.


b.

Figure 25. Photos of (a) the face and (b) the length of Monolith 2.

Monolith 3

Placed inside a rectangular stainless steel jacket, the catalyst consists of a stiffened cardboard-like material that alternates between corrugated and flat layers (See Figure 26).

Distance between "peaks" of corrugated part (i.e. wavelength): 15.0 mm (0.59 in)

Distance between flat layers (i.e. amplitude): ~7.5 mm (0.30 in)

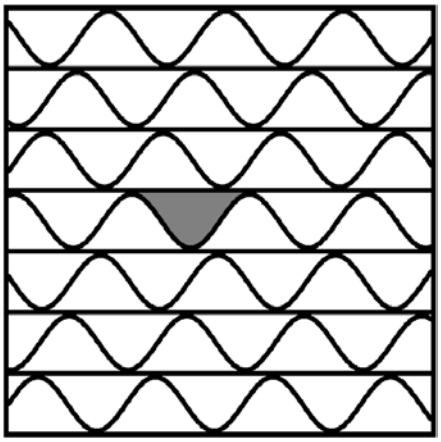

Figure 26. To-scale schematic of Monolith 3.

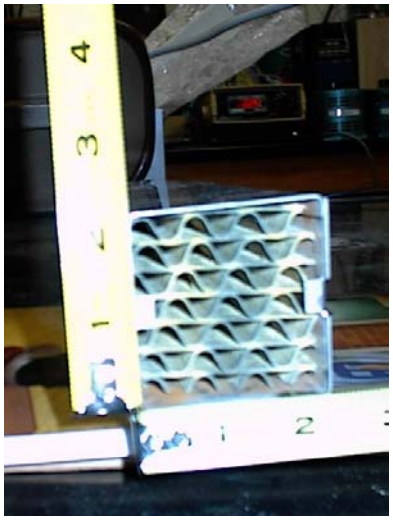
a.
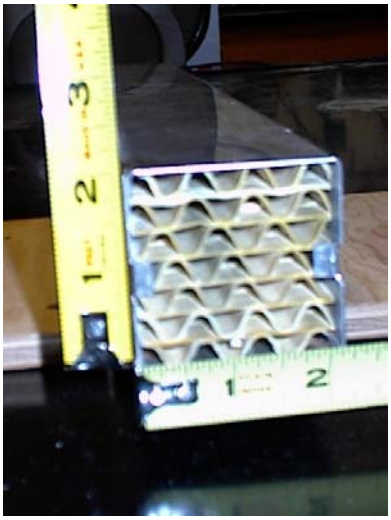
b.

c.

Figure 27. Photos of (a) and (b) the face and (c) the length of Monolith 3.

Monolith 4

This catalyst was prepared at BYU by cutting an extruded 4"x4" cordierite support lengthwise into four pieces (see Figure 28; ideal cuts would be along the dotted lines). The resulting pieces are in the form shown in Figure 29a, the breakage of the top and right edges resulting from cutting the catalyst into four equal pieces. Some wall pieces may be intact (or partially intact) where the cuts were made, as shown in Figure 29b. These monolith pieces were cut approximately 6" long.

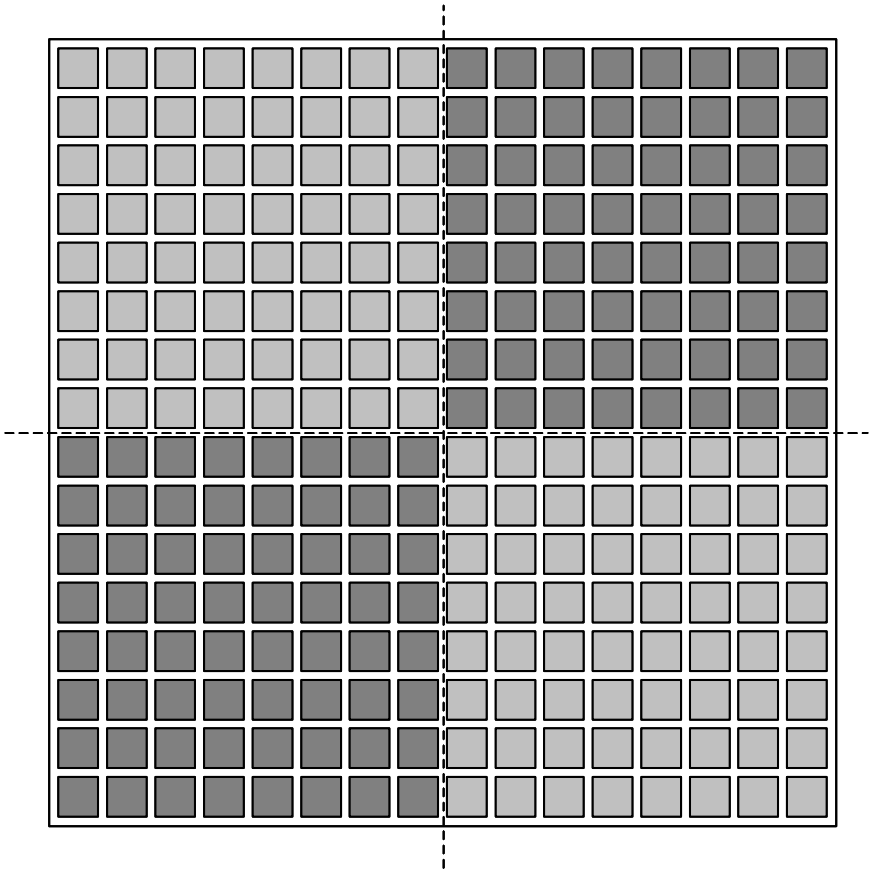

Figure 28. To-scale schematic of cordierite support with regions corresponding to smaller monolith pieces highlighted in different shades of gray.

Note that the channels in Figure 29 are slightly rounded at the corners. This is the result of dipping the cordierite pieces in a slurry consisting of the active catalytic phase supported on titania.

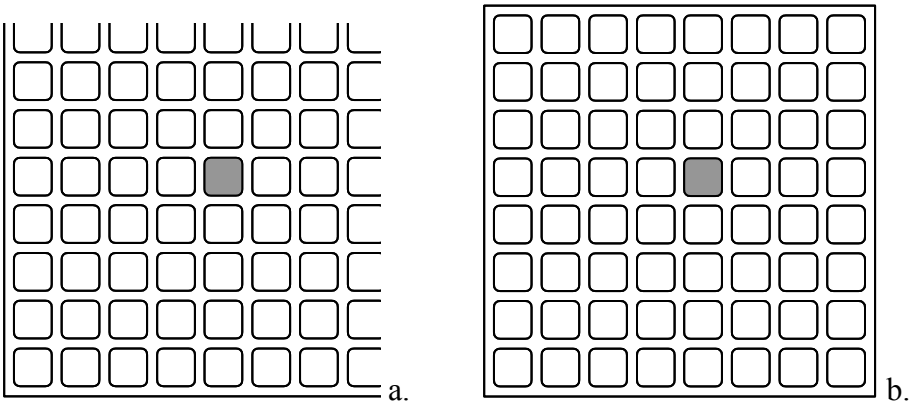
a. b.

Figure 29. To-scale schematic of Monolith 4 (BYU) after cutting (a) and as it would have turned out ideally without cutting effects (b).

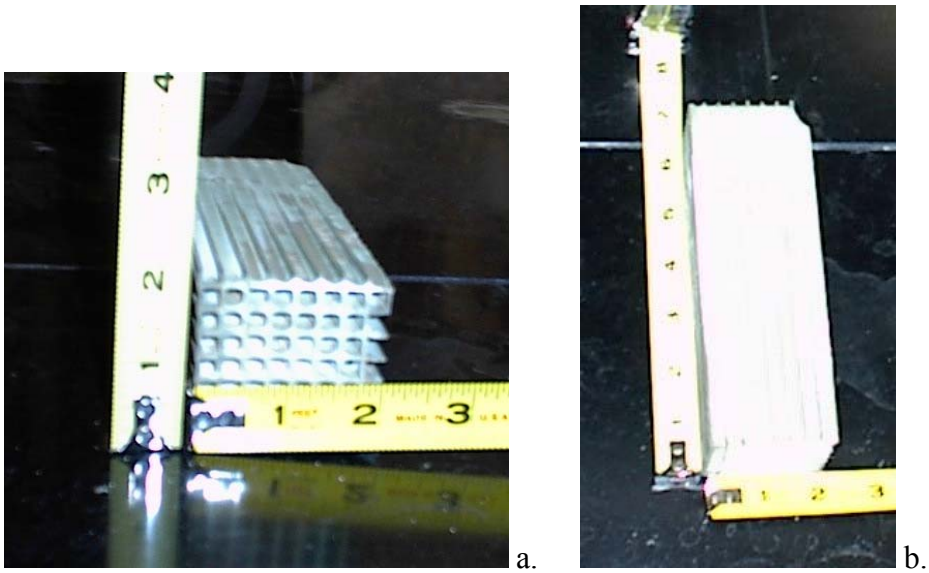
a. b.

Figure 30. Photos of (a) the face and (b) the length of Monolith 4 (BYU).

Plates 1 and 2

The plate samples are simple rectangular pieces, consisting of a perforated steel wire screen that has been coated with catalytic material. The plates are thin (<1mm thickness). The wire on Plate 1 is finer than on Plate 2, but both contain holes of similar diamond-like shape. The plate catalysts offer the advantage of being flexible and may be bent considerably without the catalyst coating flaking off (See Figure 32).

a.

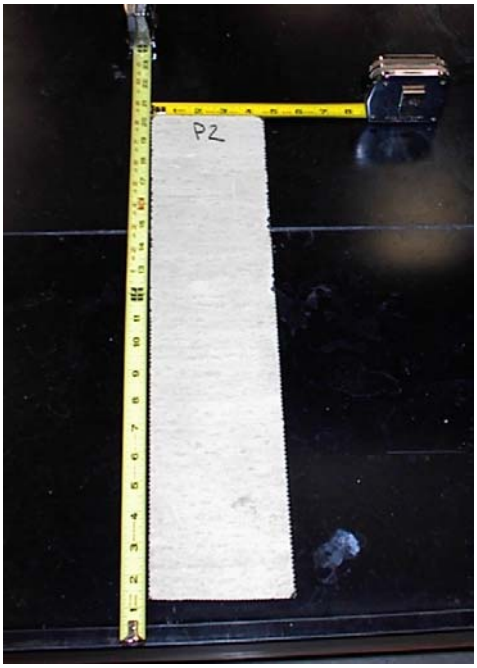

b.

Figure 31. Photographs of Plate 1 (a) and Plate 2 (b).

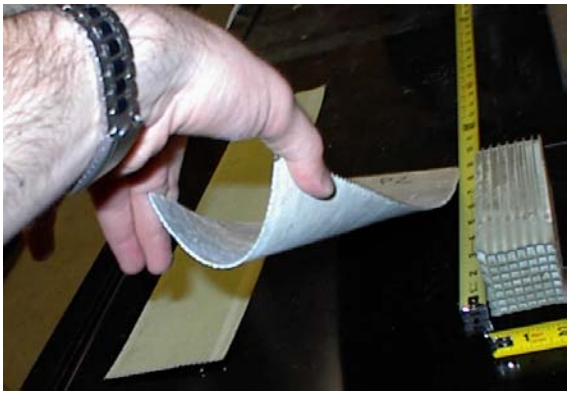

a.

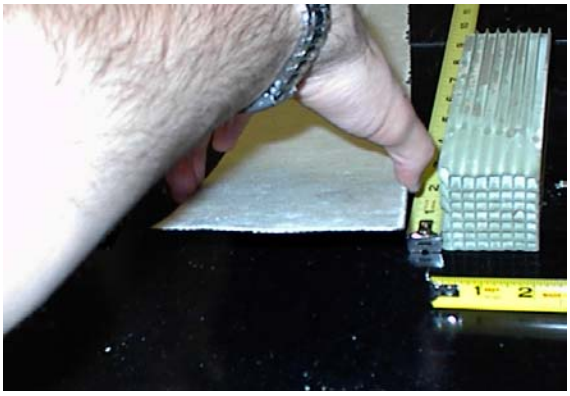

b.

Figure 32. Plate 2 can be bent (a) and will return to its original shape (b).

Housing in Slipstream Reactor

Catalysts are placed in the slipstream reactor according to Figure 33. The monolith catalysts are arranged in groups of four and are placed at the corner sections of the slipstream reactor casing. The plate catalysts are located in the middle sections. The placement of the plate catalysts is now discussed, as there has been some confusion on this issue.

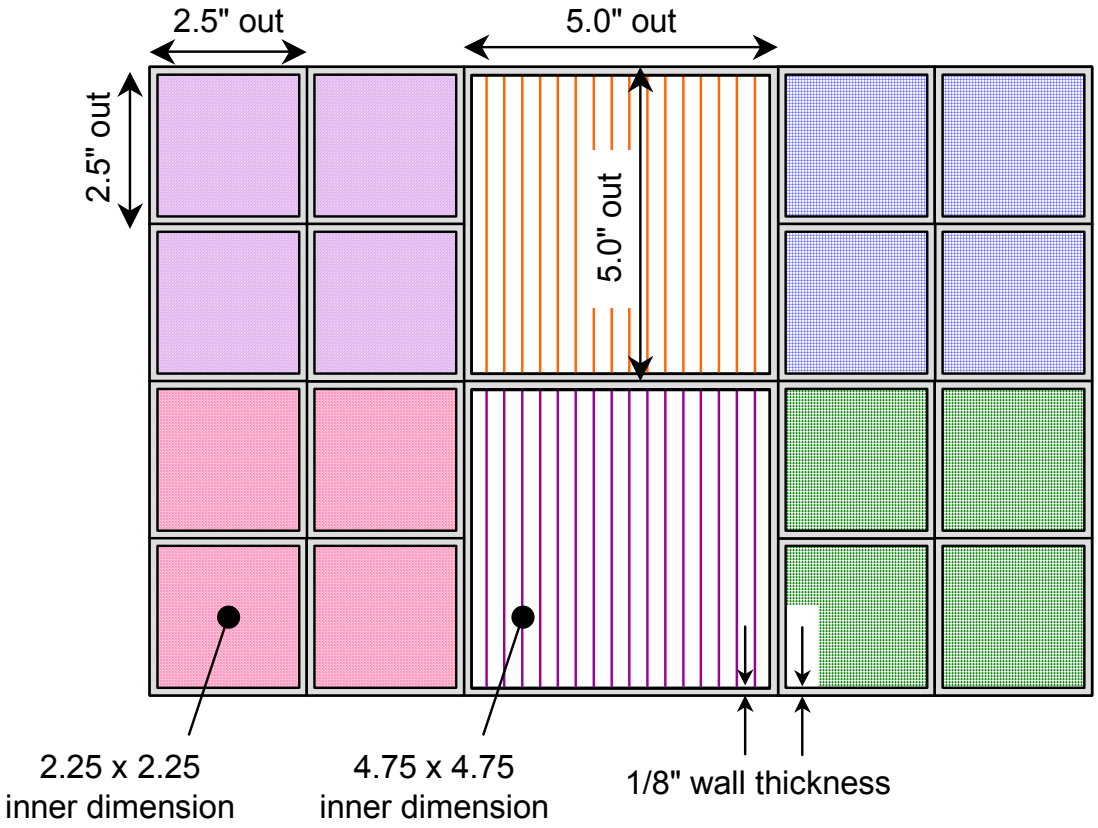

Figure 33. Layout of catalysts in slipstream reactor (picture courtesy of Kevin Whitty).

There are 40 plates in each chamber--20 on top and 20 on bottom, with the bottom plates installed transverse (or perpendicular) to the top plates. To illustrate, the plate holders for the top catalysts would be on the north and south sides, while the holders for the bottom catalysts would be on the east and west sides.

The top set of plates is installed such that the top edge of the plate is flush with (or perhaps 2-3 mm below) the top edge of the 4.75x4.75 inch square chamber tube holding the plates. The plate holders are 23 inch long, 1/4" thick aluminum plates with twenty 0.06" wide grooves machined the length of the plate (0.2231” pitch). All eight plate holders (2 top, 2 bottom in each of the 2 plate chambers) are identical. Another 1/4" thick, 1/2" high "block" is screwed onto the front side of these holders to keep the catalysts from sliding downwards. This block is positioned such that the top of the catalysts is just about flush (perhaps 2-3mm below) the top of the chamber.

The bottom edge of the bottom plate holders is just about flush with the bottom of the aluminum tube, and the "block" is about 1 inch above the bottom. Consequently, there is a space between the upper and lower set of plates. This space is estimated to be 3.5 inches for plates P1 and 7.5 inches for plates P2 (see Figure 35).

The plate holders for P2 are attached directly to the chamber tube. With two 0.25" thick plate holders secured to two sides of this (see Figure 34b), the actual inner dimensions are 4.25x4.75 inches. The grooves in the plate holders are about 0.125" deep, so the total spacing for the plate is about 4.50". The 4.375" plates slide into this nicely.

Because P1 are narrower, 0.25” thick backing plates were placed behind the catalyst holders to move them closer together. This results in a smaller chamber of dimensions 3.75x4.75 inches (Figure 34a), allowing 4.0 inches of total spacing for the 3.875 inch wide P1.

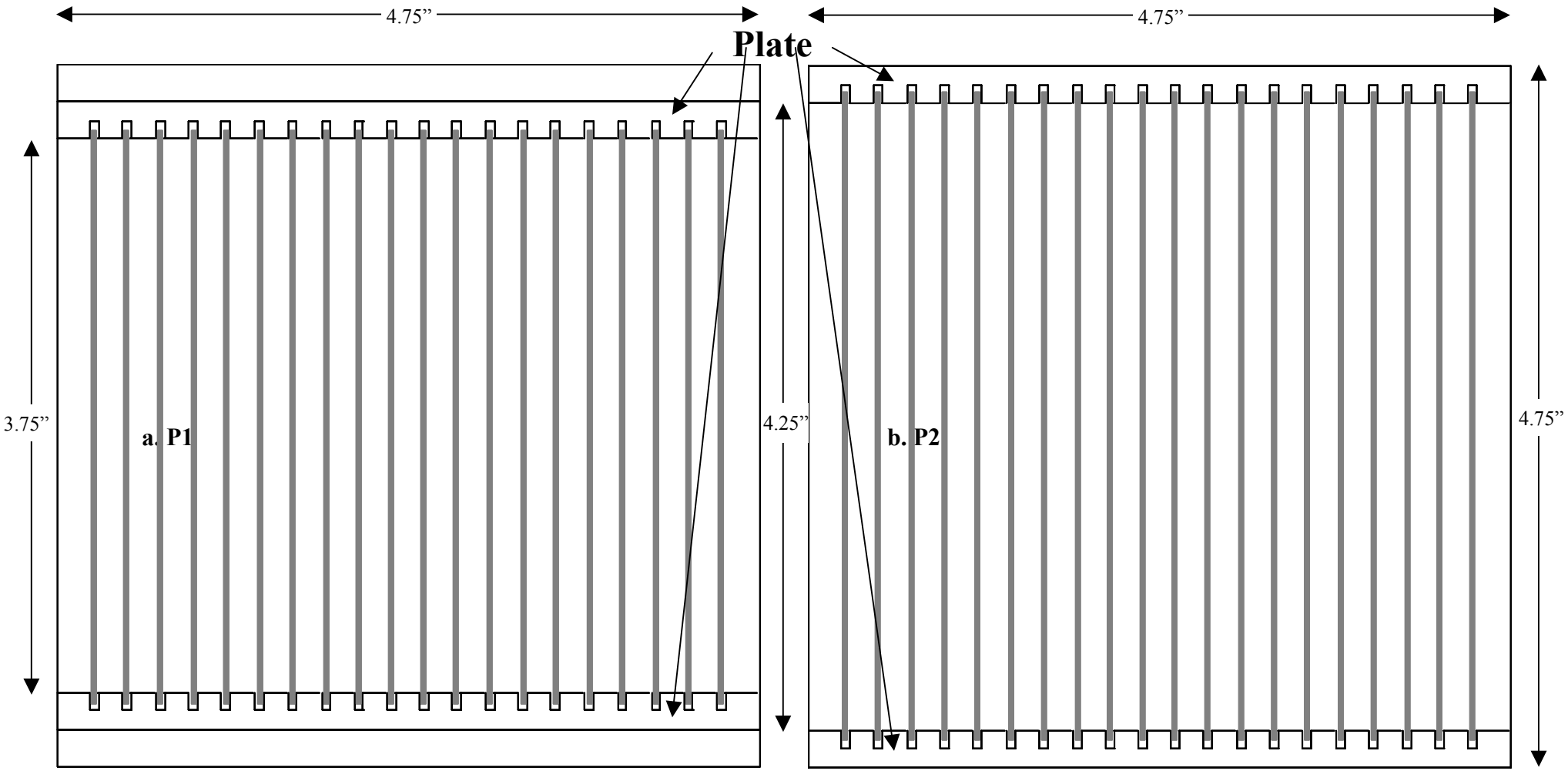

Figure 34. To-scale representation of plate catalysts as they are arranged in the slipstream reactor.

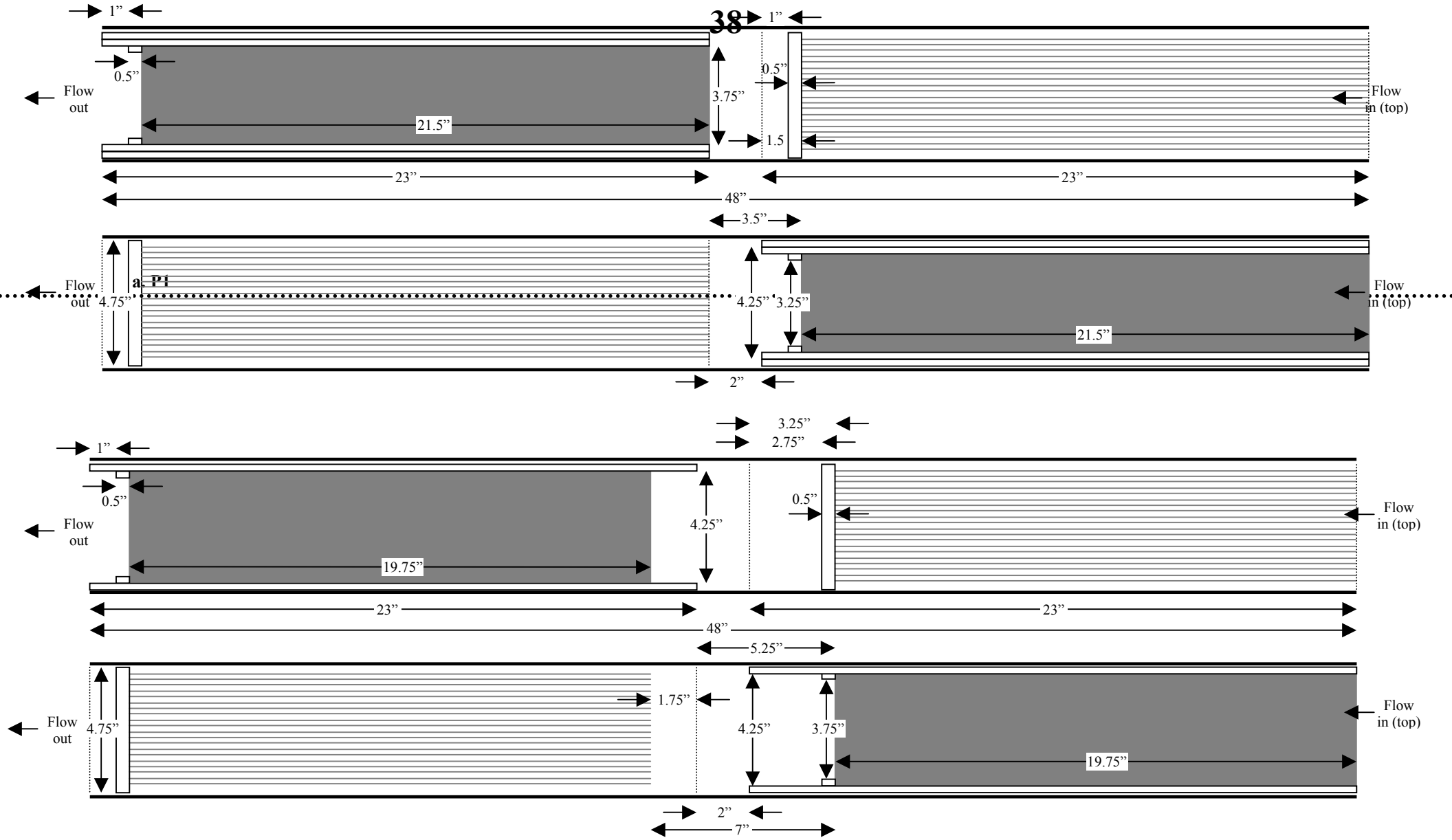

Figure 35. 1/5 scale schematic of plate catalyst layout in slipstream reactor. Note flow is from right (top) to left (bottom) [a is P1, b is P2].

Laboratory testing

Due to gas costs, flow rate restrictions, and power limitations, it has been determined that testing whole monolithic or plate catalysts will not be feasible in BYU's laboratory. The catalysts will instead be cut up into smaller pieces, likely one inch square by ½- to 1-inch tall for monoliths (see Figure 36). Only in this way can the existing equipment at BYU be used to characterize these monoliths since maximum mass flow controller flow rates are not large enough to accommodate larger monoliths.

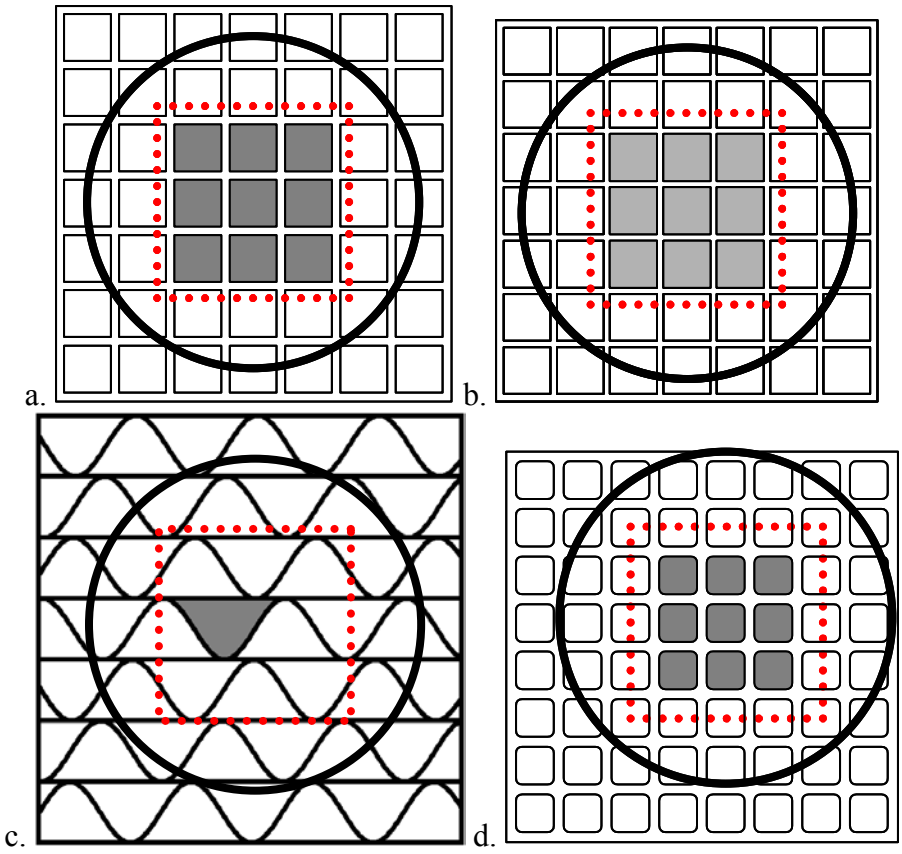

Figure 36. Schematics showing square cross-section of monoliths (dotted line) inside a circle representing the furnace inside diameter. In order, M1, M2, M3, and M4.

Task 4.2 Evaluation of Commercial Catalysts for Power Plant Conditions

The technical objective of this task is to assess deactivation of commercial catalysts exposed to a flue gas containing alkali and alkaline earth elements such as those found in low rank fuels and biomass co-fired with coal. This will be accomplished by measuring the NO_x composition of the flue gas before and after it flows through a multi-catalyst slipstream reactor in the presence of ammonia. The catalysts will then be removed periodically for physical characterization to assess the damage incurred during exposure to the ash-laden flue gas. Since deactivation of SCR catalysts depends on the length of time the catalysts are exposed to flue gas, the first step in accomplishing this task is to expose the catalysts to flue gas for sufficient time so as to be able to observe catalyst deactivation.

During this quarter, the slipstream reactor was operated at AEP's Rockport plant and a significant amount of hours on flue gas were accumulated. Figure 37 shows the gradual but steady build up of reactor operating time accrued in this quarter (April – June 2003). The catalysts have been exposed to flue gas for about 1000 hours.

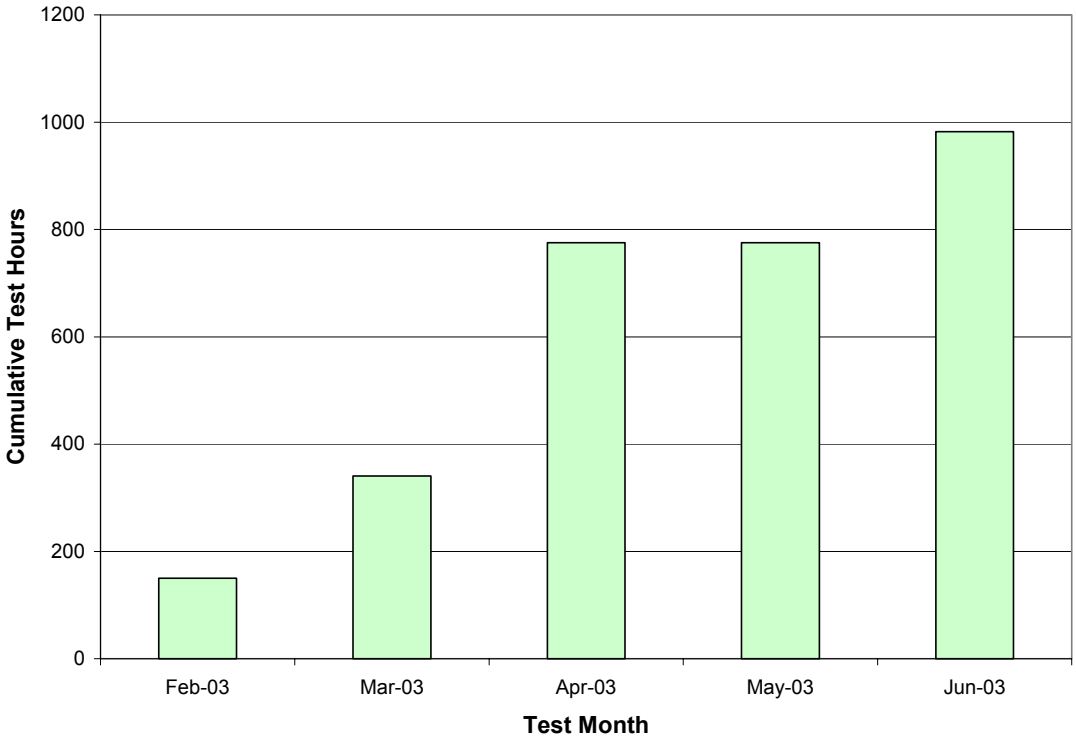

Figure 37. Cumulative catalyst exposure time to flue gas

Data Analysis

In this quarter progress was made in reactor data analysis by establishing a means for organizing the data and its analysis. Briefly, the reactor raw data are organized into daily and weekly reports. The daily reports are meant to provide information on:

(1) What is the cumulative time that the catalysts have been exposed to the flue gas?
(2) What is the cumulative flue gas flow through each catalyst?
(3) What is the cumulative amount of ammonia used?
(4) What is the activity of the catalyst based on the NO_x reduction rate as a function of temperature, space velocity and NH_3/NO_x ratio?
(5) What are the daily histories of catalyst activity, flue gas temperature, reactor temperature, space velocity, O_2 concentration, NH_3/NO_x ratio?
(6) The continuous emission monitor's (CEMs) calibration records.

From the daily reports weekly reports are generated, which also include the SCR performance status reports describing problems encountered in the week and the solutions taken to overcome them. The core of the weekly reports is aimed at providing the needed information on:

(1) What the NO_x reduction rates were last week (summary of catalyst activity).
(2) What plant operating conditions were (summary of selected PI data items) – O_2 and NO_x vs time.
(3) What the daily cumulative averages were for catalyst activity, space velocity and reactor temperatures.

Figure 38 is an example of a daily record for April 4, 2003. The figure shows a record of the temperatures of the flue gas as it leaves the economizer section of the boiler, its temperature before it enters the catalyst chambers, and the temperatures in the SCR. Notice that the rise in temperature in the SCR followed the opening of the gate valve after which the catalyst temperatures remained fairly constant.

Figure 39 shows a record of the catalyst activity for the six test catalysts for the test conditions described in Figure 38. Catalyst activity has been defined as the ratio:

$$Catalyst\ \ Activity = \left(\frac{NO_{X(in)} - NO_{X(out)}}{NO_{X(in)}} \right) \qquad (4)$$

In ideal conditions, the $NO_{X(out)}$ reading for the most effective catalyst would be zero and the catalyst activity would be 1. As the catalyst deactivates, the $NO_{X(out)}$ reading would gradually rise making the activity less than one. In the limiting condition where the catalyst is totally deactivated, $NO_{X(out)}$ would be the same as $NO_{X(in)}$ and the catalyst activity would be zero.

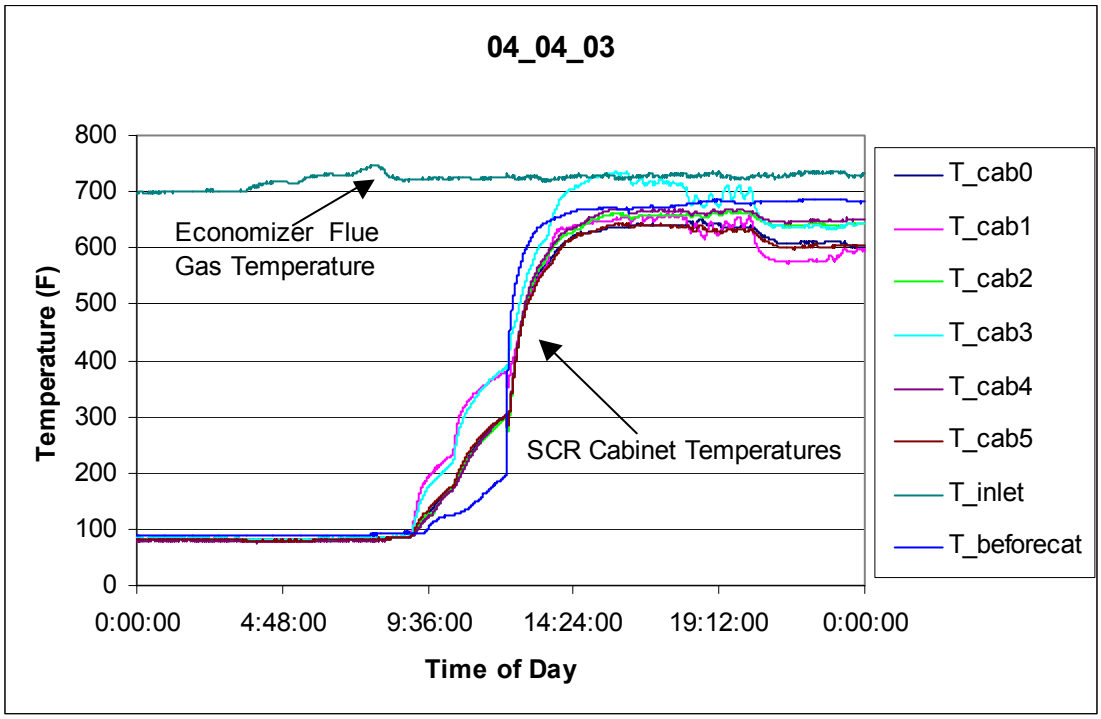

Figure 38. A snapshot of the daily record of the SCR temperature and the entering flue gas temperature.

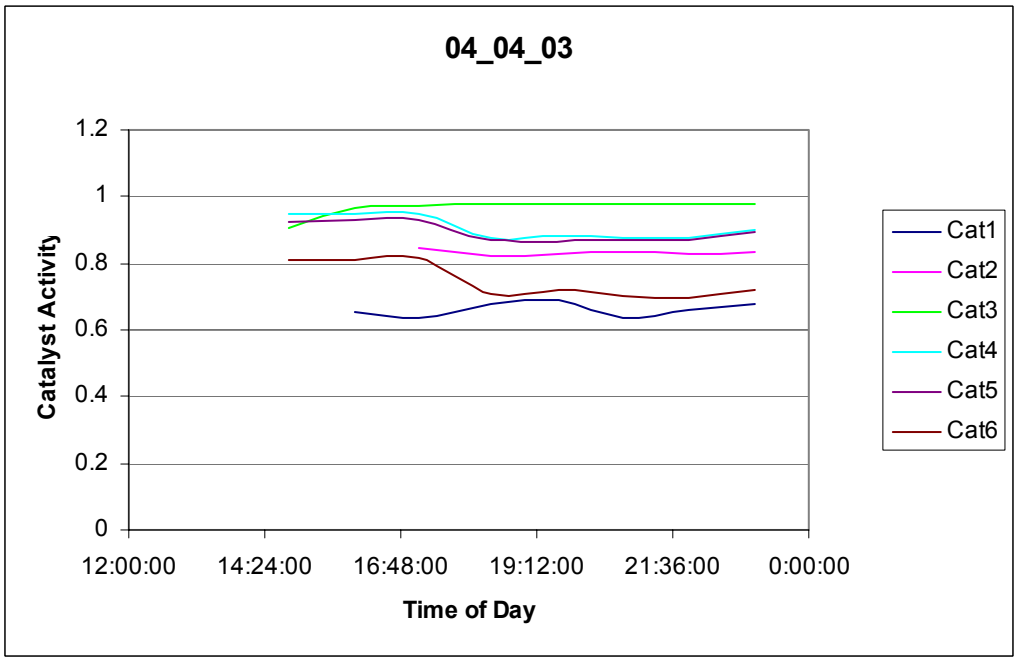

Figure 39. A comparison of activity of the six SCR catalysts as a function of time.

Problems and solutions during the quarter

This quarter saw a number of operational and equipment problems. Chief among these were sample line plugging, catalyst plugging, heater malfunction and ammonia tank pressure build-up and venting.

Sample Line Plugging

At the end of the first week of April, the CEMS stopped giving meaningful results. All sample lines were reading zero NO_x and 21 % O_2. It appeared as if the CEMS was failing to receive gas samples from the SEQUENCER. Intense troubleshooting of the SEQUENCER sampling protocol ensued. With the help of plant personnel, the SEQUENCER sample line selector switches were examined for proper positioning. The sampling pump was also checked to see if it was functioning properly. Further, with the help of Baldwin Environmental (the suppliers of the SEQUENCER) and the plant personnel, the sample line relays and switching sequence were thoroughly examined. All these did not seem to solve the problem. Eventually at the end of April Reaction Engineering International decided to send its own engineers to examine the SEQUENCER closely.

A systems engineer worked on troubleshooting the SEQUENCER for electrical faults. There were no faults found with the SEQUENCER electrical wiring. Individual troubleshooting of the pump and sample line selector solenoid valves showed that both the pump and the solenoid valves were in good working condition. Later, the systems engineer and the project engineer performed troubleshooting of flow in the sequencer, the sampling pump and the CEMS. The sampling system is configured in such a way that the SEQUENCER pump pulls gas samples from the SCR and discharges them to a filter located in the SEQUNCER unit. From the SEQUENCER filter, the sample gas is pulled by another vacuum pump located in the CEMS cabinet. When the sample line at the SEQUENCER filter was disconnected, a positive pressure in the sample line indicated that the SEQUENCER pump was working and discharged the gas sample to the filter, as it should. The sample line was then reconnected and later disconnected at the CEMS pump side at the filter. At this moment, it was noticed that there was suction in the sample line. However, upon further troubleshooting of the sample line upstream of the SEQUENCER pump it was found that when the sample line was broken at a Tee Swagelok fitting between the hot box and the sample coolers, there was no suction. It was later discovered that the sample line was clogged at the inlet to the first cooler (see Figure 40). The ash that clogged the sample line had cemented out and could not be removed even by blowing with 110 psi compressed air. The ash could only be removed with a screwdriver. Thus, flow to the CEMS was re-established and the expected NO_x and O_2 readings restored.

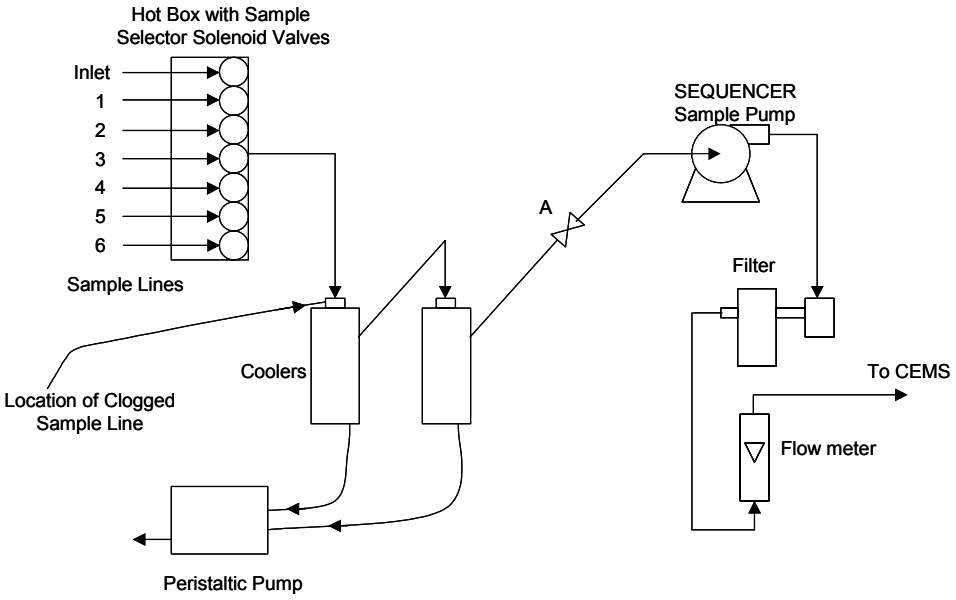

Figure 40. Simplified sample flow loop in the SEQUENCER.

Catalyst Plugging

The SCR had shut itself down due to an unscheduled outage during the weekend of April 19-20. Upon restarting the reactor on Monday April 21, 2003 it was noticed that flue gas flow through all the catalyst chambers was lost except chamber number 3. The SCR had to be taken apart and the flow tubes exiting the SCR bottom cleaned. The tube in chamber 4 was completely clogged with ash that appeared to have "cemented out". A crowbar-like tool had to be used to chisel out the ash. All the catalyst chambers were found to be clogged excerpt for a few open channels mostly in chamber number 3. Figure 41 shows pictures of the clogged catalyst chambers.

Figure 41. Catalyst channel plugging by ash due to moisture condensation.

There are two possible causes of catalyst plugging. One cause is a large quantity of ash accumulated upstream of the gate valve. When the gate valve is shut down for extended periods of time, ash accumulates in the flue gas intake pipe. Once the gate valve is opened for catalyst testing, a large quantity of ash flows into the catalyst chambers, inundating the flow channels since the eductors are unable to pull it all through the chambers. As a consequence, ash accumulates in the catalyst channels. This problem was found to be more serious with the monolith type catalysts than the plate type. The solution to this problem is to prevent accumulated ash from entering the SCR when the gate valve is first opened following a period of inactivity. To this end, a manual air blowback line has been installed upstream of the gate valve. The reactor operating procedures have now been modified to start with a blowback of the flue gas intake line prior to opening the gate valve. This measure has resulted in extended SCR operating time without the catalyst chambers plugging up with ash. In the next quarter the air blowback will be automated so that the procedure can be performed remotely.

Another identified cause of catalyst plugging is condensation of water that occurs during boiler outages. A good example of this problem is manifest on Figure 5 when an unscheduled outage resulted in the SCR shutting down. During the shutdown, the SCR heaters also stopped and the chamber temperatures dropped below the dew point of water causing ash cementation. Since the PRB ash is prone to consolidating into a cemented solid in the presence of moisture, the SCR operating procedure has been modified to keep the heaters on and maintain a temperature of 300°F during outages. The lower section of the reactor, downstream of the catalyst chambers has been insulated to prevent condensation of water in the eductor sections.

Ammonia Venting

The ammonia cylinders were connected to a manifold which supplied ammonia to the SCR. The manifold has the ability to connect to four cylinders, where two are in use and two remain on standby. For safety, the manifold was provided with pressure relief valves which would vent out the ammonia in case the cylinder pressure rose above 250 psi. During this quarter, the ammonia safety relief valves were triggered and vented the tanks. The plant reported that this happened on days when the ambient air temperatures were excessively high. Figure 42 is a schematic of the ammonia manifold setup showing the location of the safety relief valves. We are currently working with the plant and the ammonia vendors to find ways of preventing the occurrence of ammonia venting.

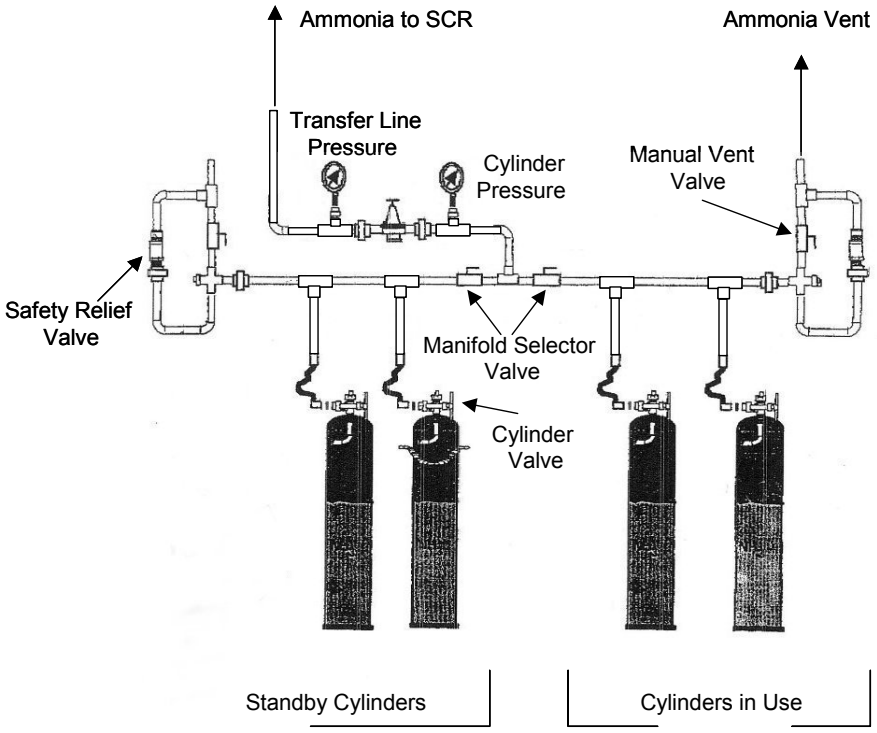

Figure 42. Ammonia supply manifold for the slipstream reactor.

Other Operational Bottlenecks Resolved this Quarter

During this quarter, a malfunctioning Fieldpoint module, heater power controller, and gate valve power supply unit were replaced. The gate valve solenoid power cables were also rewired. A longer flexible spool piece was installed at the top of the SCR to allow for expansion and improve the SCR seal. Two angle iron bars were also added to assist with fastening the SCR top in order to improve reactor sealing. The eductors were clogged and had to be taken out and cleaned. The new operating procedures require the eductors to have a flow of air all the time in order to prevent clogging with ash. The electric heater connecting cables broke several times this quarter. New and more robust wires have been identified and connected to the heaters.

Results and Discussion

The new effort was begun on the development of a corrosion management system for minimizing the impacts of low NO_x combustion systems on waterwalls. The project is based upon a novel multi-sensor real-time corrosion monitoring system using an advanced electrochemical technology; feasibility of the sensor was demonstrated in the field previously on this program. The corrosion measurements will be coupled with REI's in-house CFD modeling tools and the recently developed EPRI-REI corrosion correlations for utility boilers for the identification of key corrosion locations and to provide up-front insight as to how corrosion patterns might change during variations in operating conditions and fuel selection. In addition, an advanced precision metrology technique and simple screw-in type coupons will be used to verify predicted and measured corrosion rates.

This quarter, a project kick-off meeting was held at AEP's Gavin Plant, in Chesire, Ohio. The meeting attendees were able to inspect the current probe locations where the REI and EPRI probes would be installed. During the site visit attendees also inspected the control room where the host PC would be located. Work began on the fabrication of electrochemical noise probes and the KEMCOP probes.

At BYU, *in situ*, spectroscopic experiments, which were partially reported last quarter, were completed. The most significant finding of these investigations is a consistent indication that vanadium does not sulfate during SCR activity in the presence of gas-phase SO_2 while both the substrate (anatase) and modifiers (molybdenum) do. Adsorption tests indicated that ammonia appears to adsorb on Brønsted acid sites present on the sulfated surface, suggesting sulfating the catalyst produced Brønsted acid sites. NO did not appear to adsorb on the sulfated catalyst surface, with or without pre-adsorption of ammonia. Improvements on the mass-spectrometer system at BYU have been made and work on the steady state reactor system shakedown neared completion. Due to gas costs, flow rate restrictions, and power limitations, it has been determined that testing whole monolithic or plate catalysts will not be feasible in BYU's laboratory. The catalysts will instead be cut up into smaller pieces, likely one inch square by ½- to 1-inch tall for monoliths. Only in this way can the existing equipment at BYU be used to characterize these monoliths since the maximum flow rates are not large enough to accommodate larger monoliths.

During this quarter, the slipstream reactor was operated at AEP's Rockport plant and a significant amount of hours on flue gas were accumulated. At the end of the performance period, the catalysts had been exposed to flue gas for about 1000 hours. This quarter saw a number of operational and equipment problems with the slipstream reaction. Chief among these were sample line plugging, catalyst plugging, heater malfunction and ammonia tank pressure build-up and venting. Minor modifications were made to the reactor to address some of the operational problems; in addition, operating procedures were changed to prevent plugging. As a result of these changes, the reactor ran well for the latter part of the quarter. Progress was made in reactor data analysis by establishing a means for organizing the data and its analysis into daily and weekly reports.

Conclusions

Good progress has been made on several fronts during the last three months. In particular:

- The new effort to develop and test the corrosion management system kicked off this quarter with a meeting at AEP's Gavin plant. Work commenced on fabrication of the probes.
- During this quarter, FTIR experiments for SCR catalyst sulfation were finished at BYU and indicated no vanadium/vanadyl sulfate formation at reactor conditions. Improvements on the mass-spectrometer system at BYU have been made and work on the steady state reactor system shakedown neared completion.
- The slipstream reactor continued to operate at AEP's Rockport plant; at the end of the quarter, the catalysts had been exposed to flue gas for about 1000 hours. Some operational problems were addressed this quarter that enable the reactor to run without excessive downtime by the end of the quarter.

During the next quarter activities planned for the active tasks in the project are as follows.

Corrosion Management System:

- Plans for the next quarter will focus on the fabrication of electrochemical noise probes, procurement of electronic equipment for data acquisition and building the software tools for probe control and data processing.

- Field measurements at Gavin are scheduled to commence in the next quarter.

Laboratory Studies of Catalyst Activity:

- Further XPS analysis will be conducted of the powdered catalyst samples exposed to various gases in the ISSR in order to measure surface elemental concentrations.

- NO adsorption experiments will be conducted on fresh catalyst and sulfated catalyst without pre-adsorption of ammonia.

- NO adsorption on a wet sulfated catalyst is under investigation and will be reported in next quarterly report.
- The following is a list of items pertaining to the powdered catalyst test reactor that will be accomplished before the next quarterly report:
    - Examine catalytic effects of hot stainless steel reactors and replace with an inert material if necessary.
    - Verify that the condenser removes sufficient amount of water or else the NO_x analyzer and GC will be affected; need to also see how much NO it removes, if any, since NO_x analyzer is downstream.
    - Quantify amount of water that bubblers release, and compare consistency of all four bubblers; might want to investigate effect of height of water in bubbler tube, which drops over time.

- Quantify effects that uncontrollable inconsistencies in MFC flow rates have on observed catalyst activity.
- Ensure that catalyst packing/loading methods give consistent results (i.e. channeling or gas bypass effects are negligible).
- Investigate methods of sampling reactor feed streams.
- Work on Labview software to facilitate data analysis further.
- Get gas chromatograph working.
- Take preliminary data on actual catalysts in order to fine-tune necessary amount of catalyst, reactor temperature, and space velocity.
- Design a list of catalysts to test and begin that work.

Slipstream Reactor Testing of Catalyst Activity:

- In the next quarter work will continue to resolve the ammonia-venting problem and resume tests under ammonia flow.
- We plan to complete the second campaign of mercury oxidation in SCR catalysts.
- Following the mercury oxidation testing, the first set of catalyst samples will be removed from the reactor and sent to BYU for analysis.
- To improve the SCR reactor operation, a remote-controlled blowback of the flue gas intake pipe upstream of the gate valve will be installed together with relays that will allow individual sample line blowback. This swill help alleviate sample line plugging problems.
- The unit at Rockport is scheduled for an eight-week outage beginning on September 19 in order to install low-NO_x burners. Before the outage, therefore, we must complete the mercury testing and pull catalyst samples.

Literature References

Busca, Guido, Lietti, Luca, Ramis, Gianguido, Berti, Francesco, *Appl. Catal*. B 18 (1998) 1.

Cremer, M.A., Adams, B.R., and O'Connor, D., "Improved Rich Reagent Injection Performance for NO_x Control in Coal Fired Utility Boilers," EPRI-DOE-EPA Combined Utility Air Pollution Symposium: The MEGA Symposium, Washington, D.C. May 2003.

Appendix

Waterwall Corrosion Management

Kick-off Meeting Presentations

Field Testing of a Corrosion Advisor System

Project Update

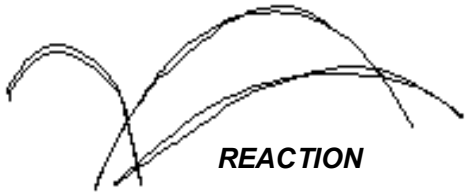

REACTION
ENGINEERING
INTERNATIONAL

Team Members

Project Sponsors: OCDO, US DOE, AEP

Participants by Tasks

- CFD Modeling: REI, AEP, EPRI
- Equipment: REI, CM, University of Utah (U of U)
- Demonstration: REI, AEP, EPRI
- Metrology: REI, U of U
- Correlation: NS Harding & Associates, REI, AEP, EPRI
- Project Management: REI, AEP

Outline

- Project Tasks and Current Status
- CFD Corrosion Modeling of the Test Boiler
- Installation of Probe Ports
- Equipment
- Plans for Next 6 Months

Project Tasks and Timeline

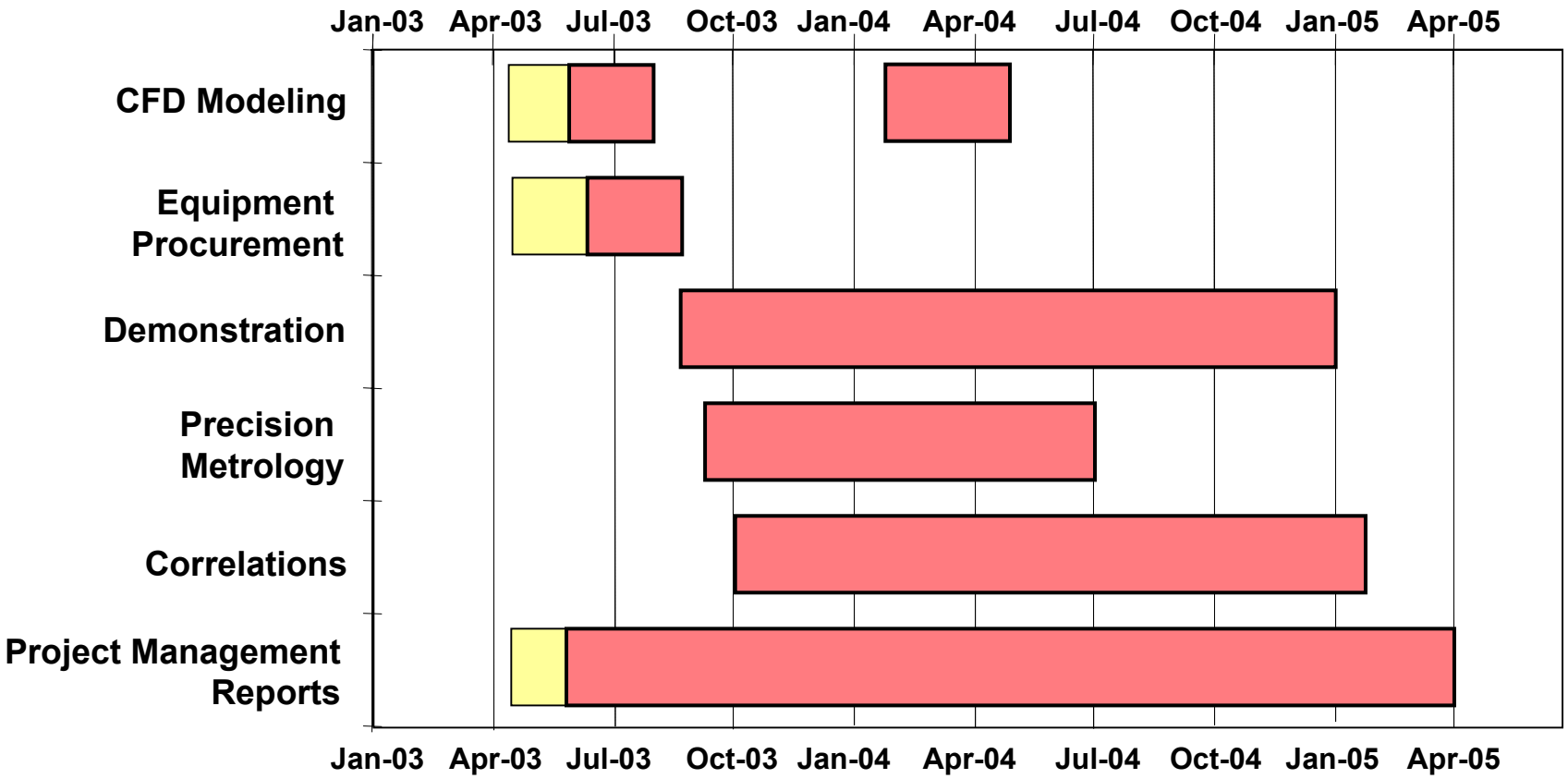

Current Project Status

Task description	***Start date***	***End date***	**% Done**
CFD Modeling	15-Apr-03	31-Jul-03	27
Equipment	1-Jun-03	31-Aug-03	15
Demonstration	15-Aug-03	31-Dec-04	
Metrology	1-Sep-03	30-Jun-04	
Correlations	1-Oct-03	28-Feb-05	
Management	15-Apr-03	31-Mar-05	6

CFD Corrosion Modeling for AEP Gavin Unit 2

Baseline Model

Model Geometry

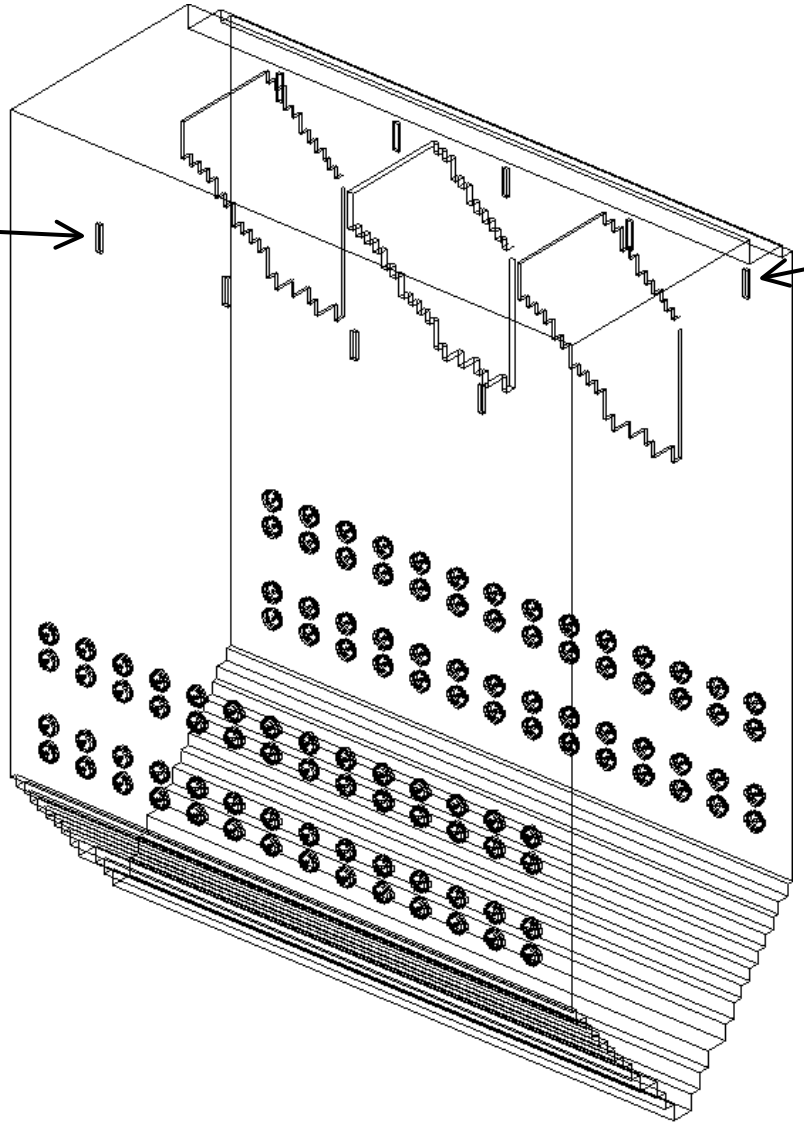

4 Front Wall GT Ports

5 Rear Wall GT Ports

112 DB Riley Single Register CCV Low NO_x Burners in a Cell Arrangement

REACTION ENGINEERING INTERNATIONAL

Predicted Flue Gas Temperature

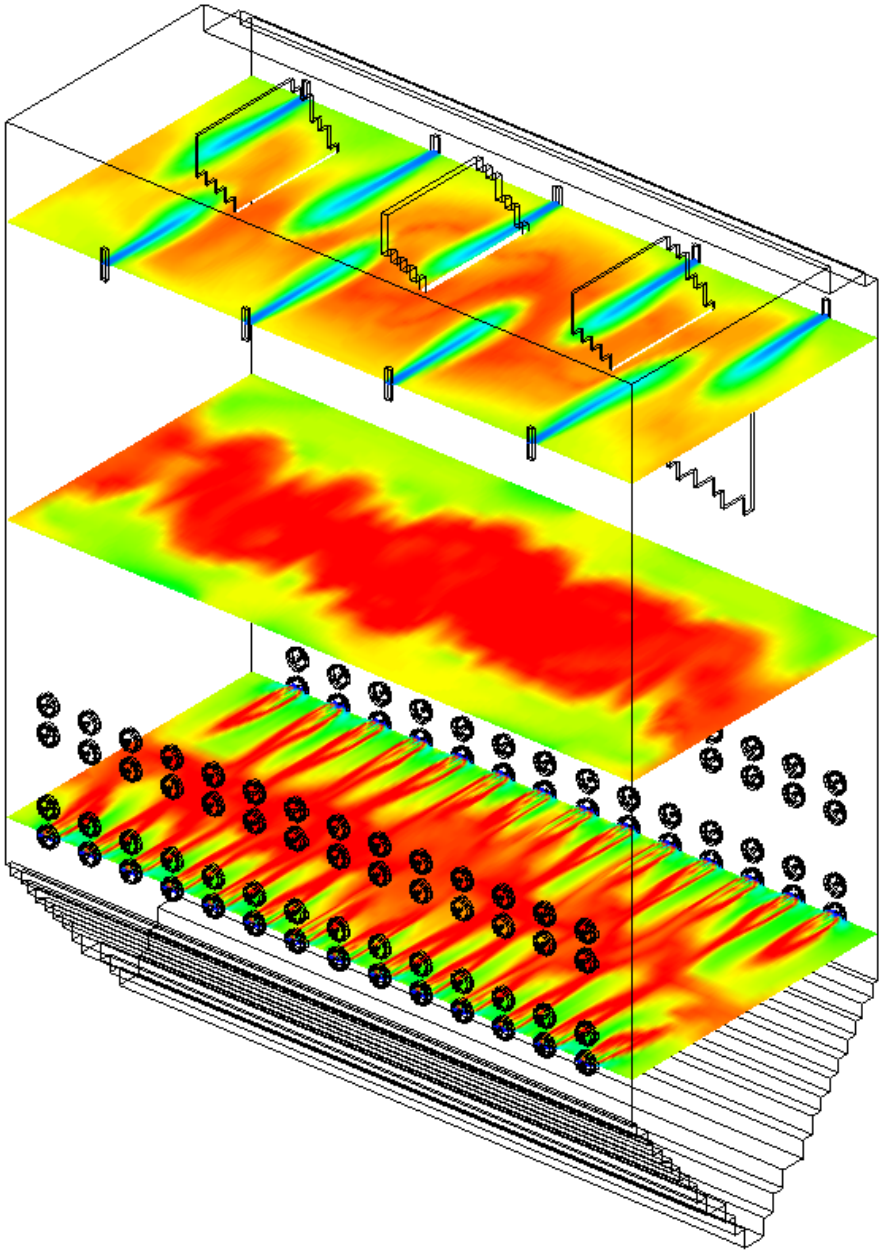

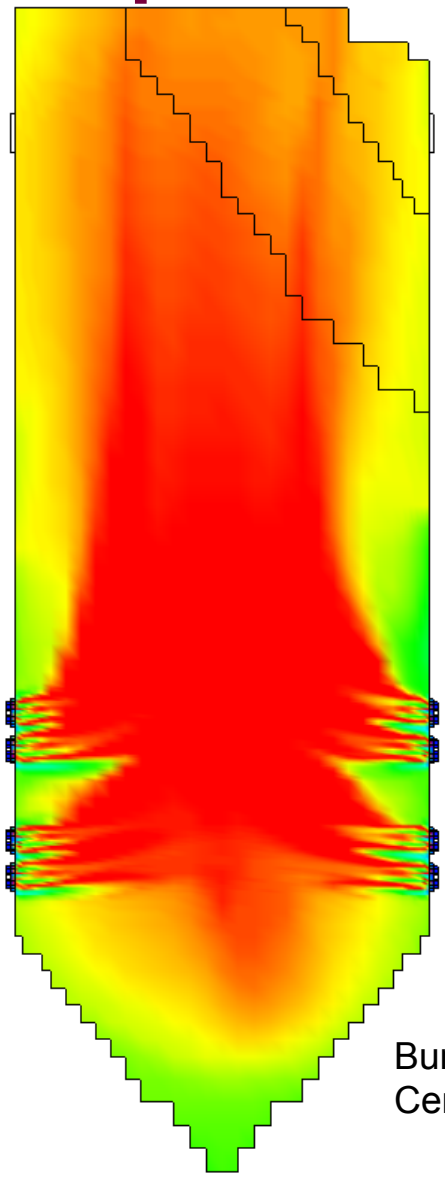

Predicted CO Concentration

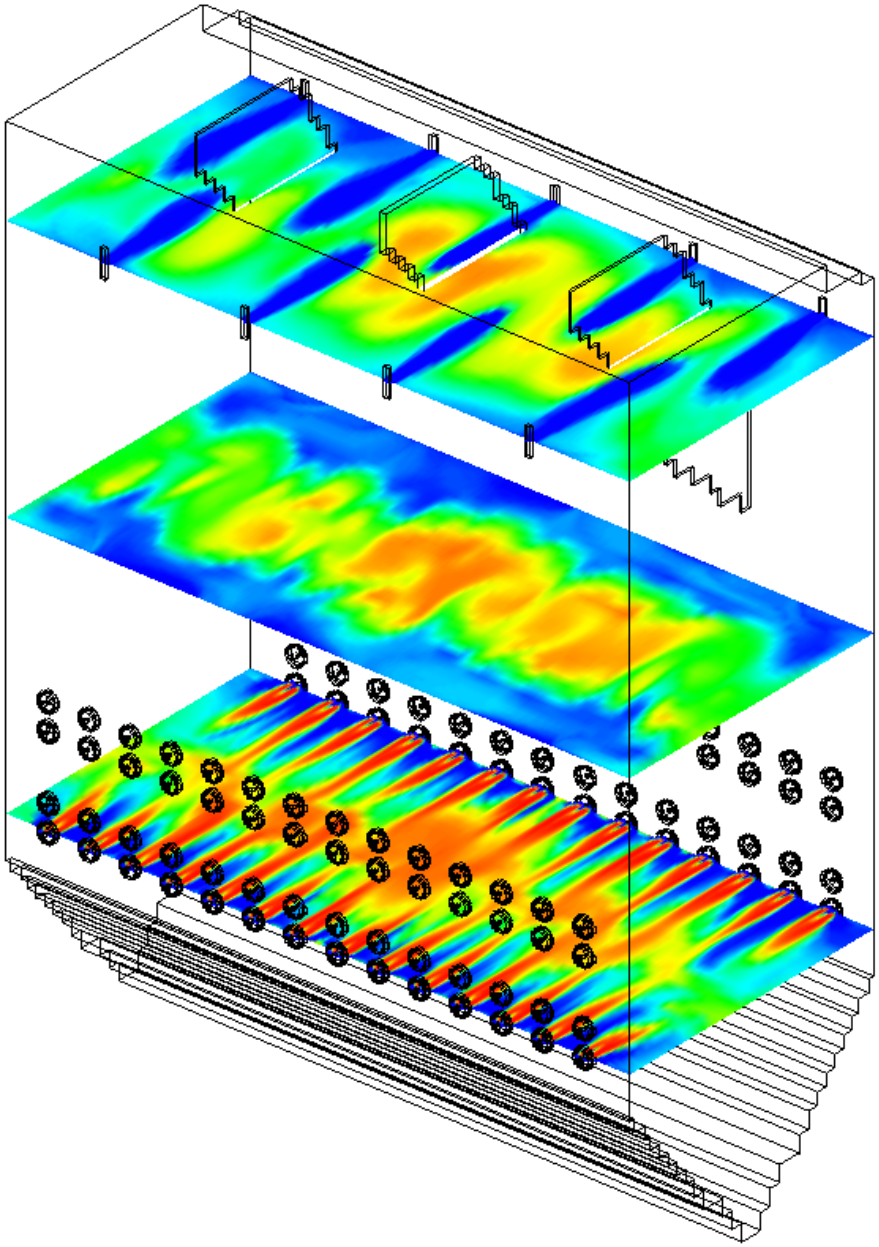

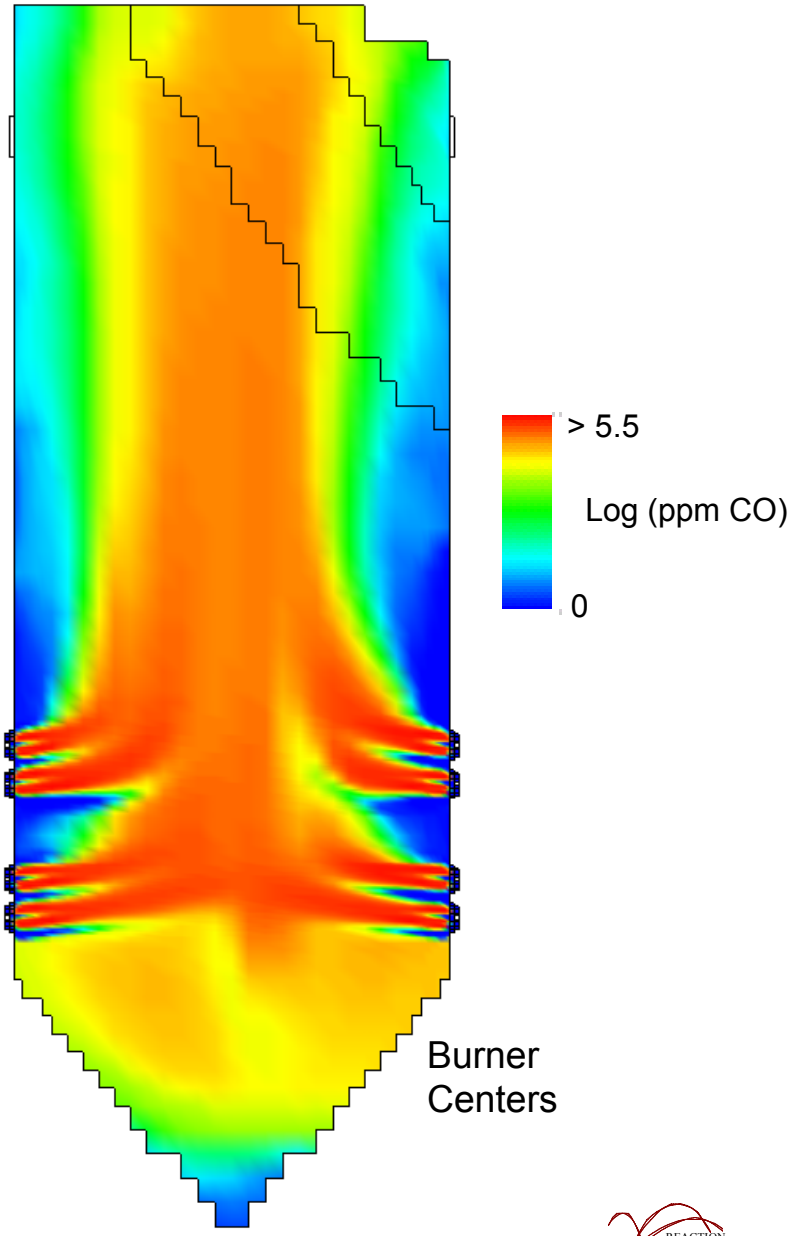

Predicted O_2 Concentration

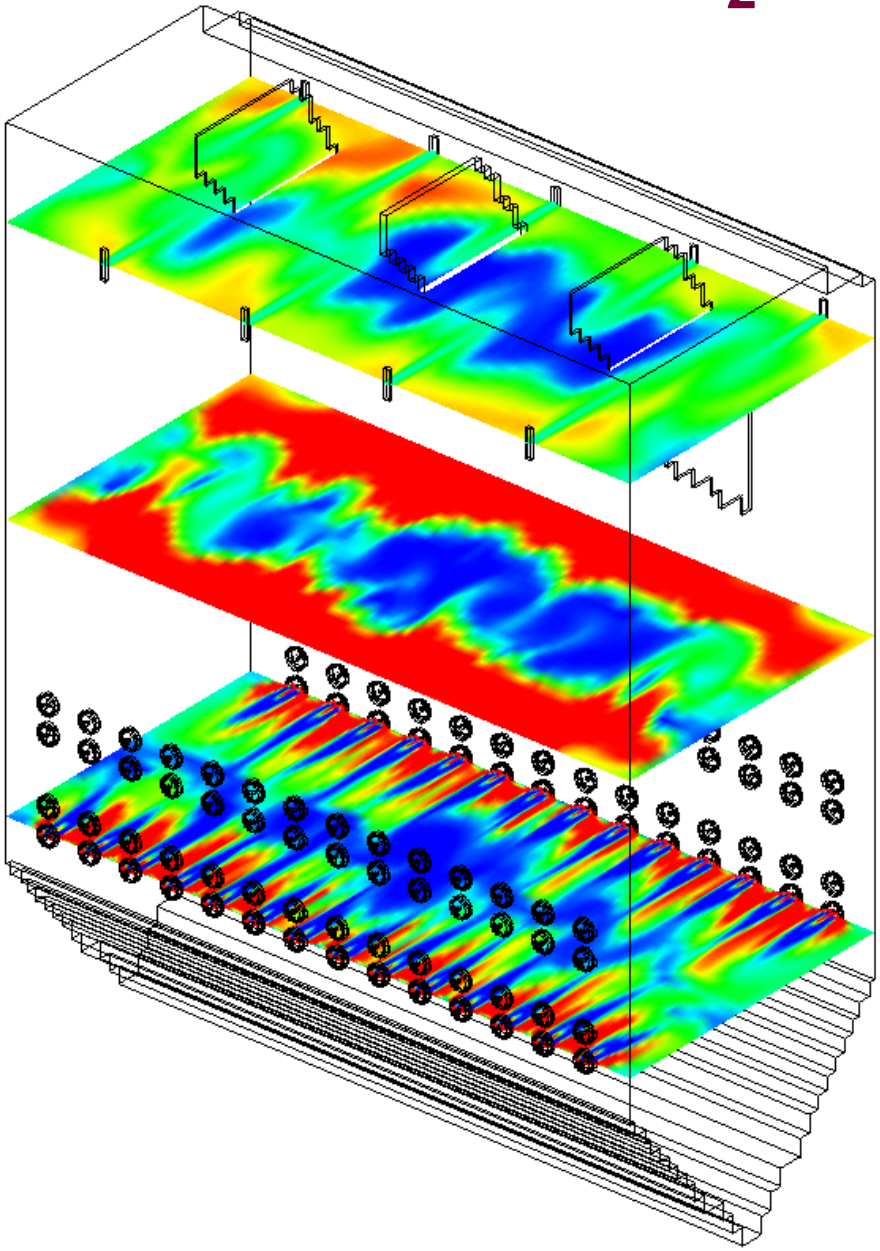

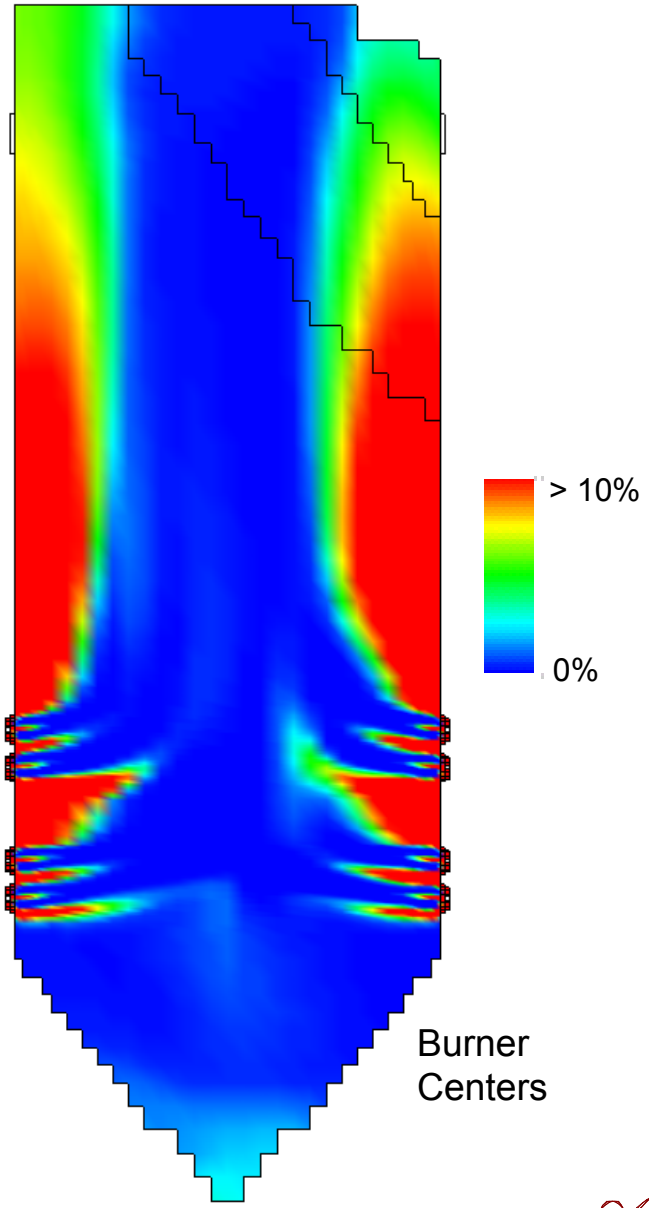

REACTION ENGINEERING INTERNATIONAL

Predicted Net Wall Heat Flux

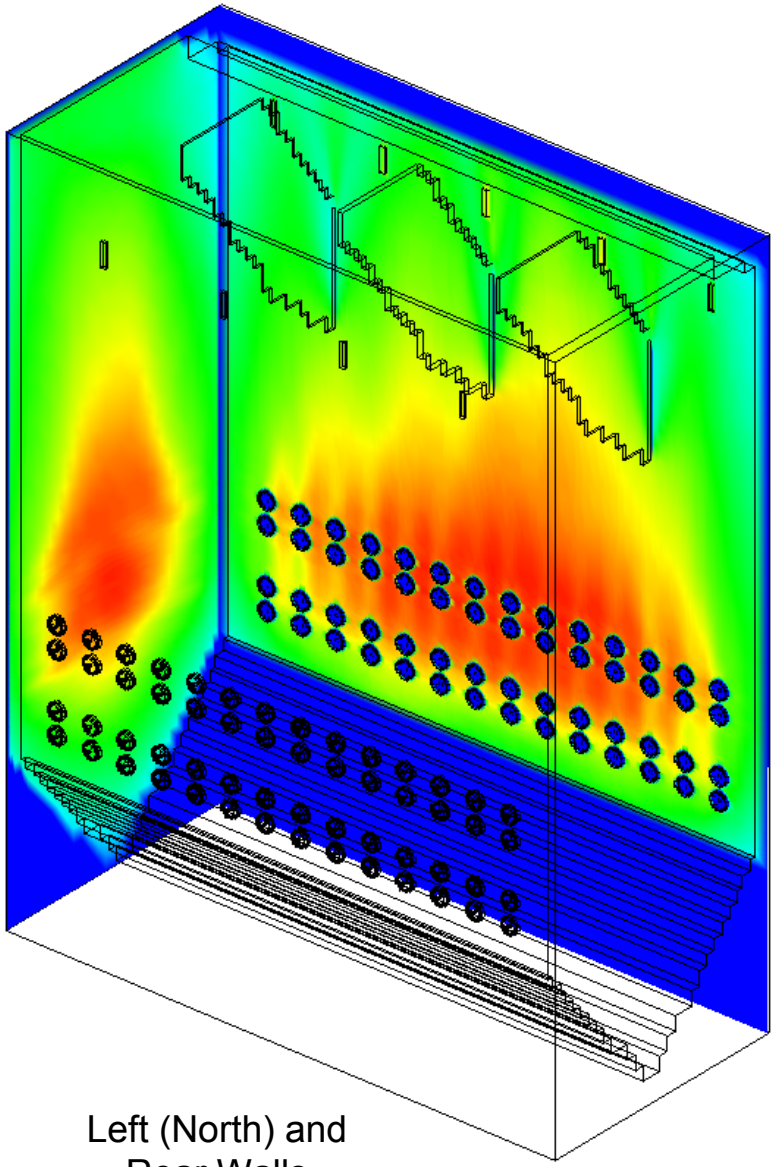

Left (North) and
Rear Walls

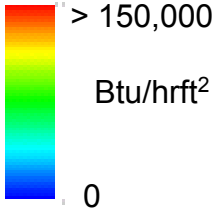

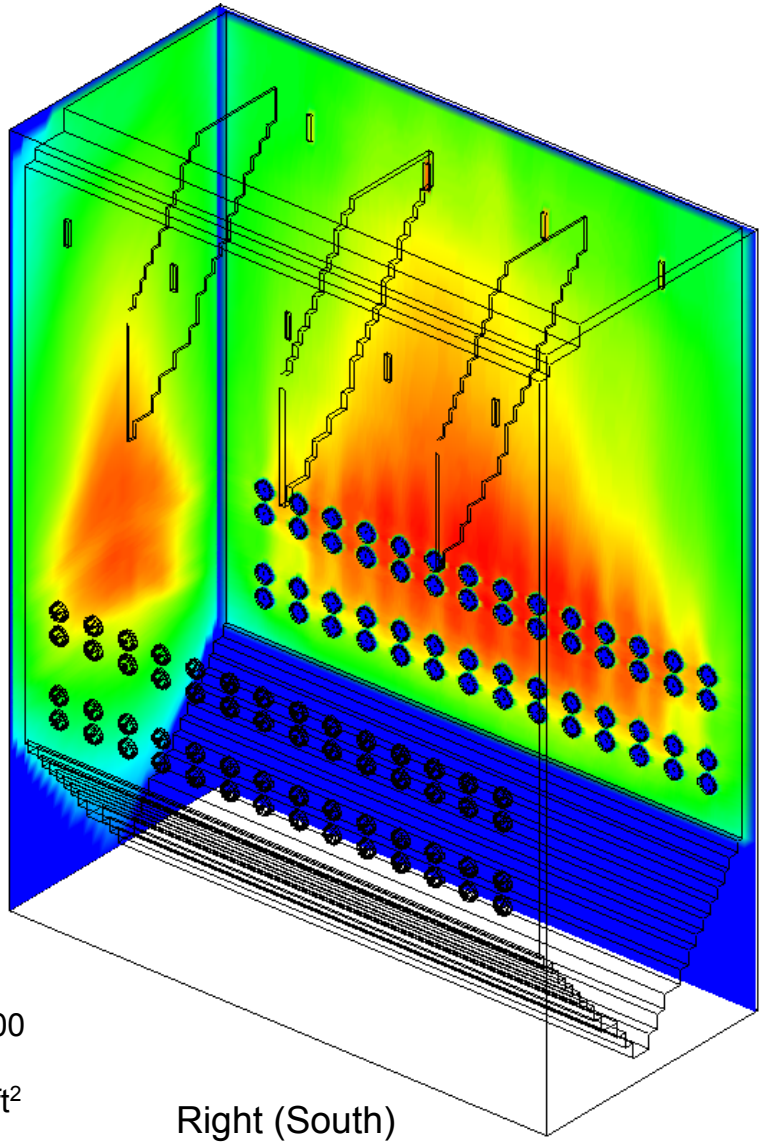

Right (South)
and Front Walls

REACTION
ENGINEERING
INTERNATIONAL

Fraction Unburned Material in Deposit

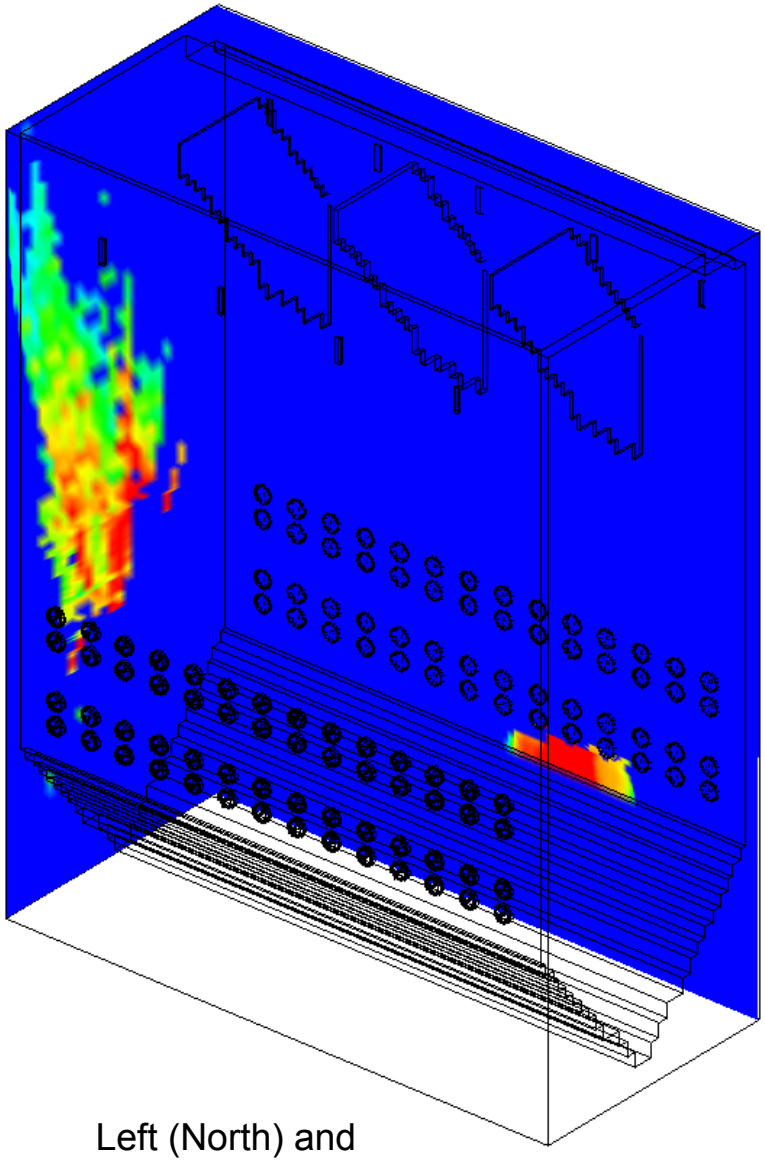

Left (North) and
Rear Walls

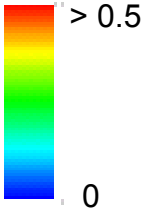

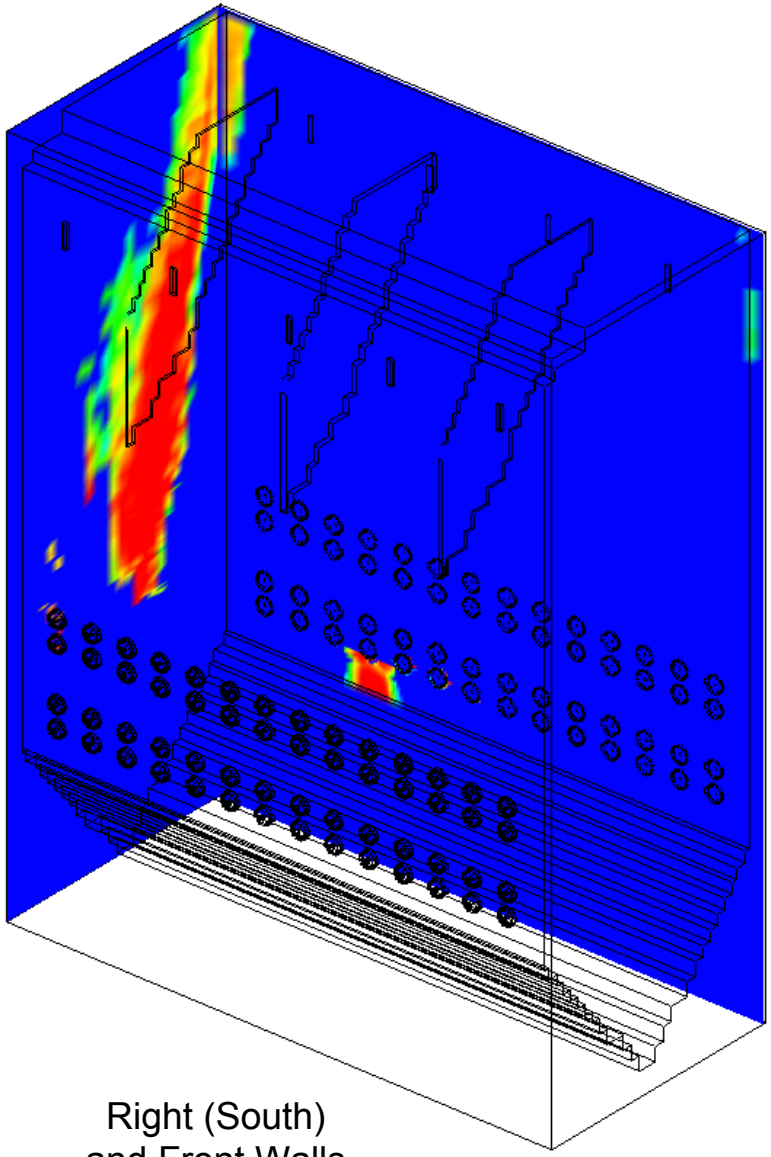

Right (South)
and Front Walls

REACTION
ENGINEERING
INTERNATIONAL

Predicted Corrosion Rate

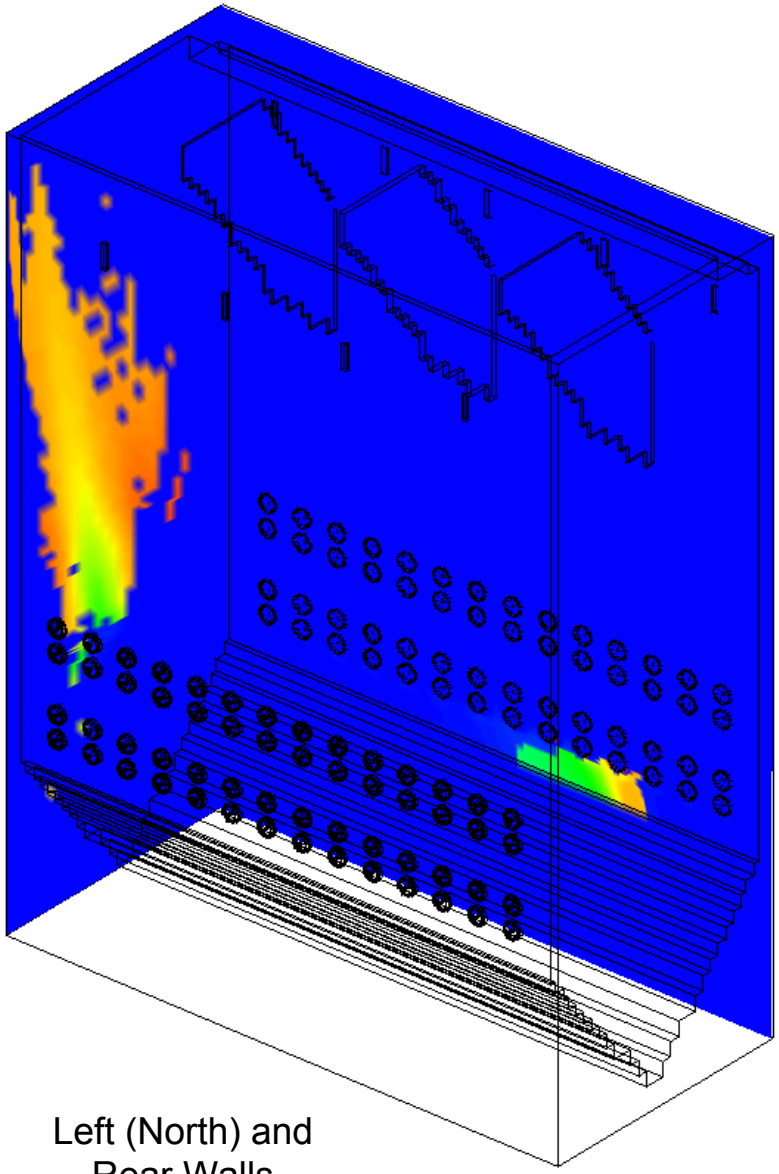

Left (North) and
Rear Walls

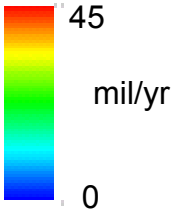

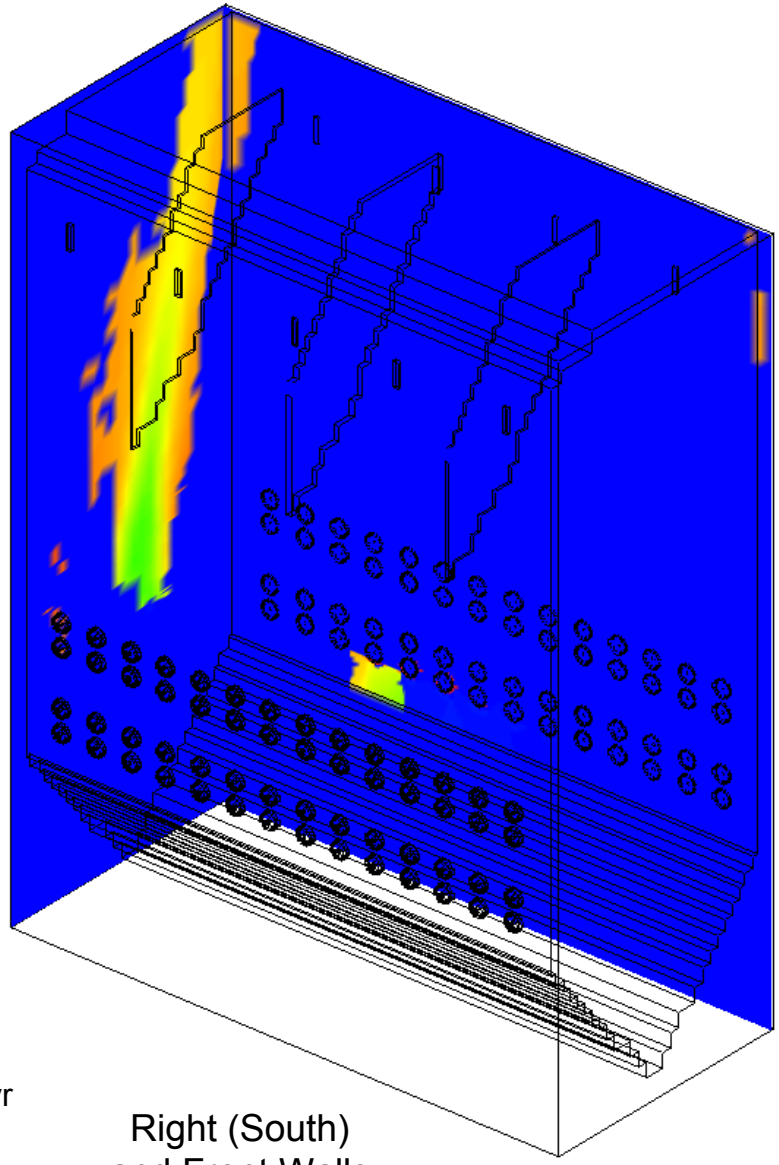

Right (South)
and Front Walls

REACTION
ENGINEERING
INTERNATIONAL

Equipment

Equipment Status

- KEMCOP probes are ready
- EN modules have been ordered
- Sensor plates are under preparation

Plans for the Next 6 Months

- Complete detailed CFD modeling of the boiler
- Completion of equipment procurement and assembly of EN corrosion probes
- Shakedown testing of the probes at the U of U
- Commencement of corrosion measurements at Gavin
- Initial precision metrology

Roundtable Discussions

Corrosion Probe Requirements

- Air cooled – 50-80 SCFM instrument air
- Electrical – 120 V 20 amp circuit
- Central area about 3 ft X 6 ft for control boxes on each side of boiler
- Air conditioned room for computer within 500 feet of control boxes

On-line High-Temperature Corrosion Monitoring Technology

June 12, 2003

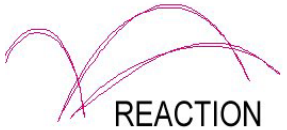

REACTION
ENGINEERING
INTERNATIONAL

Outline

- Introduction
- State of the Technology
- Advanced Real Time Corrosion Monitoring
- CFD Corrosion Simulation Tools
- Electrochemical Corrosion Monitoring
- Surface Profilometry
- Corrosion Advisor
- Summary

Introduction

Cost of Fireside Corrosion in Electric Utility Boilers

- Waterwall Tubes - $325m
- Superheater and Reheater Tubes - $148m

Source: Barry Syrett (EPRI), in Materials Performance, Feb 2003 p32-38.

Corrosion Monitoring Methods

- Visual Inspection
- Ultrasonic Tube Wall Thickness
- Weight Loss Coupons
- Precision Metrology
- Electrical Resistance
- Linear Polarization Resistance
- Electrochemical Impedance Measurement
- Electrochemical Noise

State of the Technology

Achievements of the Single Probe Program

- Successfully conducted corrosion monitoring tests at the lab-scale, pilot-scale and full-scale plant size
- Developed a benchmark technique based on surface profilometry
- World's first demonstration of EN real time corrosion monitoring in the radiant section of a large utility boiler

Examples of REI Experience

- 130 MWe cyclone-fired boiler
  - Rugged and robust system development
  - Qualitatively and quantitatively reasonable response verified
- 600 MWe pc-fired boiler
  - Quantitative validation for multiple mechanisms of corrosion
  - Air-cooled design tested
  - Remote operation procedures developed

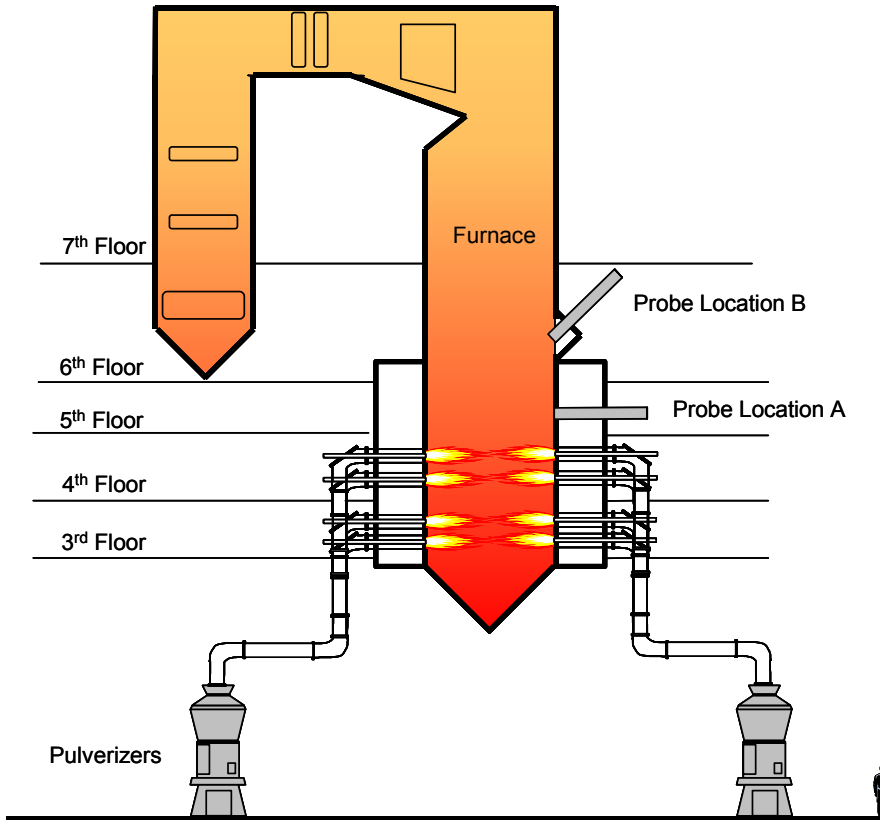

Utility Boiler Field Test

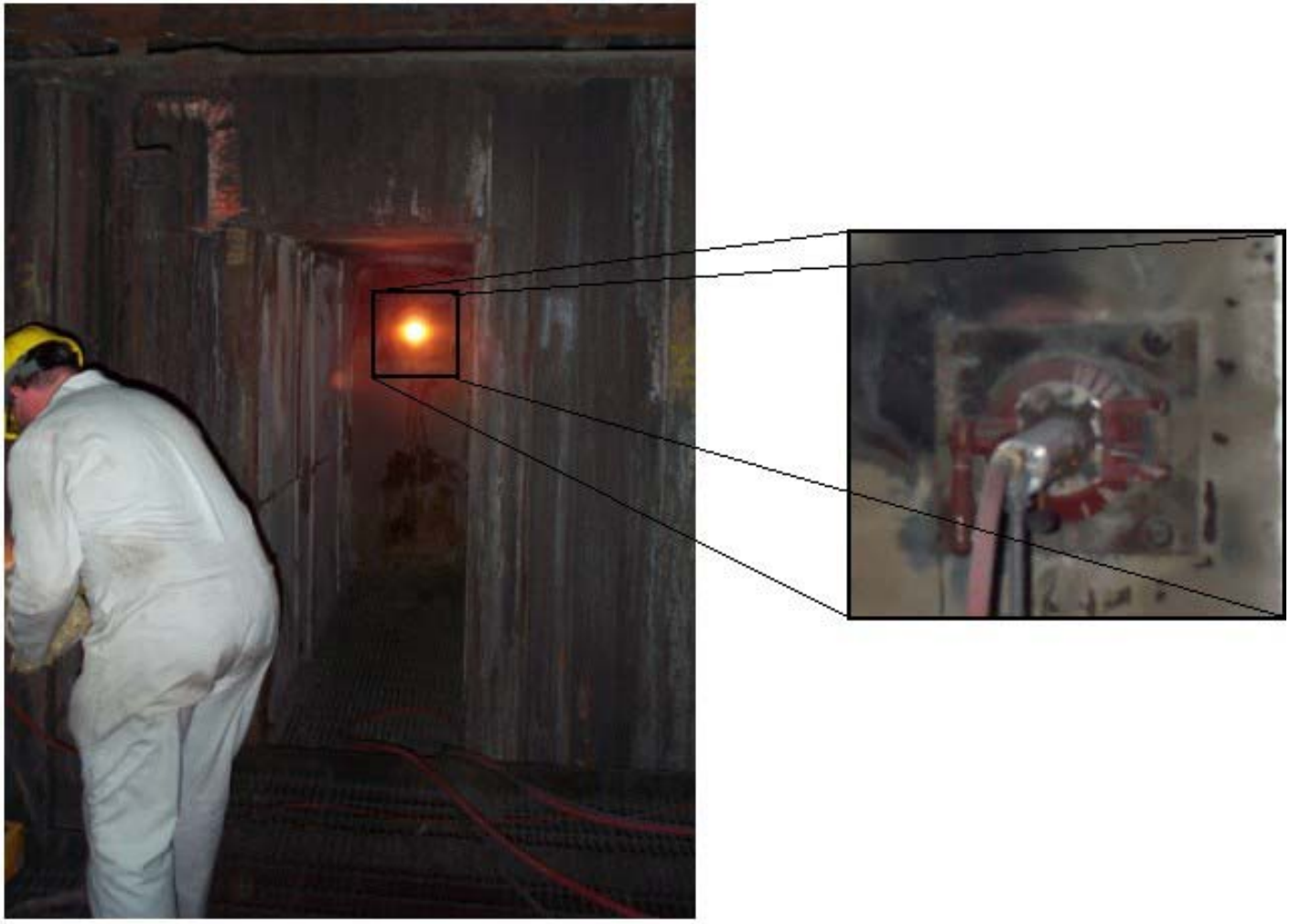

Advanced Corrosion Monitoring Technology

Comprehensive Approach to Corrosion Management

- **Identification of high risk locations**
  - application of empirical correlations and CFD modeling
  - plant measurements and/or tube failures
- **Installation of real time monitoring system**
- **Validation using physical measurements**
- **Corrosion advisor system**

I. CFD Simulation Tools

Corrosion & CFD

- CFD model predicts conditions that contribute to increased waterwall wastage
  - Gas composition at the wall
  - Tube temperature
  - Incident/net heat flux
  - Composition of depositing material
- Empirical correlations quantify wastage rates based on local conditions involving:
  - Sulfur
    - Gas-phase $CO/O_2/H_2S$ concentration
    - deposition of unreacted sulfur
    - waterwall tube metal temperature
    - near wall reducing conditions
  - Chlorine
    - weight % chlorine in fuel
    - waterwall tube metal temperature
    - waterwall heat flux
    - near wall reducing conditions

Sulfur Waterwall Attack

Rear Wall

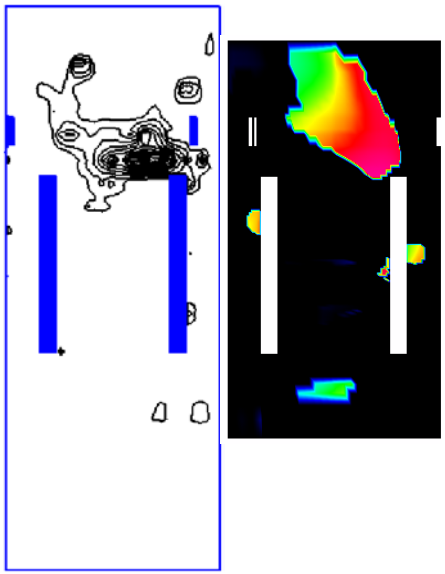

(max = 81 mil/yr)

Side Wall

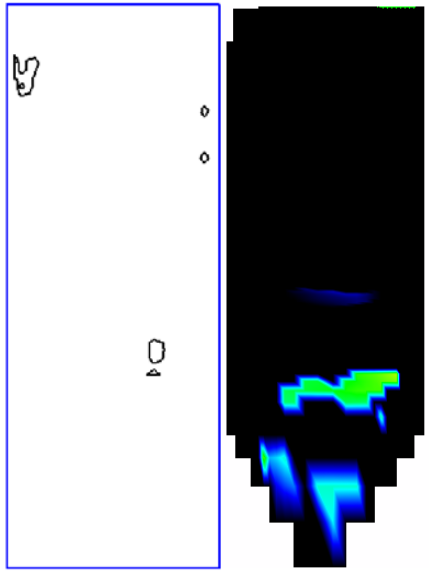

(max = 26 mil/yr)

Front Wall

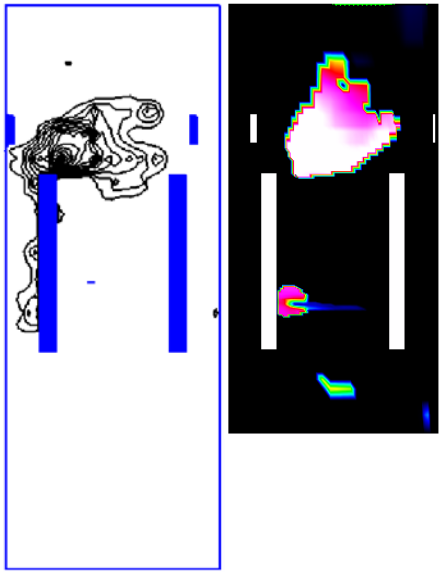

(max = 94 mil/yr)

Center Wall

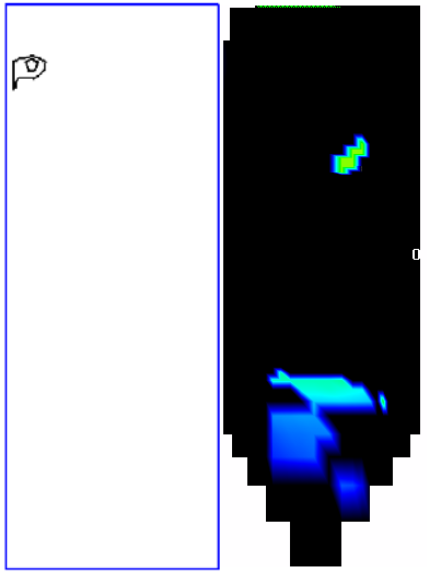

(max = 29 mil/yr)

(scale for simulations)

> 70

mils/yr

0

REACTION ENGINEERING INTERNATIONAL

II. Electrochemical Monitoring

Real-time Data

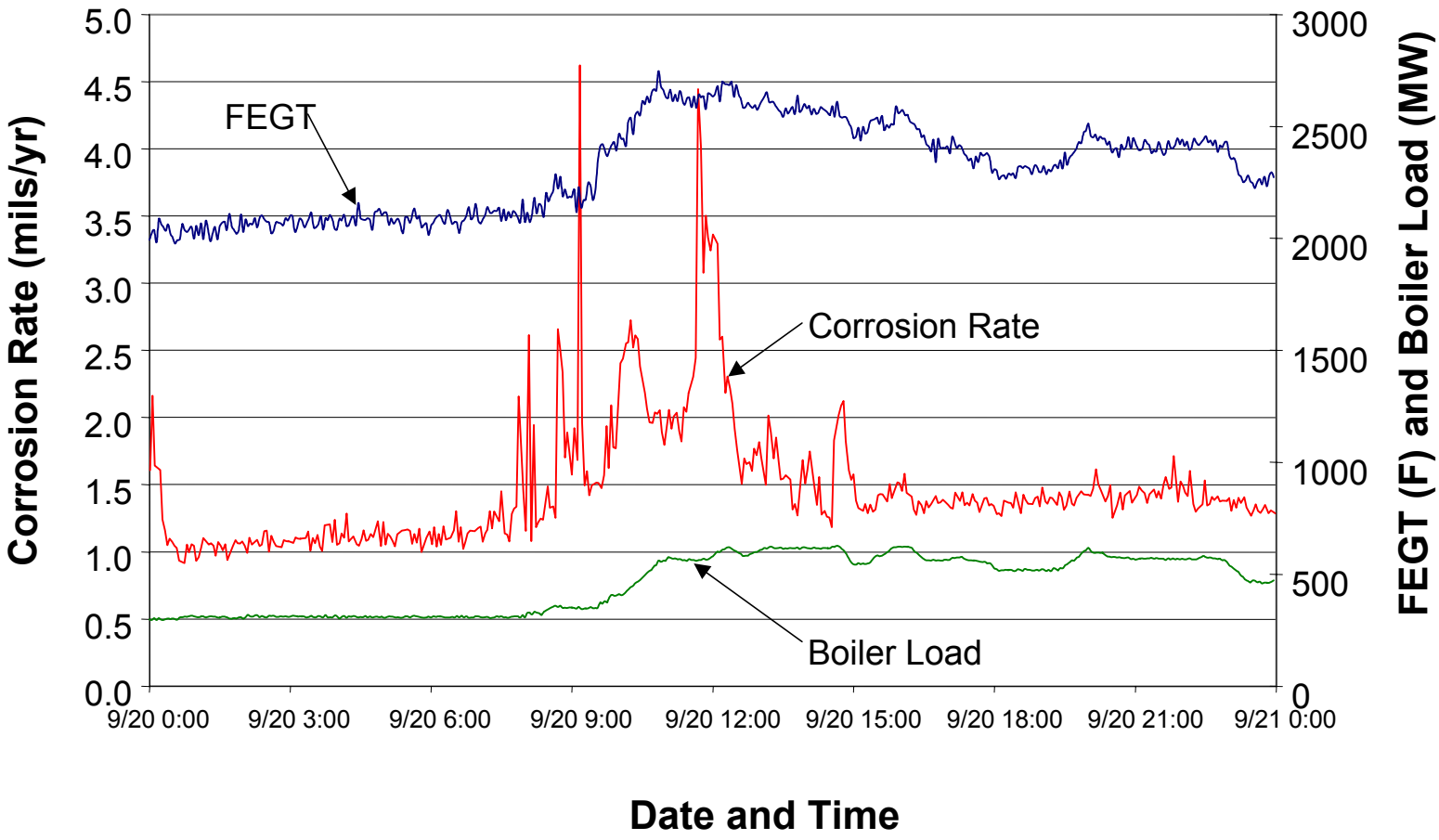

REACTION ENGINEERING INTERNATIONAL

III. Surface Profilometry

Verification with Surface Profilometry

- Requires late model profilometer and mounting jig
- Modified sensor elements to provide a corrosion resistant surface for comparison
- In-house software for border recognition and volume removal calculation
- Effective resolution to corrosion depths <0.1 micron

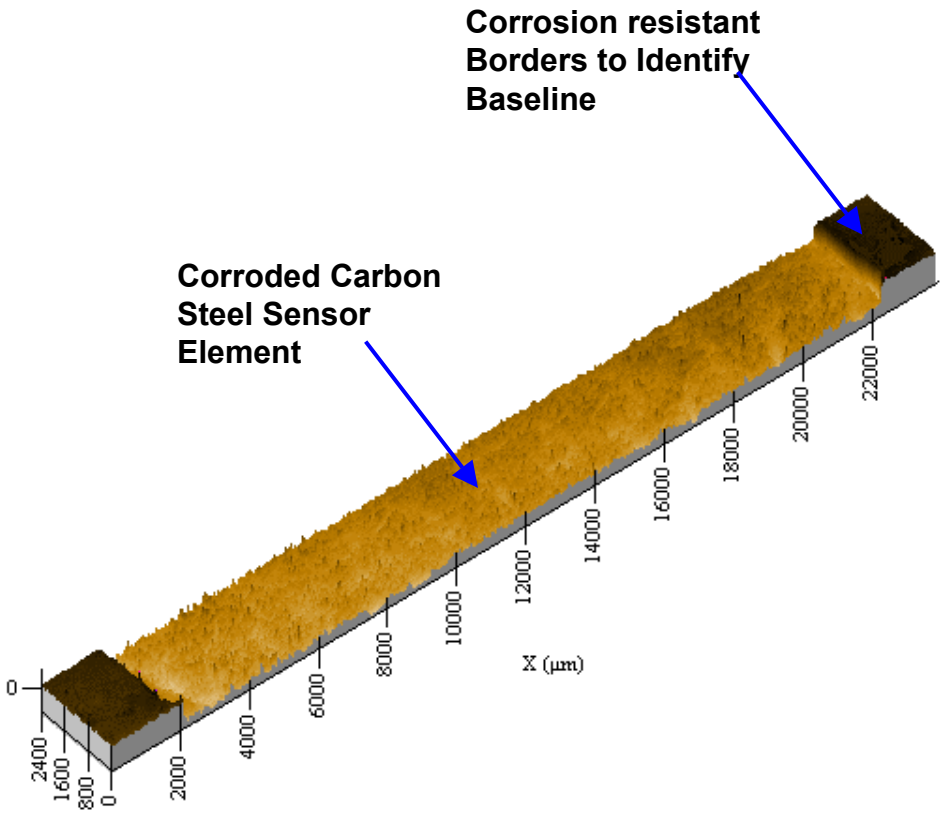

REACTION ENGINEERING INTERNATIONAL

Profilometry and EN Corrosion Measurement

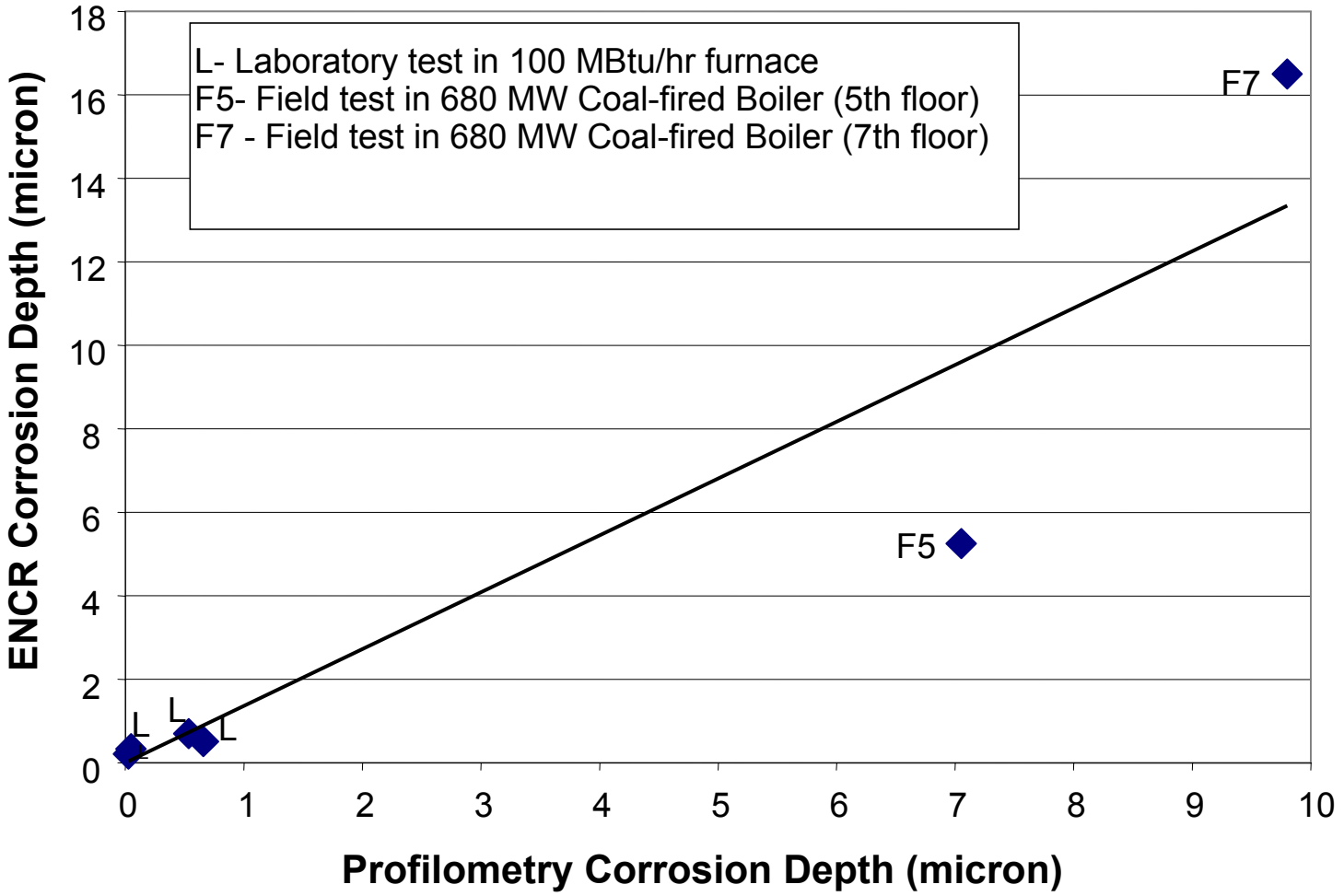

REACTION ENGINEERING INTERNATIONAL

Corrosion Advisor

Current State of the Technology

- **Advice is based on:**
  - Observations made by plant personnel during outages
  - Ultrasonic tube thickness (UT) data obtained annually
  - Weight loss coupons

- **Disadvantages of this approach**
  - Observations and UT data can only be obtained during outages
  - Weight loss coupons do not provide real time data
  - Coupons require a considerable amount of time to provide meaningful data
  - Corrosion information is obtained after the damage has already been done

New Approach to Corrosion Management

- **Advice is based on:**
  - CFD-derived corrosion map of the boiler
  - Multi-sensor EN technique provides real time corrosion rates
  - High-resolution surface profilometry instead of weight loss coupons is used as a benchmark for corrosion rates
- **Major Advantages**
  - EN ties operating conditions to real time corrosion rates
  - Can identify the risk of attack (operating conditions) in real time before significant damage is done
- **Advice provided on:**
  - Improving unit performance – timely feedback to unit operators on detrimental burner operating conditions
  - Maintenance
  - Materials selection
  - Life cycle budgeting
  - NO_x control optimization

REACTION ENGINEERING INTERNATIONAL

Identification of Risk of Damaging Corrosion Attack

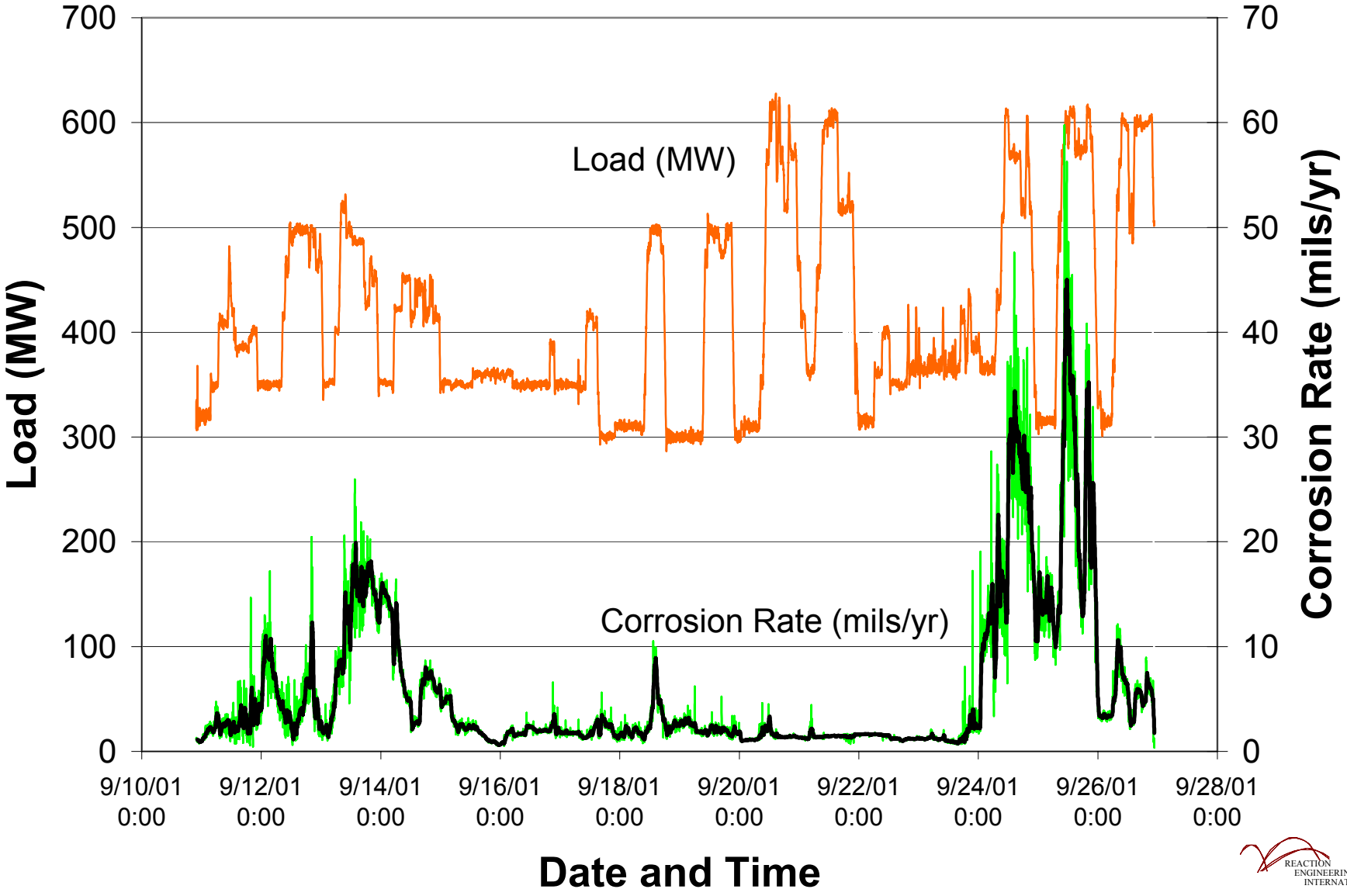

REACTION ENGINEERING INTERNATIONAL

Summary

- Application of a single EN probe for real time monitoring of corrosion in the radiant section of a boiler has been demonstrated
- Combination of the EN technique, surface profilometry and CFD tools offers a powerful system for corrosion management
- The purpose of the current program is to demonstrate the advanced multi-probe system which combines these elements

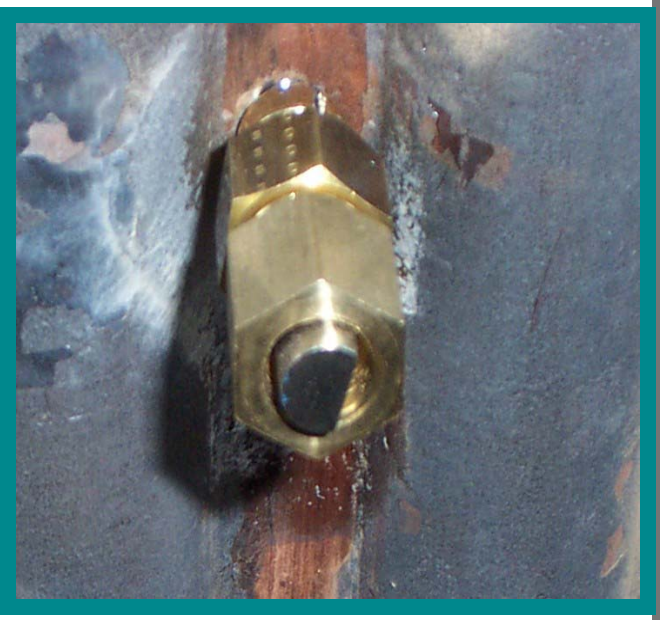

Passive Corrosion Probes

Wate T. Bakker
EPRI

Why Use Passive Corrosion Probes

- Waterwall Wastage rates are frequently variable, especially if chlorine is one of the corrosive species.
- Therefore a large number of probes is desirable to characterize corrosion mechanisms and measure corrosion rates at various locations.
- This requires the use of inexpensive probes which can be installed in the web between tubes and do not require cooling.

Corrosion Probe Installation at Dairyland's Genoa # 3 Boiler

Objectives of the Project

1. Determine the corrosion rate of Alloy 625 weld overlay
2. Determine if corrosion of bare T-11 / T-22 tubes occurs on edges of weld overlay
3. Determine if corrosion rates increase with increased staging
4. Determine corrosion mechanisms
5. Establish operability and benefits of the system selected

The KEMCOP Corrosion Probe

Newly Installed KEMCOP Probe

- Probe is small enough to be installed in web between tubes (8 mm .32”)
- Probes are removable during boiler operation
- Losses ≥ 0.5 mil (12 micron) can be measured, at least in theory
- Analysis of scales and deposits is carried out to determine corrosion mechanisms
- Installation of 25-50 probes in 1-3 days
  - Access hatches in insulation
  - Drill holes in webs
  - Insert probes
  - Reinstall installation
- 300 probes installed in Dutch boilers and waste incinerators

Corrosion Probe Installation at Dairyland's Genoa #3

- 22 T-11(13CrMo4.4), 6 625 (inconel 625), and 2 622 (inconel 622) probes were installed at the inconel 625 overlayed waterwall
- 4 T-22 (10CrMo9.10) probes were installed at walls with no overlay

Corrosion Probe Installation Grid at Dairyland's Genoa #3

- Probe Grid Configuration

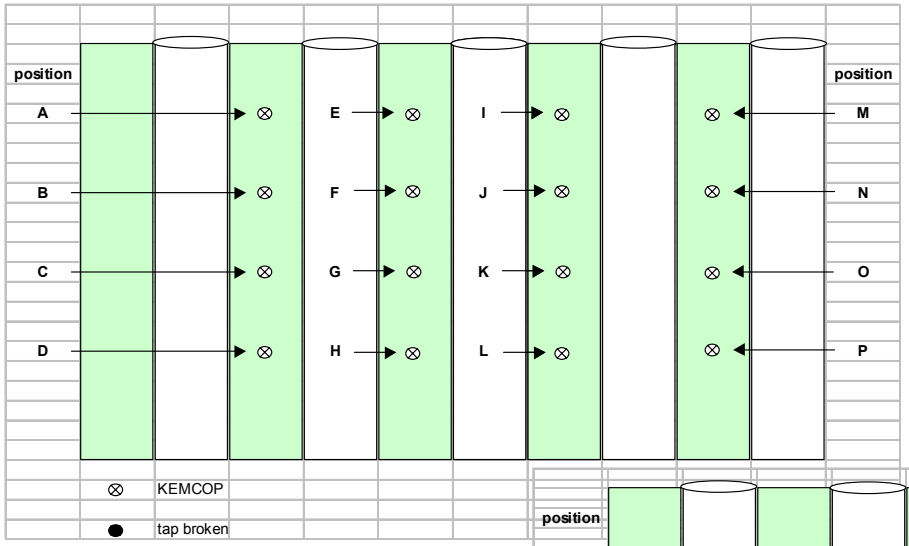

Location I
Rear wall 5th elevation

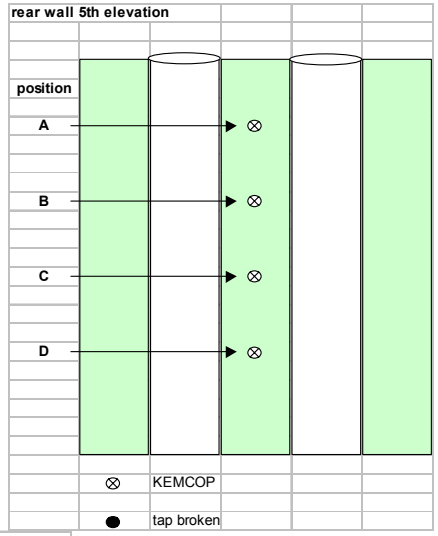

Location II
North side wall 5th elevation

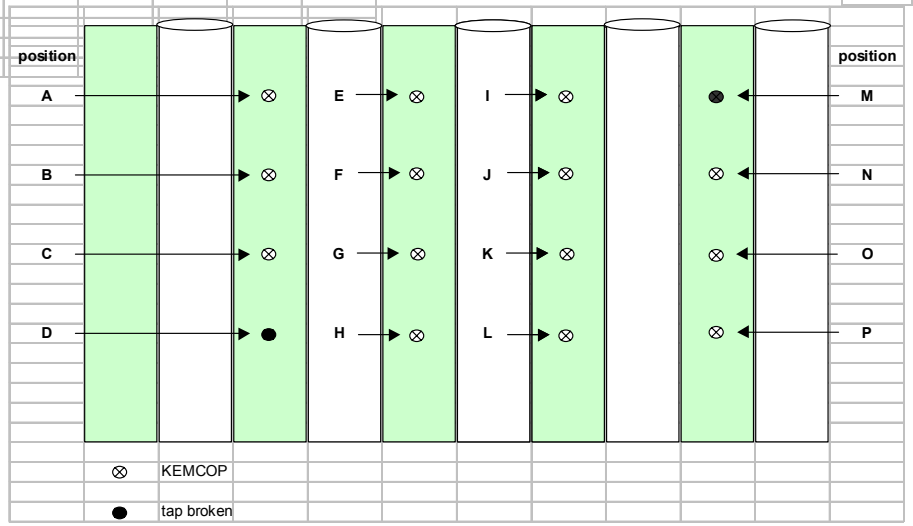

Location III
Rear wall 4th elevation

Temperature Measurements at Dairyland Power Genoa #3

Three KEMA Temperature KEMCOP thread fitted K Type thermocouples were used to determine water wall temperatures as well as near wall temperatures allowable by thermocouple type.

Thermocouple Installation and Testing at Genoa #3

EPRI

T-11 and 625 KEMCOP

After Exposure (~2000hrs)

T11/30

T11/24

625/11

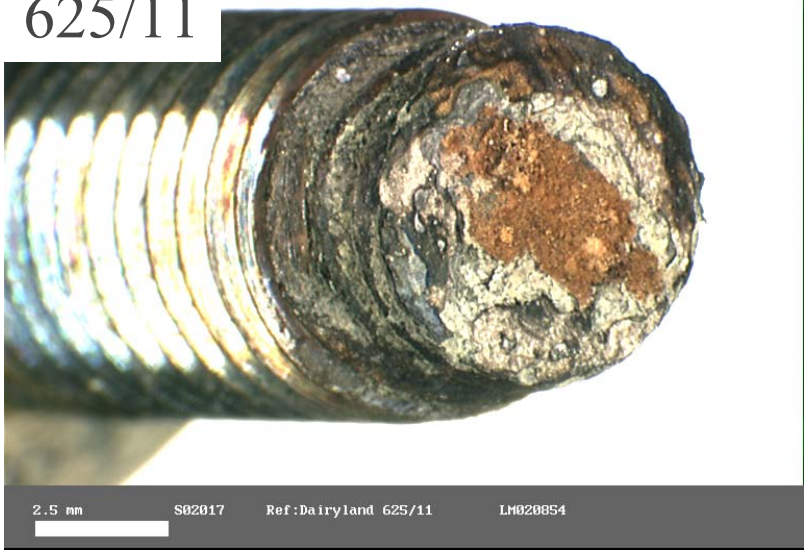

T11/41

FWDC SEM Analysis (T-11/30)

Probe T11/30

- The probe exhibited a layer of remnant deposit/scale along the tip.
- The outer deposit region was comprised of a mixture of iron, sulfur, oxygen, calcium, silicon, and aluminum along with traces of potassium, magnesium, and sodium.
- Evidence of residual chlorides was noted in scattered locations (arrows) along the interface of the deposit/scale and corrosion probe tip. Semi quantitative analysis revealed that the chlorides ranged from 2 to 7 wt.-Percent.

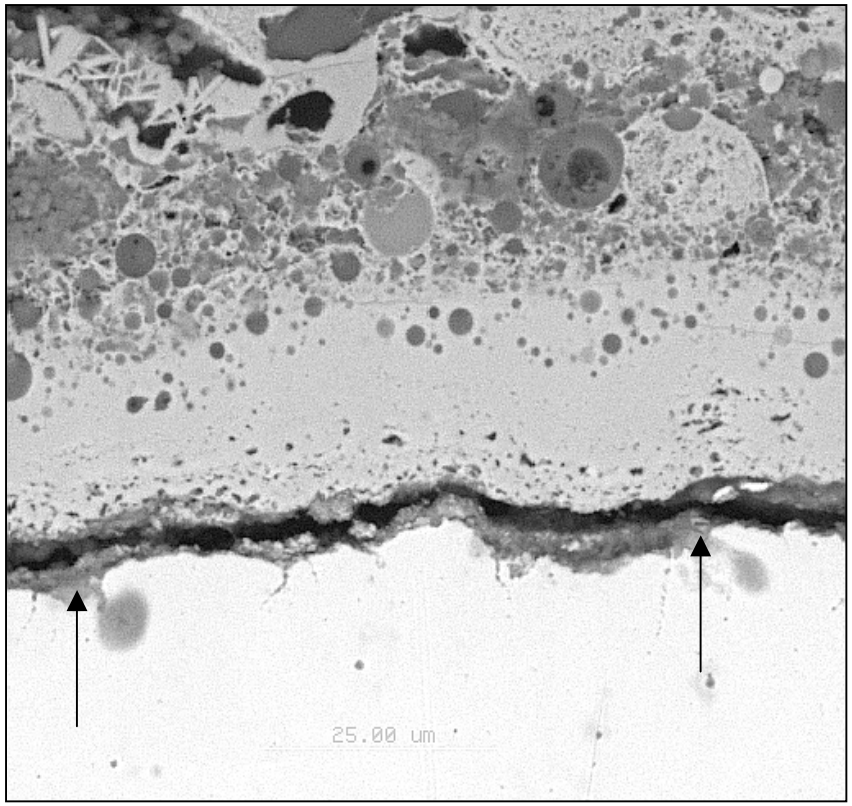

T11/30 SEM backscatter image

Preliminary Results

First exposure period (2523 hrs, minimum SOFA)

- Some T-11 and inconel 625 probes were exposed to high temperatures, leading to high wastage.

  150 mils/yr for T-11 and 48 mils/yr for inconel 625

- Most T-11 probes had relative low wastage rates, maximum wastage rate 24 mils/yr.
- The majority of the scales contained Iron sulfide, indicative of reducing conditions, one sample contained $FeCl_2$ as corrosion product. It had the highest corrosion rate.
- All inconel 625 probes showed significant hardness increases from 98 HRB to 41 HRC. This may make them more susceptible to cracking.

Preliminary Results

Second Exposure Period
(2616 hours, minimum SOFA)

- All 625 and 622 probes showed increase in hardness of the exposed surface, when mounted flush with the web surface.
- Wastage of both inconel 625 and 622 probes was negligible.
- Wastage of T-11 probes was variable, maximum wastage rate 80 mils/yr.
- Wastage of T-22 probes, exposed above weld overlay was variable, maximum wastage rate 32 mils/yr.
- One T-11 probe contained 1-2 wt. % Chlorides.

Preliminary Evaluation of Passive Probes

1. Wastage rate very sensitive to probe temperature, but generally lower than the maximum tube wastage observed prior to weld overlay installation.
2. Probes can provide early information on corrosion mechanism from which corrosion rates ranges can be estimated.
3. Consistent increases in hardness of weld overlay materials indicates weld overlay surface may be hotter than expected.
4. Information obtained will complement data from active probes.

Installation at Gavin

- Compare results from passive probes with active, electrochemical probes installed by REI.
- Installed 24 probes during March/April outage. Four probes close to each active probe.
- New probes will be installed when testing of REI probes starts.
- Probes installed protrude at different lengths (0.5-2 mm) to create range of exposure temperatures.

Corrosion Probe Installation at AEP's Gavin #1

- 18 T-11 and 6 inconel 625 probes were installed at six locations in the inconel 625 overlayed waterwall. The probes were placed between tubes close to the REI probes.

EPRI Installation of KEMCOP Corrosion Probes